Markus Berli

Compaction of agricultural subsoils
by tracked heavy construction machinery

Diss. ETH No. 14132

Compaction of Agricultural Subsoils
by Tracked Heavy Construction Machinery

Dissertation submitted to the

SWISS FEDERAL INSTITUTE OF TECHNOLOGY ZÜRICH

for the degree of

DOCTOR OF TECHNICAL SCIENCES

presented by

MARKUS BERLI

Dipl. Umwelting., ETH Zürich

born 1 January 1968

citizen of Birmensdorf and Ottenbach ZH

Prof. Dr. Rainer Schulin, examiner

Prof. Dr. Sarah Springman, co-examiner

Prof. Dr. Hannes Flühler, co-examiner

2001

Für meine Eltern

Contents

Preface

This work was carried out in the context of a joint research project entitled 'Assessment and prediction of subsoil compaction sensitivity in the course of pipeline construction work through agricultural land'. The project was jointly sponsored by the Institute of terrestrial Ecology (ITÖ) of the Swiss Federal Institute of Technology (ETH) Zurich and the Research and Development Fund of the Swiss Gas Industry (FOGA). This collaboration was initiated as a result of discussions concerning the validity of tolerance limits which regulate the maximum weights and contact stresses of heavy tracked machinery used for gas pipeline construction.

Vorwort

Diese Arbeit entstand im Rahmen einer Forschungszusammenarbeit zum Thema „Beurteilung und Vorhersage der mechanischen Belastbarkeit des Unterbodens beim Verlegen unterirdischer Rohrleitungen durch Kulturland" zwischen dem Institut für terrestrische Ökologie (ITÖ) der ETH Zürich und dem Forschungs- und Entwicklungsfonds der Schweizer Gasindustrie (FOGA). Ausgelöst wurde die Zusammenarbeit durch die Diskussion um Grenzwerte für den Einsatz schwerer Maschinen beim Gasleitungsbau, um den Unterboden vor bleibenden Verdichtungen zu schützen.

Summary

In the past century mechanisation has revolutionised agriculture. In the course of the desired increase in crop production, negative effects such as an increased risk of soil compaction due to heavy machinery have also emerged threatening soil fertility. Particularly problematic is the compaction of subsoils because it is extremely persistent and often hard, if feasible at all, to restore to non-compacted state. Apart from agricultural activities, the use of agricultural land as temporary access way for road-, overland high voltage transmission line- and pipeline construction work has added to the problem of subsoil compaction. In recent years, heavy tracked machinery weighing up to 6×10^4 kg with mean normal stresses in the contact area up to 100 kPa was used for overland gas pipeline construction work in Switzerland.

To prevent subsoil compaction damages, precompression stress, i.e. the yield point between elastic and plastic compression behaviour, has been proposed as a key criterion for allowable mechanic loads on agricultural subsoils. As the available knowledge about the validity and feasibility of this criterion for such application to heterogeneous, unsaturated field soils was insufficien, this study was performed. In particular, the study addressed the applicability of the precompression stress criterion to regulate the use of heavy tracked construction machinery. For this purpose the criterion was tested under real-world conditions in field experiments. A particular problem was the moisture dependence of soil mechanical parameters of unsaturated structured agricultural soil. A soil mechanical model was evaluated to predict subsoil compaction by computer simulation.

On three selected field sites along a gas pipeline under construction, wet and dry test plots were experimentally trafficked with heavy tracked machines used for construction work. Compaction effects were determined by comparing precompression stress, bulk density and macroporosity values as well as water flow pattern from trafficked and non-trafficked soil. Precompression stress was determined by the Casagrande-procedure from confined uniaxial compression tests carried out in the laboratory on undisturbed samples at -6 kPa initial soil water potential. For one of the three test sites, a silt loam Haplic Luvisol, additionally precompression stress, compression- and recompression index were determined at five different initial water potentials between -1 and -32 kPa. For this site,

the outcome of the field trial was interpreted with a finite-element model based on the concept of critical state soil mechanics.

No significant increase of precompression stress and bulk density and decrease of macroporosity occurred in the subsoil if the mean stress in the contact area of the tracks did not reach precompression stress. This findings were supported by the lack of significant changes in water flow pattern. The lack of statistical significance in the subsoil does not mean, however, that compaction effects can be entirely excluded. They may have simply remained insignificant in comparison to the rather large background variability of the parameters used to assess the compaction effects.

A negative logarithmic correlation was found between precompression stress and water potential and a negative linear correlation between precompression stress and gravimetric water content. Precompression stress increased very strongly with water tension in the subsoil but was almost independent of soil moisture (in the range between -1 and -32 kPa water potential) in the topsoil. The compression index slightly increased with decreasing water potential. But it was stronger correlated to initial void ratio of the samples. The recompression index slightly decreased with decreasing water potential. Like precompression stress, also compression and recompression index showed stronger moisture dependence in the subsoil than in the topsoil. No correlation was found between stress-compression characteristics and initial water saturation degree.

For the silt loam Haplic Luvisol, both direct measurement and modelling showed that the dry soil was strong enough to resist compaction. The wet soil was too weak to resist compaction in the topsoil, strong enough in the ploughpan, and probably also strong enough in the subsoil. For the wet soil, the modelling results suggested that only partially drained conditions prevailed in the soil beneath the tracks during passage of the machines.

Given the good agreement between experimentally observed and expected compaction effects and the surprisingly accurate stress predictions of the used critical state soil mechanics model, it was concluded that precompression stress represents a useful and practical parameter to access subsoil compaction susceptibility for the used traffic and soil conditions investigated in this study.

Zusammenfassung

Die Landwirtschaft wurde im 20. Jahrhundert durch die starke Mechanisierung revolutioniert. Mit den dadurch erreichten Ertragssteigerungen gehen allerdings auch negative Einflüsse auf die Umwelt einher. Ein Beispiel dafür ist die Gefährdung der Bodenfruchtbarkeit durch Verdichtungen. Unterbodenverdichtungen gelten dabei als besonders problematisch, da sie sehr persistent und wenn überhaupt, nur schwer wieder zu entfernen sind. Zusätzlich zur immer intensiveren landwirtschaftlichen Nutzung wird Kulturland auch zunehmend mit schwere Baumaschinen im Zusammenhang mit Strassen- oder Überland-Leitungsbauten befahren. Die in den letzten Jahren beim Gasleitungsbau durch Kulturland in der Schweiz eingesetzten Raupenfahrzeuge weisen Gewichte bis 6×10^4 kg und mittlere Kontakflächendrücken bis 100 kPa auf und können daher Unterbodenverdichtungen verursachen.

Um Verdichtungsschäden in Unterböden zu vermeiden, wurde die Vorbelastung, d.h. der Übergang von elastischem zu plastischem Verdichtungsverhalten des Bodens, als Schlüsselkriterium zur Beurteilung der zulässigen mechanischen Belastung vorgeschlagen. Da die Kenntnisse über die Verlässlichkeit und Anwendbarkeit dieses Kriteriums für inhomogene, ungesättigte Kulturböden bisher ungenügend waren, wurde diese Untersuchung durchgeführt. Untersucht wurde, ob sich die Vorbelastung als Kriterium zur Beurteilung der Verdichtungsempfindlichkeit von Unterböden beim Einsatz schwerer Raupenfahrzeuge unter realen Baubedingungen eignet. Ein spezielles Problem stellte dabei die Feuchtigkeitsabhängigkeit der Verformungseigenschaften des ungesättigten, strukturierten Bodens dar. Ein bodenmechanisches Modell wurde evaluiert, um Unterbodenverdichtungen mittels Computersimulation vorhersagen zu können.

An drei Untersuchungssstandorten entlang einer Gasleitungsbaustelle wurden feuchte und trockene Versuchsflächen mit schweren Raupenfahrzeugen, wie sie beim Bau verwendet wurden, befahren. Um Verdichtungseffekte festzustellen, wurden Vorbelastung, Lagerungsdichte und Grobporenvolumen sowie die Fliesspfade von Wasser in befahrenem und unbefahrenem Boden untersucht. Die Vorbelastung wurde mit der Casagrande-Methode, angewendet auf Drucksetzungskurven aus Ödometerversuchen an ungestörten Proben bei 6 kPa Anfangssaugspannung, bestimmt. Für eine der drei Versuchsflächen, einer Parabraunerde aus lehmigem Schluff, wurden zusätzlich zur Vorbe-

lastung auch die Kompressions- und Wiederverdichtungsbeiwerte bei verschiedenen Anfangssaugspannungen zwischen 1 und 32 kPa bestimmt. Für dieselbe Versuchsfläche wurden die Resultate des Befahrungsversuches mit einem Finite-Elemente Modell, basierend auf dem Konzept der critical state soil mechanics, interpretiert.

In den Unterböden wurden keine signifikant grösseren Vorbelastungen und Lagerungsdichten sowie kleinere Grobporenvolumina gefunden, sofern der mittlere Kontaktflächendruck unter den Raupen die Vorbelastung im Boden nicht erreichte. Auch wurden keine signifikanten Veränderungen der Fliesspfade für Wassers festgestellt. Fehlende Signifikanz bedeutet nicht, dass Verdichtungen vollständig ausgeschlossen werden können. Kleine Verdichtungseffekte könnten durch die natürliche Variabilität der untersuchten Parameter überdeckt worden sein.

Die Vorbelastung war positiv logarithmisch mit der Anfangssaugspannung, sowie negativ linear mit dem gravimetrischen Wassergehalt korreliert. Im betrachteten Saugspannungsbereich zwischen 1 und 32 kPa war die Vorbelastung im Unterboden, im Gegensatz zum Oberboden, sehr stark saugspannungsabhängig. Der Kompressionsbeiwert wurde mit zunehmender Anfangssaugspannung tendentiell grösser. Er war jedoch deutlich stärker mit der Anfangsporenziffer als mit der Feuchtigkeit korreliert. Der Wiederverdichtungsbeiwert wurde mit zunehmender Anfangssaugspannung tendentiell kleiner. Wie die Vorbelastung waren auch Kompressions- und Wiederverdichtungsbeiwert im Unterboden stärker feuchtigkeitsabhängig als im Oberboden. Zwischen dem Anfangssättigungsgrad und der Vorbelastung sowie dem Kompressions- und Wiederverdichtungsbeiwert wurden keine Korrelationen gefunden.

Für die Parabraunerde aus lehmigem Schluff zeigten Messung und Modellierung, dass der trockene Boden sowie die Pflugsohle im feuchten Boden durch die Befahrung nicht verdichtet wurden. Der Oberboden der feuchten Versuchsfläche wurde signifikant verdichtet, während der Unterboden wahrscheinlich nicht weiter verdichtet wurde. Die Modellrechnungen zeigten auch, dass während der Belastung im feuchten Unterboden unter den Raupen Porenwasserüberdrücke auftraten und diesen damit möglicherweise vor Verdichtung schützten.

Die gute Übereinstimmung zwischen erwarteten und experimentell beobachteten Unterbodenverdichtungen sowie die überraschend gut zutreffenden Modellvorhersagen lassen den Schluss zu, dass die Vorbelastung, zumindest unter den gewählten Belastungs- und Bodenverhältnissen, einen brauchbaren und praktischen Parameter darstellt, um die Verdichtungsempfindlichkeit von Unterböden zu beurteilen.

1

Introduction

In the past century, mechanisation has revolutionised agriculture. Apart from the desired increase of crop production this has, however, also brought negative impacts on the environment. Among these, the risk of soil compaction by using heavy machinery has been recognised as a major threat to soil fertility. Oldeman et al. (1991) estimated that compaction is by far the most important type of physical deterioration of agricultural soils, being responsible for soil degradation of an area of 6.8×10^4 km^2 world-wide of which 3.3×10^4 km^2 is found in Europe. Compaction does not only adversely affect crop production by decreasing rootability and conductivity for water and air and increasing the requirement for fertilisers and energy but also on environmental quality (emission of greenhouse gases, runoff of water and pollutants into surface waters, movements of nitrate and pesticides into ground water) as reviewed by Soane and van Ouwerkerk (1995). What makes the problem worse is that the restoration of compacted soils by technical means is difficult, if feasible at all. Subsoil compaction especially is regarded as very persistent. Structural regeneration by natural processes (reviewed by Håkansson and Reeder, 1994) or artificial techniques (Kooistra et al., 1984) seems to be in most cases extremely slow, except for the topsoil, while artificial deep loosening often leads to secondary compaction which may be even worse.

Not only agricultural activities but also the use of agricultural land as temporary access way during construction of roads, overland high voltage transmission lines and gas pipeline construction work bears a high risk of soil compaction. Since the early 1990s, controversy about the use of heavy machines for the construction of transport gas pipelines through agricultural land led to an increased awareness of the problem of physical soil degradation in Switzerland. Farmers worried because of negative experiences with persistent soil damages caused by pipeline construction work in the 1970s and demanded tight restrictions on the allowable use of construction machines. Soil protection agencies saw the main problem in subsoil compaction since many of the tracked vehicles used for gas pipeline construction weighed 3×10^4 kg and more; some even exceeded 6×10^4 kg. In order to protect subsoils from mechanical overloading, regulations were set and enforced

1

as part of the pipeline concessions. Limits were imposed on the allowable weight and contact stress of the used construction machinery as a function of water tension in the subsoil (0.3-0.35 m depth). As a sound data basis was lacking, these tolerance limits had to be based primarily on expert opinions and were set rather restrictive for precautionary reasons. As the resulting restrictions on the construction works were not only costly for the construction but also felt undue in many cases, the present study was initiated in order to establish a sound data basis for setting tolerance limits which would still warrant sufficient soil protection without being over-restrictive for construction work.

Following Horn (1981; 1988), Lebert (1989) and Kirby (1991b), precompression stress, i.e. the yield point in the transition from elastic to plastic compression behaviour, has been proposed as a key criterion in the regulation of tolerable mechanic stresses on agricultural soils. The concept of precompression stress states that compression of a soil is elastic and thus reversible up to a certain limit, the precompression stress. Only stresses above that limit cause plastic and, thus, thermodynamically irreversible deformation. Thus, if stresses beyond the precompression stress are avoided, there should be no irreversible mechanical damage to the soil. The underlying soil mechanical concept appeared to be well suited to account for the mechanical stress situation in particular under wide, rigid steel tracks of construction machinery, without being too complex for regulative purposes.

Although theoretically very appealing, the practical applicability and suitability of precompression stress as a regulatory criterion to prevent soil compaction under real-world conditions was not evident a priori. Precompression stress is usually measured in the laboratory on undisturbed samples, which are subjected to defined stress conditions. Such conditions can never exactly reproduce the mechanical stress as well as the air and water drainage situation in the soil environment of the field, even if the sampling does not cause any damage to the sample itself. How representative a laboratory test is, may also depend on the size of the sample. This should be sufficiently large to reproduce the structural features of the soil, which determine its mechanical properties, adequately. The mechanical representative elementary volume of soil will in general be much larger for undisturbed field soils than for fine grained, remoulded 'engineering' soils.

Further complications arise from the fact that we deal with unsaturated soils and that, therefore, the influence of soil moisture on the mechanical properties has to be taken into account. A number of previous studies (Söhne, 1953; Söhne, 1958; Greacen, 1960; Larson et al., 1980; Stone and Larson, 1980; Leeson and Campbell, 1983; Hettiaratchi and O'Callaghan, 1985; Culley and Larson, 1987; Horn, 1988; Kirby, 1991a; Petersen, 1993; O'Sullivan et al., 1994; O'Sullivan and Robertson, 1996; Panayiotopoulos, 1996;

Adams and Wulfsohn, 1997) have clearly shown that the compression behaviour of un-saturated agricultural soils, including precompression stress, can strongly depend on moisture status.

Moisture dependence also complicates the task of determining the stresses which are exerted by the load of a machine in the subsoil. Apart from the problem of calculating the stress propagation in the soil profile a major difficulty already consists in assessing stress boundary conditions at the soil surface below the wheels or tracks of a vehicle.

While the available literature suggests that the precompression stress concept is very promising for regulatory application in soil protection, it does not provide sufficient an-swers to these questions. Addressing the task to show the feasibility of applying the pre-compression stress criterion to real-word situations, the specific objectives of this study were to

- assess whether precompression stress, experimentally determined in the laboratory, can provide a suitable criterion for the compressibility of unsaturated agricultural soils under field conditions and stresses exerted by tracked heavy construction machinery.

- describe the stress propagation under such conditions in the continuum by an appro-priate soil mechanics constitutive model.

- determine the dependence of relevant compression properties on the moisture status of undisturbed soil samples.

This study accordingly proceeded in three main steps which are described each in one of the following chapters:

- Field experiments were performed along a gas pipeline under construction on three test sites in which heavy tracked construction machinery trafficked test plots of vari-ous soil moisture under controlled and well-defined mechanical conditions. Precom-pression stress, bulk density, coarse porosity and water flow paths of trafficked and non-trafficked soil were compared (chapter 3).

- Soil samples from one test site were conditioned to different initial moisture status and then subjected to confined uniaxial compression tests. From the resulting stress-strain curves effects of soil moisture on precompression stress, compression and re-compression index were evaluated (chapter 4).

- For one field experiment, stress propagation in the soil was calculated using the critical state soil mechanics model 'Modified Cam Clay', implemented in the finite-element code 'Crisp' (Britto and Gunn, 1987). Compression characteristics including their moisture dependence determined in the previous step and shear properties additionally measured from the same site were used as input parameters. Calculated vertical stresses were compared with measured precompression stresses (chapter 5).

References

Adams, B.A. and Wulfsohn, D., 1997. Variation of the critical-state boundaries of an agricultural soil. European Journal of Soil Science, 48: 739-748.

Britto, A.M. and Gunn, M.J., 1987. Critical State Soil Mechanics via Finite Elements. Ellis Horwood, Chichester, 488 pp.

Culley, J.L.B. and Larson, W.E., 1987. Susceptibility to compression of a clay loam Haplaquoll. Soil Science Society of American Journal, 51: 562-567.

Greacen, E.L., 1960. Water content and soil strength. Journal of Soil Science, 11(2): 313-333.

Håkansson, I. and Reeder, R.C., 1994. Subsoil compaction by vehicles with high axial load - extend, persistence and crop response. Soil & Tillage Research, 29: 277-304.

Hettiaratchi, D.R.P. and O'Callaghan, J.R., 1985. The mechanical behaviour of unsaturated soils. International Conference on Soil Dynamics, Auburn, Alabama. pp. 266-281.

Horn, R., 1981. Eine Methode zur Ermittlung der Druckbelastung von Böden anhand von Drucksetzungsversuchen. Zeitschrift für Kulturtechnik und Flurbereinigung, 22(1): 20-26.

Horn, R., 1988. Compressibility of arable land. In: J. Drescher, R. Horn and M. De Boodt (Editors). Impact of Water and External Forces on Soil Structure, Catena Supplement 11. Catena-Verlag, Cremlingen-Destedt, pp. 53-71.

Kirby, J.M., 1991a. Critical-state soil mechanics parameters and their variation for Vertisols in eastern Australia. Journal of Soil Science, 42: 487-499.

Kirby, J.M., 1991b. Strength and deformation of agricultural soil: measurement and practical significance. Soil Use and Management, 7: 223-229.

Kooistra, M.J., Bouma, J., Boersma, O.H. and Jager, A., 1984. Physical and morphological characterisation of undisturbed and disturbed ploughpans in a sandy loam soil. Soil & Tillage Research, 4: 405-417.

Larson, W.E., Gupta, S.C. and Useche, R.A., 1980. Compression of agricultural soils from eight soil orders. Soil Science Society of America Journal, 44: 450-457.

Lebert, M., 1989. Beurteilung und Vorhersage der mechanischen Belastbarkeit von Ackerböden. PhD Thesis, Fakultät für Biologie, Chemie und Geowissenschaften, Universität Bayreuth, Bayreuth, 131 pp.

Leeson, J.J. and Campbell, D.J., 1983. The variation of soil critical state parameters with water content and its relevance to the compaction of two agricultural soils. Journal of Soil Science, 34: 33-44.

Oldeman, L.R., Hakkeling, R.T.A. and Sombroeck, W.G., 1991. World Map of the Status of Human-Induced Soil Degradation: An Explanatory Note, International Soil Reference and Information Centre (ISRIC), Wageningen.

O'Sullivan, M.F., Campbell, D.J. and Hettiaratchi, D.R.P., 1994. Critical state parameters derived from constant cell volume triaxial tests. European Journal of Soil Science, 45: 249-256.

O'Sullivan, M.F. and Robertson, E.A.G., 1996. Critical state parameters from intact samples of two agricultural topsoils. Soil & Tillage Research, 39: 161-173.

Panayiotopoulos, K.P., 1996. The effect of matric suction on stress-strain relation and strength of three Alfisoils. Soil & Tillage Research, 39: 45-59.

Petersen, C.T., 1993. The variation of critical-state parameters with water content for two agricultural soils. Journal of Soil Science, 44: 397-410.

Soane, B.D. and Van Ouwerkerk, C., 1995. Implications of soil compaction in crop production for the quality of the environment. Soil & Tillage Research, 35: 5-22.

Söhne, W., 1953. Druckverteilung im Boden und Bodenverformung unter Schlepperreifen. Grundlagen der Landtechnik, 5: 49-63.

Söhne, W., 1958. Fundamentals of pressure distribution and soil compaction under tractor tires. Agricultural Engineering, May: 276-291.

Stone, J.A. and Larson, W.E., 1980. Rebound of five one-dimensionally compressed unsaturated granular soils. Soil Science Society of America Journal, 44: 819-822.

2

Soil physics and soil mechanics - theoretical aspects

2.1 Objectives

This study was carried out at the interface of 'classical' soil physics and soil mechanics. Although both disciplines deal with the same material, i.e. the soil, different notation and terms for the same properties are in use. Therefore the first aim of chapter 2 is to define the terms 'topsoil', 'subsoil', 'compression' and 'compaction' as well as the volume and mass relationships of the soil constituents used in this study. Secondly an introduction into the soil physical/mechanical concepts of 'soil water potential', 'tensiometry' and 'soil water characteristic', as well as a short introduction into critical state soil mechanics is given.

2.2 Definitions

In soil science, the **topsoil** (in agricultural soils usually identical with the A-horizon) is defined as the top layer of a soil which is characterised by the incorporation of humified organic matter and/or the loss of mineral constituents (e.g. by dissolution and leaching) resulting in a relative enrichment of the organic matter content of the mineral soil (sand, silt, clay) relative to the soil below. Usually the organic matter content is above 0.02 kg organic matter per kg dry soil. In arable land the topsoil is in general equivalent with the plough layer. i.e. the layer in which the soil is more or less regularly mixed by cultivation.

The **subsoil** is the part of a soil profile below the topsoil which is enriched by pedogenic mineral phases due to weathering and transformation of the primary, i.e. geogenic, minerals and/or accumulation of constituents from the topsoil by illuviation. In general, the subsoil is equivalent to the B-horizon, i.e. the layer between the topsoil and the non-weathered parent material of the underground below (C-horizon).

In geotechnical engineering **compression** denotes a decrease in void space due to external (applied load) or internal (suction) forces. In soil science a reduction in pore volume is called **compaction**. Often compaction is used to refer to any change in pore size distribution resulting in a reduction of permeability for water or air. In contrast to this wide meaning of the term in soil science, geotechnic reserves its use strictly for the

mechanical operation applied to a soil to increase its dry bulk density (i.e. densification) (Fredlund and Rahardjo, 1993, p. 33). In this study compaction in the sense of reduction of porosity, in particular of coarse porosity, is used following its usage in soil science.

Table 2.1.   Volumetric and mass properties of soil constituents

Parameter	Definition	Definitions according to
Bulk density	$\rho_b = \dfrac{M_s}{V_t}$	Jury et al. (1991)
Mineral density	$\rho_s = \dfrac{M_s}{V_s}$	Jury et al. (1991)
Porosity	$n = \dfrac{V_w + V_a}{V_t}$	Wood (1990)
Void ratio	$e = \dfrac{V_w + V_a}{V_s}$	Wood (1990)
Specific volume	$v = \dfrac{V_t}{V_s}$	Wood (1990)
Gravimetric water content	$\Theta_g = \dfrac{M_w}{M_s}$	Jury et al. (1991)
Volumetric water content	$\Theta_v = \dfrac{V_w}{V_t}$	Jury et al. (1991)
Degree of saturation	$S_r = \dfrac{V_w}{V_w + V_a}$	Wood (1990)

M_t: total soil mass; M_s, M_w, M_a: fraction of soil solid (s), water (w) and air (a) mass.

V_t: total soil volume; V_s, V_w, V_a: fraction of soil solid (s), water (w) and air (a) volume.

The notation for the definitions given in Table 2.1 were chosen according to the text-books of Jury et al. (1991) and Wood (1990) being aware that most of the definitions were already formulated earlier e.g. by Terzaghi (1925).

2.3 Soil physics

2.3.1 Soil water potentials

According to the Soil Science Society of America (SSSA, 1997) the total soil water potential is defined as «the amount of work that must be done per unit quantity of pure water in order to transport reversibly and isothermally an infinitesimal quantity of water from a pool of pure water at a specific elevation at atmospheric pressure to the soil water (at a specific point)». The total soil water potential Ψ_t can be thought of as a sum of separate components due to system variables. Jury et al. (1991, p. 52) give the following definitions:

$$\Psi_t = \Psi_z + \Psi_s + \Psi_{tp}$$
$$\Psi_{tp} = \Psi_a + \Psi_m \qquad\qquad (2.1\ a\text{-}c)$$
$$\Psi_m = \Psi_b + \Psi_w$$

where $\Psi_z = \rho_w\, g\left(z_{soil} - z_o\right)$ is the gravitational potential, Ψ_s is the solute potential and Ψ_{tp} is the tensiometer pressure potential. The tensiometer pressure potential can be subdivided into the air pressure potential Ψ_a and the matric potential Ψ_m. The former arises due to different air pressures in the soil and the atmosphere. The latter results from the capillary and adsorptive interactions between water and soil matrix. If the soil is assumed to be a non-rigid material, it is useful to subdivide the matric potential Ψ_m into an overburden pressure potential Ψ_b and a wetness potential Ψ_w (Jury et al., 1991, p. 52). Ψ_w is the result of the adsorptive forces between water and soil matrix. Ψ_b arises due to mechanical pressure exerted by the solid soil on the soil water as the result of e.g. the weight of the overlying soil material or a load on the soil surface.

In practice, the gravitational water potential at a point z_{soil} is given by ist elevation from a reference level z_o. The solute potential is measured as the pressure difference across a semi-permeable membrane and the tensiometer potential as the hydraulic water pressure in the ceramic cup of a tensiometer (see Fig. 2.1a). The ceramic cup of a tensiometer is permeable for solutes, thus the tensiometer potential refers to the soil solution in its actual composition and the solute potential is zero. Except for conditions of trapped air or very low air permeability of the soil, differences in soil air and atmospheric air pressure can usually be neglected. In this study, tensiometer potential was considered to be equivalent to matric potential because sufficient time was always given for air pressure equilibration. With solute and air potential being zero, tensiometer potential was simply referred as soil water potential.

a)   b)
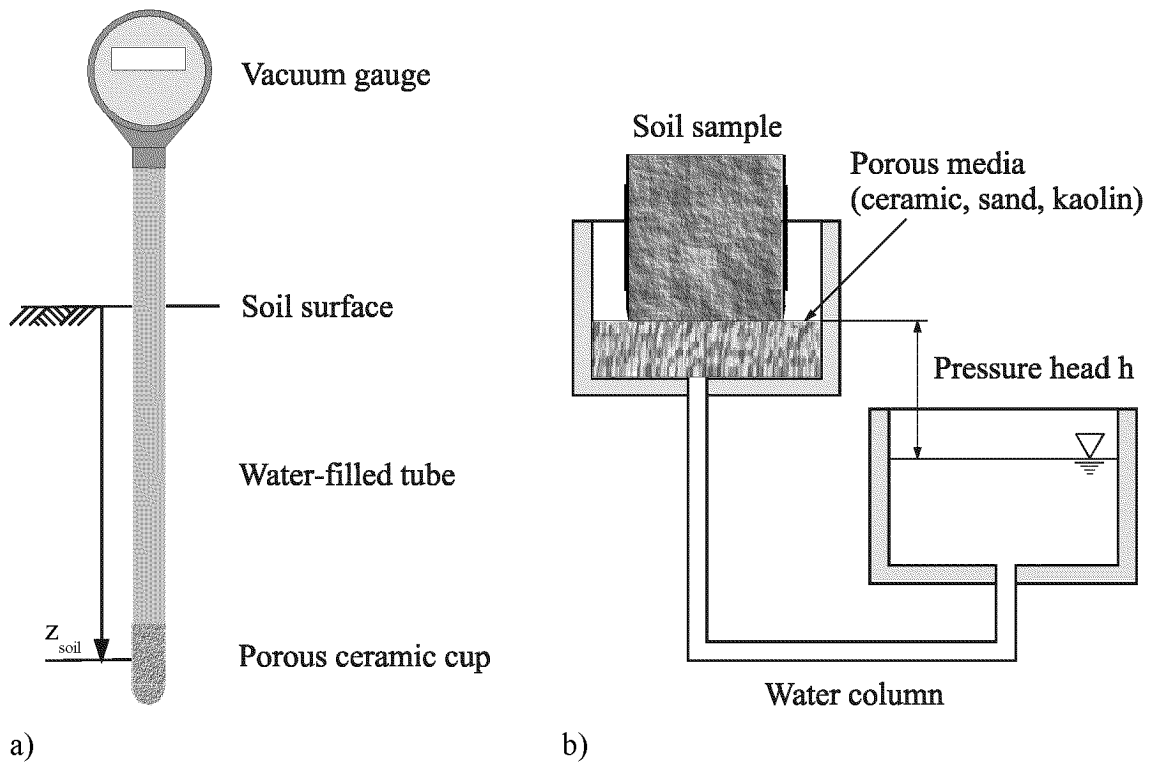
Fig. 2.1.   Vacuum gauge tensiometer (a) and desaturation of soil samples to a matric potential $\Psi_m = \rho_w\, g\, h$ with a hanging water column (b) (following Jury et al. (1991)).

2.3.2 Soil water characteristic

The functional relationship between the matric potential Ψ_m and the gravimetric or volumetric water content (Θ_g, Θ_v) is called the soil water characteristic, characteristic curve or water retention curve (SSSA, 1997). The desorbtion curve is the drying branch of this hysteretic relationship. It can be determined by drying a soil sample using a hanging water column for matrix potentials down to -20 kPa (see Fig. 2.1b) or a pressure membrane apparatus (e.g. Richards, 1941; Richards and Fireman, 1941; ASTM, 1994) for matric potentials down to -1500 kPa. The water characteristic function depends on texture (Fig. 2.2a) as well as on structure (Fig. 2.2b). Changes in the soil water characteristic can be interpreted as an equivalent change in pore size distribution. This provides an indicator for structural soil deformation (Hillel, 1998, p. 157). Compaction will primarily decrease coarse porosity (matric potential 0 to -6 kPa, equivalent pore diameter $> 5 \times 10^{-5}$ m) while the amount of finer pores (matric potential -6 to -30 kPa, equivalent pore diameter 5×10^{-5}-5×10^{-6} m) may increase due to the collapse of coarser pores.
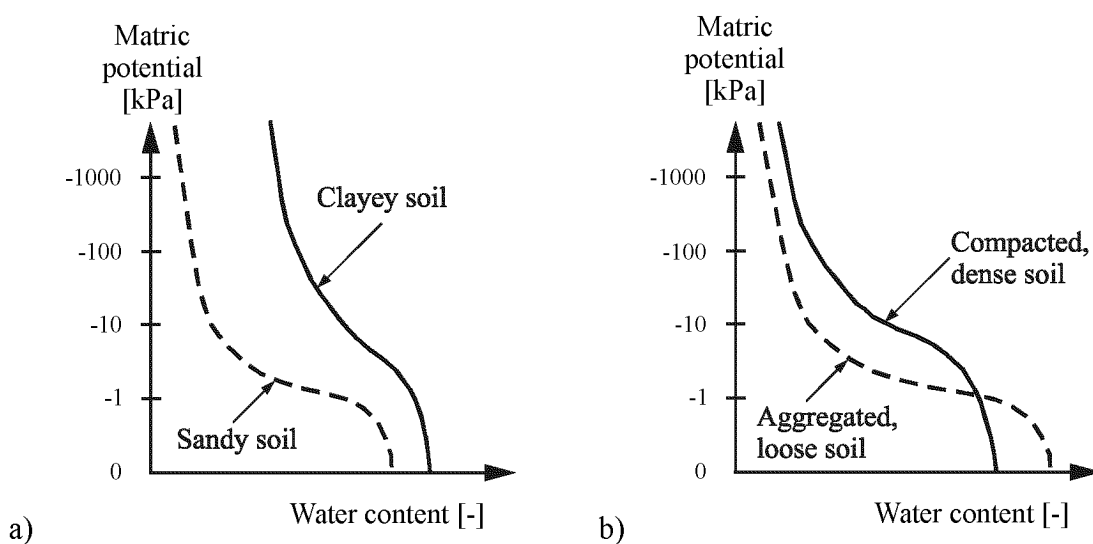
Fig. 2.2. The effect of soil texture (a) and soil structure (b) on the water characteristic function (adapted from Hillel (1998)).

2.4 Soil mechanics

The design of structures made of soil or founded on or in soil is a basic objective in civil engineering work. These structures may not collapse, should experience only moderate soil deformations and should be built with an adequate factor of safety. To solve these design problems in practice, since the mid 18th century (Coulomb, 1776; Rankine, 1857; Terzaghi, 1925) soil mechanics has developed to provide constitutive laws which allow soil deformation and failure states to be predicted as a function of the applied load as well as the soil stiffness and strength (see e.g. Terzaghi and Peck (1967)). In the 1940s, soil mechanics concepts were recognised as potentially valuable for understanding deterioration problems in agricultural soils (Söhne, 1958). As a first step, mainly soil compaction, i.e. the increase of bulk density due to the trafficking of agricultural land with heavy machinery, should be prevented. For that purpose, soil mechanics frameworks like the 'critical state concept', presented by Roscoe et al. (1958) and Schofield and Wroth (1968), could be a suitable way to understand the processes which lead to non-reversible soil compaction. The critical state concept considers that a continuously deformed particulate material will come to a critical state in which further deformation proceeds with no change in stress or volume. Critical state constitutive models describe soil as elasto-plastic material that undergoes changes in bulk density due to applied compressive and shear stresses.

Although very appealing for agricultural soil mechanics (Kurtay and Reece, 1970; Reece, 1977; Hettiaratchi and O'Callaghan, 1980; Koolen and Kuipers, 1983), the applicability of the critical state concept to unsaturated agricultural soils was not obvious (Spoor and Godwin, 1979; Towner, 1983; McKyes, 1986, p. 33) since it was developed for saturated 'engineering' soils (see chapter 2.4.1). However, a number of authors (Greacen, 1960; Bailey and VandenBerg, 1968; Hettiaratchi and O'Callaghan, 1980; Leeson and Campbell, 1983; Hettiaratchi, 1987; Kirby, 1989; Kirby, 1991; Petersen, 1993; Kirby, 1994; Adams and Wulfsohn, 1997; Kirby et al., 1997) successfully applied the critical state concept to unsaturated agricultural soils. Most of them worked with total instead of effective stresses. The total stress approach is simpler and seems more convenient for the usually very complex loading and soil characteristics under wheels and tracks in practice. But it has the disadvantage that it cannot describe properly the influence of water and air pressure on the stress-strain behaviour of the soil. Toll (1990), Alonso et al. (1990) and Wheeler and Sivakumar (1995) presented critical state frameworks for unsaturated soils, introducing water suction as an additional independent stress parameter (chapter 2.4.2).

2.4.1 Critical state soil mechanics for saturated soil

The critical state concept for saturated soils is usually described for triaxial stress conditions (Fig. 2.3) in terms of the mean effective stress p' and the deviator stress q (Britto and Gunn, 1987; Wood, 1990) where

$$p' = \frac{\sigma_1' + \sigma_2' + \sigma_3'}{3} \qquad \text{is the mean effective stress and} \qquad (2.2)$$

$$q = \sigma_1' - \sigma_3' \qquad \text{the deviator stress.} \qquad (2.3)$$

$\sigma_1', \sigma_2', \sigma_3'$ are the effective principal stresses and $\varepsilon_1, \varepsilon_2, \varepsilon_3$ are the corresponding principal strains (see Fig. 2.3). According to Terzaghi (1936), the effective principal stresses $\sigma_1', \sigma_2', \sigma_3'$ are defined as

$$\sigma_1' = \sigma_1 - u_w, \quad \sigma_2' = \sigma_2 - u_w, \quad \sigma_3' = \sigma_3 - u_w \qquad (2.4 \text{ a-c})$$

where $\sigma_1, \sigma_2, \sigma_3$ are the total principal stresses and u_w is the pore water pressure.

A change in effective principal stresses applied to a cylindrical soil sample (Fig. 2.3) leads to changes in volumetric strain (ε_p) and, if $q \neq 0$, to deviator strain (ε_q)

$$\partial \varepsilon_p = \partial \varepsilon_1 + \partial \varepsilon_2 + \partial \varepsilon_3 \qquad (2.5)$$

$$\partial \varepsilon_q = \frac{\left\{ 2 \left[\left(\partial \varepsilon_1 - \partial \varepsilon_2 \right)^2 + \left(\partial \varepsilon_1 - \partial \varepsilon_3 \right)^2 + \left(\partial \varepsilon_2 - \partial \varepsilon_3 \right)^2 \right] \right\}^{0.5}}{3} \qquad (2.6)$$

$\partial \varepsilon_1, \partial \varepsilon_2, \partial \varepsilon_3$ are the total strain increments in the principal stress directions.

$$\varepsilon_1 = \frac{l_{01} - l_1}{l_{01}}, \quad \varepsilon_2 = \frac{l_{02} - l_2}{l_{02}}, \quad \varepsilon_3 = \frac{l_{03} - l_3}{l_{03}},$$
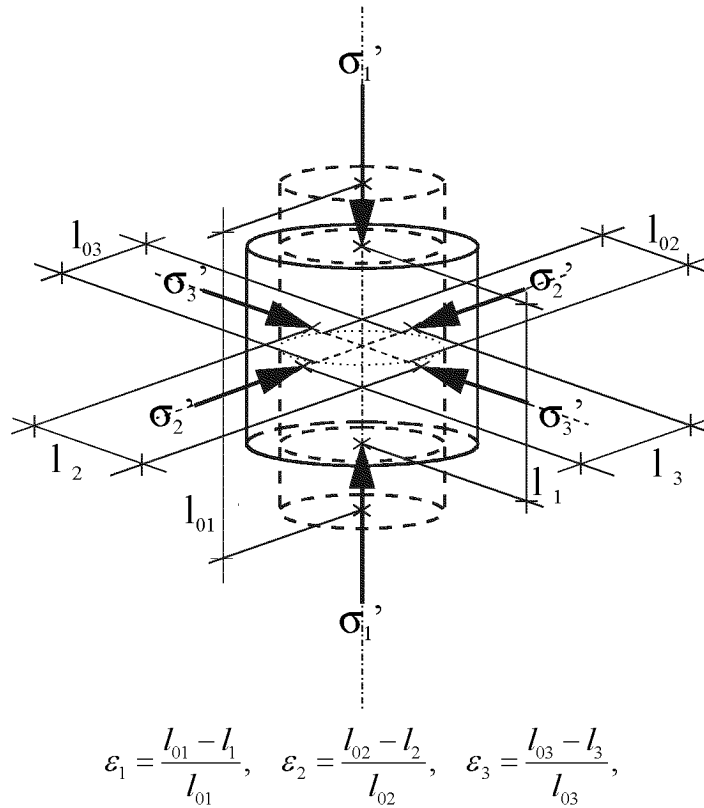
Fig. 2.3.   A cylindrical soil sample under triaxial principal stress conditions.

The volumetric state of a sample during a triaxial test is usually expressed as specific volume $v = 1 + e$. e is the void ratio. The volumetric strain increment $\partial \varepsilon_p$ is related to the specific volume v according to

$$\partial \varepsilon_p = \frac{-\partial v}{v} \tag{2.7}$$

The work input increment per unit volume ∂W of a soil sample under triaxial stress conditions can be defined as

$$\partial W = p' \, \partial \varepsilon_p + q \, \partial \varepsilon_q \tag{2.8}$$

14

The critical state concept can be broadened to incorporate the idea of state boundary or yield surfaces. The critical state is defined by a unique line in deviator stress-mean effective stress-specific volume space. With reference to Fig. 2.4, a soil can exist in a stress state on or within a yield surface in deviator stress-mean effective stress-specific volume space. Within the yield surface, behaviour is assumed to be elastic, and can be described as 'elastic walls' along an unload-reload line.
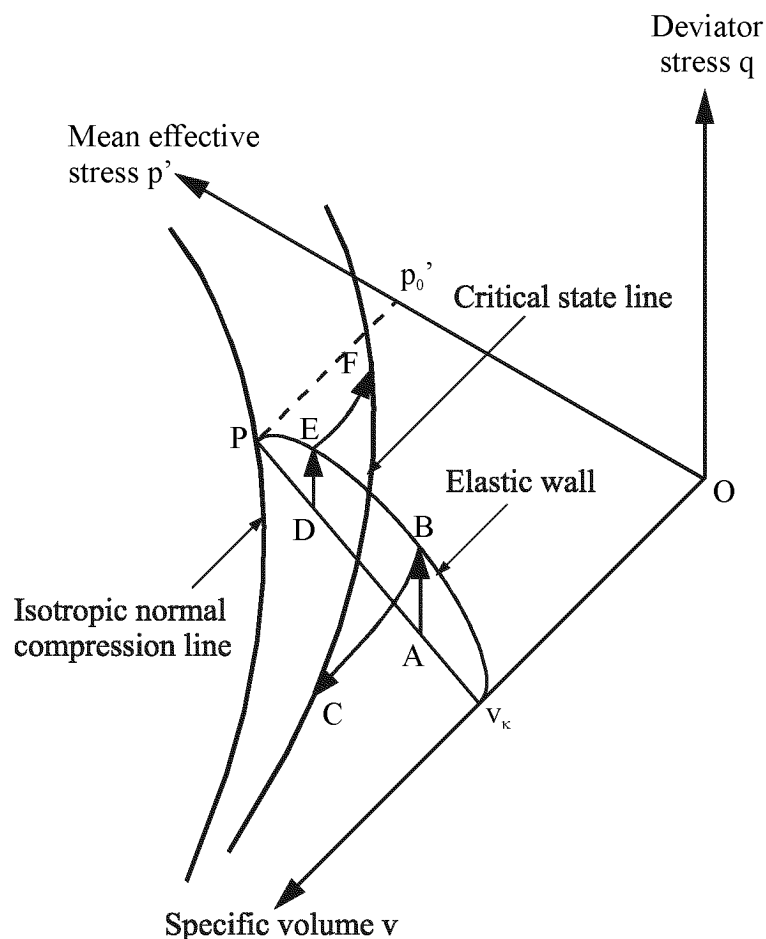
Fig. 2.4.   The critical state line and an elastic wall depicted in the deviator stress-mean effective stress-specific volume space (adapted from Kirby (1989)).

For instance, a sample with a mean effective stress on the isotropic normal consolidation line P (Fig. 2.4) would, on removal of the mean effective stress to 0, experience an increase in volume due to elastic rebound (specific volume = v_κ). The elastic wall is, therefore, not parallel to the mean effective stress axis. The elastic walls increase in size with decreasing specific volume, i.e. the sample is becoming stronger with increasing density. According to Wood (1990, p. 69), the yield surface can be regarded as generalised pre-

compression stress, determined under various mean effective stress and deviator stress conditions. The precompression stress observed in a uniaxial compression test corresponds to just one point on this yield surface.
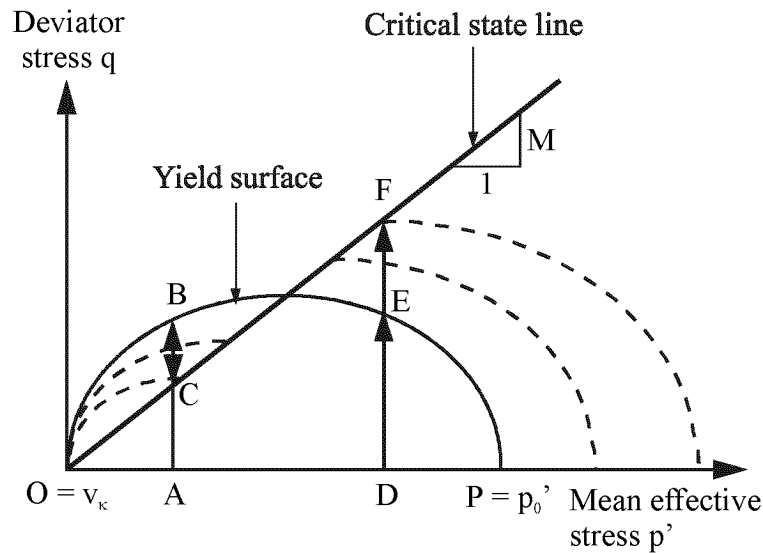
Fig. 2.5.   Projection of an elastic wall onto the deviator stress-mean effective stress plane (adapted from Kirby (1989)).

The locus of critical states in the deviator stress-mean effective stress plane (Fig. 2.5) is described by the critical state line in the p' - q space.

$$q_{cs} = M \ p'_{cs} \qquad (2.9)$$

where q_{cs} is the deviator stress and p'_{cs} is the mean effective stress at the critical state. The slope of the critical state line M under triaxial compression can be calculated with the effective angle of internal friction ϕ' as

$$M = \frac{6 \sin \phi'}{3 - \sin \phi'} \qquad (2.10)$$

Fig. 2.5 shows the projection of an elastic wall onto the deviator stress-mean effective stress plane. The shape of the elastic wall projection in Fig. 2.5 is assumed to be elliptical. This is one possible idealisation of the yield locus/surface of the findings of numerous investigations which was also used for the constitutive model 'Modified Cam Clay' (Roscoe and Burland, 1968).

The elliptical elastic wall can be defined as

$$q^2 = M^2 \left(p' \, p'_o - p'^2 \right) \tag{2.11}$$

with M the slope of the critical state line and p_o' the isotropic precompression stress.

On the yield locus on the left of the critical state line, shearing causes strain-softening and is accompanied by a volume increase. On the yield locus to the right of the critical state line, shearing is strain-hardening and is accompanied by a volume decrease. Shear at constant mean effective stress (stress paths BC and EF) to the original locus defined by P causes the loci to develop as shown in Fig. 2.5, once yielding has began at points B and E, respectively.

Projecting the yield surface onto a specific volume-ln(mean effective stress) plane gives Fig. 2.6.
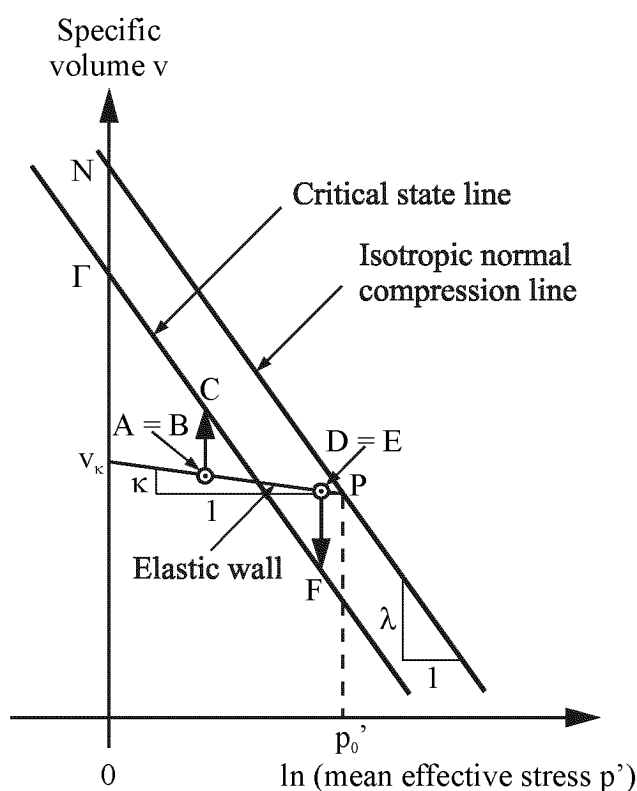
Fig. 2.6. Projection of the critical state line and an elastic wall onto the specific volume-ln(mean effective stress) plane (adapted from Kirby (1989)).

The isotropic normal compression line is that formed by isotropic triaxial compression ($p'=\sigma'_1 = \sigma'_2 = \sigma'_3$, $q = 0$) and can be expressed as

$$v_{iso} = N - \lambda \ln p'_{iso} \qquad (2.12)$$

where $N = v_{iso}\left(p'_{iso} = 1\,kPa\right)$.

In the specific volume-ln(mean effective stress) plane, the critical state line is parallel to the isotropic normal compression line but has a lower specific volume

$$v_{cs} = \Gamma - \lambda \ln p'_{cs} \qquad (2.13)$$

where $\Gamma = v_{cs}\left(p'_{cs} = 1\,kPa\right)$.

An elastic wall projects as an unload/reload-line with a slope κ

$$v = v_\kappa - \kappa \ln p' \qquad (2.14)$$

where $v_\kappa = v\left(p' = 1\,kPa\right)$.

A remoulded soil sample loaded with isotropic stress will travel down the isotropic normal compression line (Fig. 2.6), and upon unloading it will rebound back along the elastic wall. It can be seen that isotropic compression involves both elastic (recoverable) and plastic (irrecoverable) strain. The strain hardening and strain softening behaviour depicted by the stress paths BC and EF in Fig. 2.4 and Fig. 2.5 is shown also in Fig. 2.6. The specific volume decrease (bulk density increase) of the latter, and specific volume increase (bulk density decrease) of the former is readily apparent.

Since critical state soil mechanics considers elastic as well as plastic deformations, volumetric strain $\partial \varepsilon_p$ and deviator strain $\partial \varepsilon_q$ are divided up into an elastic and a plastic part, given by equation (2.15) and (2.16)

$$\partial \varepsilon_p = \delta \varepsilon_p^e + \delta \varepsilon_p^p \qquad (2.15)$$

$$\partial \varepsilon_q = \delta \varepsilon_q^e + \delta \varepsilon_q^p \qquad (2.16)$$

$\partial \varepsilon_p^e$ is the elastic and $\partial \varepsilon_p^p$ the plastic volumetric strain increment, $\partial \varepsilon_q^e$ is the elastic and $\partial \varepsilon_q^p$ the plastic deviator strain increment.

The elastic stress-strain behaviour, i.e. the behaviour inside the yield surface, can be described with the vector equation (2.17) in terms of two of the four (dependent) elastic material properties (Timoshenko and Goodier, 1970). In critical state soil mechanics, the slope of the unload-reload line κ and the effective shear modulus G' are usually used as elastic material properties (Wood, 1990).

$$\begin{bmatrix} \partial \varepsilon_p^e \\ \partial \varepsilon_q^e \end{bmatrix} = \begin{bmatrix} \kappa \left(v\, p' \right)^{-1} & 0 \\ 0 & \left(3\, G' \right)^{-1} \end{bmatrix} \begin{bmatrix} \delta p' \\ \delta q \end{bmatrix} \tag{2.17}$$

Critical state soil mechanics uses a plastic potential approach to describe plastic stress-strain behaviour, i.e. the behaviour on the yield surface of a soil. A plastic potential g can be defined as given in equation (2.18) as a scalar function of the mean effective stress p', the deviator stress q and a factor ζ which controls the size of the potential (Wood, 1990, p. 106).

$$g\,(p',q,\zeta) = 0 \tag{2.18}$$

The plastic strain increments $\partial \varepsilon_p^p$ and $\partial \varepsilon_q^p$ form a mechanism of plastic deformation re-lated to the normal to the plastic potential g at the current effective stress state p'-q so that

$$\partial \varepsilon_p^p = k\,\frac{\partial g}{\partial p'} \tag{2.19}$$

$$\partial \varepsilon_q^p = k\,\frac{\partial g}{\partial q} \tag{2.20}$$

where k is a scalar multiplier, characterising soil hardening.

For the 'Modified Cam Clay' model, normality is assumed, i.e. the plastic potential g and the yield function f, defined by equation (2.21)

$$f = q^2 - M^2 \left(p'\, p'_o - p'^2 \right), \tag{2.21}$$

(see also equation (2.9) for the definition of the elastic wall) coincide and, hence, $g = f$.

The plastic strains $\partial\varepsilon^p$, $\partial\varepsilon_p^p$ and $\partial\varepsilon_q^p$ can be depicted graphically for the 'Modified Cam Clay' model as given in Fig. 2.7.
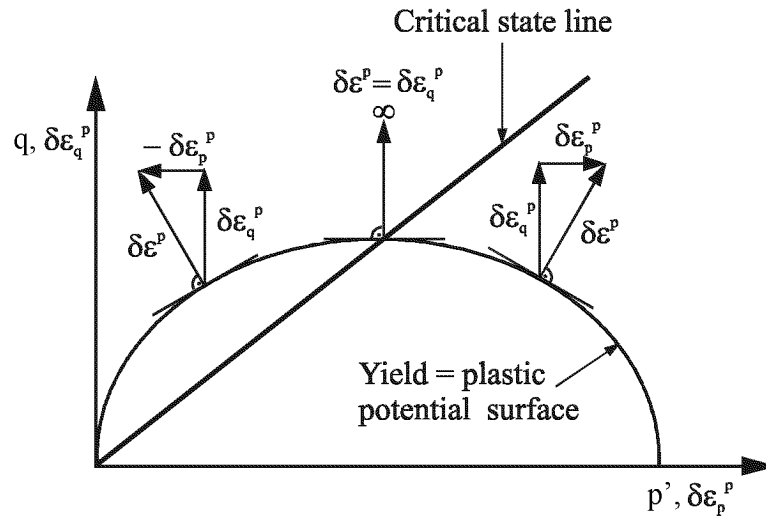
Fig. 2.7.   The plastic strains $\partial\varepsilon^p$, $\partial\varepsilon_p^p$ and $\partial\varepsilon_q^p$ in the p'-q space.

For $\partial\varepsilon_p^p > 0$, compaction and for $\partial\varepsilon_p^p < 0$ dilation (loosening) occurs. For $\partial\varepsilon_p^p = 0$ and $\partial\varepsilon_q^p = \infty$, the soil reaches its critical state which means infinite shear deformation at with no change in stress and volume occurs. This can be expressed mathematically according to Wood (1990, p. 139) with equation (2.22)

$$\frac{\partial p'}{\partial\varepsilon_q} = \frac{\partial q}{\partial\varepsilon_q} = \frac{\partial v}{\partial\varepsilon_q} = 0 \tag{2.22}$$

With equations (2.19) to (2.21), the normality condition and the plastic soil hardening characteristic, given by Wood (1990, p. 94)) as

$$\partial \varepsilon_p^p = \left(\lambda - \kappa\right) \frac{\partial p'_0}{v \, p'_0},$$ (2.23)

the plastic stress-strain behaviour can be described with the vector equation (2.24)

$$\begin{bmatrix} \partial \varepsilon_p^p \\ \partial \varepsilon_q^p \end{bmatrix} = \frac{\left(\lambda - \kappa\right)}{v \, p' \left(M^2 + \eta^2\right)} \begin{bmatrix} M^2 - \eta^2 & 2\,\eta \\ 2\,\eta & 4\,\eta^2 \left(M^2 - \eta^2\right)^{-1} \end{bmatrix} \begin{bmatrix} \delta p' \\ \delta q \end{bmatrix}$$ (2.24)

with $\eta = \dfrac{q}{p'}$,

λ is the slope of the isotropic compression line (equation (2.12) and (2.13)), κ is the slope of the unload-reload line (equation (2.14)), v is the specific volume and M is the slope of the critical state line (equation (2.9)). For the detailed derivation of equations (2.17) and (2.24) refer to Wood (1990, p. 84ff).

2.4.2 Some remarks on critical state soil mechanics for unsaturated soil

Volume change and shear strength of unsaturated soil cannot be related to a single effective stress as shown e.g. by Jennings and Burland (1962). Instead, the total stress σ, pore-air pressure u_a and pore-water pressure u_w must be combined in two independent stress variables, typically chosen as the net stress $\sigma - u_a$ and the water suction $u_a - u_w$ (Bishop and Blight, 1963). Net stress $\sigma - u_a$ and water suction $u_a - u_w$ can be combined to define the effective stress σ' under unsaturated conditions as

$$\sigma' = \sigma - u_a + \chi\left(u_a - u_w\right) \qquad (2.25)$$

as proposed by Bishop (1959), where χ is a function of water content as well as wetting and drying history ($\chi = 1$ for fully water saturated and $\chi = 0$ for dry soil). Toll (1990), Alonso et al. (1990) and Wheeler and Sivakumar (1995) presented critical state frameworks for unsaturated soils. The general idea is to define the effective stress as given in equation (2.25) instead of (2.4a-c). Thus, equation (2.2) changes to

$$p' = \frac{\sigma_1 + \sigma_2 + \sigma_3}{3} - u_a + \chi\left(u_a - u_w\right) \qquad (2.26)$$

while equation (2.3) $q = \sigma_1' - \sigma_3'$ stays the same. Not only the stress state parameter p' but also the specific volume v, the critical state parameter λ, κ and M as well as the precompression stress p_0' become a function of water suction $u_a - u_w$ and pore-air pressure u_a. These considerations are supported by practical experience with unsaturated agricultural and forest soils. Their compression and shear behaviour depends considerably on suction or water content (see chapter 4). Thus the critical state concept for unsaturated soil provides realistic constitutive models to describe stress-strain behaviour of agricultural and forest soils. Unfortunately the determination of stresses and material properties under controlled suction and pore-air pressure conditions is still very difficult.

2.5 References

Adams, B.A. and Wulfsohn, D., 1997. Variation of the critical-state boundaries of an agricultural soil. European Journal of Soil Science, 48: 739-748.

Alonso, E.E., Gens, A. and Josa, A., 1990. A constitutive model for partially saturated soils. Géotechnique, 40(3): 405-430.

ASTM, 1994. Standard test method for capillarity-moisture relationships for coarse- and medium-textured soils by porous-plate apparatus (ASTM D2325-68). Annual Books of ASTM Standards. American Society for Testing an Materials (ASTM), Philadelphia, pp. 195-201.

Bailey, A.C. and VandenBerg, G.E., 1968. Yielding by shear and compaction in unsaturated soils. Transactions of the American Society of Agricultural Engineers, 11(2): 307-311, 317.

Bishop, A.W., 1959. The principle of effective stress. Teknisk Ukeblad, 106(39): 859-863.

Bishop, A.W. and Blight, G.E., 1963. Some aspects of effective stress in saturated and partially saturated soils. Géotechnique, 13(3): 177-197.

Britto, A.M. and Gunn, M.J., 1987. Critical State Soil Mechanics via Finite Elements. Ellis Horwood, Chichester, 488 pp.

Coulomb, C.A., 1776. Essai sur une application des règles des maximis et minimis à quelques problèmes des statique relatifs à l'architecture. Memoires de Mathematique et de Physique, présentés à l' Academie Royal de Science par divers Savans, 7: 343-382.

Greacen, E.L., 1960. Water content and soil strength. Journal of Soil Science, 11(2): 313-333.

Hettiaratchi, D.R.P., 1987. A critical state soil mechanics model for agricultural soils. Soil Use and Manangement, 3(3): 94-105.

Hettiaratchi, D.R.P. and O'Callaghan, J.R., 1980. Mechanical behaviour of agricultural soils. Journal of agricultural Engineering Research, 25: 239-259.

Hillel, D., 1998. Environmental Soil Physics. Academic Press, San Diego, 771 pp.

Jennings, J.E.B. and Burland, J.B., 1962. Limitations of the use of effective stresses in partially saturated soils. Géotechnique, 12(1): 125-144.

Jury, W.A., Gardner, W.R. and Gardner, W.H., 1991. Soil Physics. John Wiley & Sons, New York, 328 pp.

Kirby, J.M., 1989. Measurements of the yield surfaces and critical state of some unsaturated agricultural soils. Journal of Soil Science, 40: 167-182.

Kirby, J.M., 1991. Critical-state soil mechanics parameters and their variation for Vertisols in eastern Australia. Journal of Soil Science, 42: 487-499.

Kirby, J.M., 1994. Simulating soil deformation using a critical-state model: I. Laboratory tests. European Journal of Soil Science, 45: 239-248.

Kirby, J.M., Blunden, B.G. and Trein, C.R., 1997. Simulating soil deformation using a critical-state model: II. Soil compaction beneath tyres and tracks. European Journal of Soil Science, 48: 59-70.

Koolen, A.J. and Kuipers, H., 1983. Agricultural Soil Mechanics. Advanced Series in Agricultural Sciences 13. Springer-Verlag, Berlin, 241 pp.

Kurtay, T. and Reece, A.R., 1970. Plasticity theory and critical state soil mechanics. Journal of Terramechanics, 7(3&4): 23-56.

Leeson, J.J. and Campbell, D.J., 1983. The variation of soil critical state parameters with water content and its relevance to the compaction of two agricultural soils. Journal of Soil Science, 34: 33-44.

McKyes, E., 1986. Soil Cutting and Tillage. Elsevier, Amsterdam, 161 pp.

Petersen, C.T., 1993. The variation of critical-state parameters with water content for two agricultural soils. Journal of Soil Science, 44: 397-410.

Rankine, W.J.M., 1857. On the stability of loose earth. Philosophical Transactions of the Royal Society of London, 147: 9-27.

Reece, A.R., 1977. Soil mechanics of agricultural soils. Soil Science, 123(5): 332-337.

Richards, L.A., 1941. A pressure-membrane extraction apparatus for soil solution. Soil Science, 51: 377-386.

Richards, L.A. and Fireman, M., 1941. A pressure-plate apparatus for measuring moisture sorption and transmission by soils. Soil Science, 56: 395-404.

Roscoe, K.H. and Burland, J.B., 1968. On the generalised stress-strain behaviour of 'wet' clay. In: J. Heyman and F.A. Leckie (Editors). Engineering plasticity. Cambridge University Press, Cambridge, pp. 535-609.

Roscoe, K.H., Schofield, A.N. and Wroth, C.P., 1958. On the yielding of soils. Géotechnique, 8: 22-53.

Schofield, A.N. and Wroth, C.P., 1968. Critical State Soil Mechanics. McGraw-Hill, London, 310 pp.

Söhne, W., 1958. Fundamentals of pressure distribution and soil compaction under tractor tires. Agricultural Engineering, May: 276-291.

Spoor, G. and Godwin, R.J., 1979. Soil deformation and shear strength characteristics of some clay soils at different moisture contents. Journal of Soil Science, 30: 429-436.

SSSA, 1997. Glossary of Soil Science Terms. Soil Science Society of America (SSSA), Madison WI, 138 pp.

Terzaghi, K., 1925. Erdbaumechanik auf bodenphysikalischer Grundlage. Franz Deuticke, Wien, 399 pp.

Terzaghi, K., 1936. The shearing resitstance of saturated soils. 1st International Conference on Soil Mechanics and Foundation Engineering, Harvard University, Cambridge, Massachusetts. pp. 54-56.

Terzaghi, K. and Peck, R.B., 1967. Soil Mechanics in Engineering Practice. John Wiley & Sons, New York, 729 pp.

Timoshenko, S.P. and Goodier, J.N., 1970. Theory of Elasticity. Engineering Society Monograph. MacGraw-Hill, Tokyo, 567 pp.

Toll, D.G., 1990. A framework for unsaturated soil behaviour. Géotechnique, 40(1): 31-44.

Towner, G.D., 1983. Effective stresses in unsaturated soils and their applicability in the theory of critical state soil mechanics. Journal of Soil Science, 34: 429-435.

Wheeler, S.J. and Sivakumar, V., 1995. An elasto-plastic critical state framework for unsaturated soil. Géotechnique, 45(1): 35-53.

Wood, D.M., 1990. Soil Behaviour and Critical State Soil Mechanics. Cambridge University Press, Cambridge, 462 pp.

3

Compaction of agricultural and forest subsoils by tracked heavy construction machinery

M. Berli, B. Kulli, W. Attinger, M. Keller, J. Leuenberger,
H. Flühler, S.M. Springman and R. Schulin
Submitted for Publication in Soil & Tillage Research

Abstract

Precompression stress has been proposed as a criterion for subsoil compression sensitivity in regulations, limiting mechanical loads by vehicles, trafficking on agricultural and forest soils. In this study we investigated the applicability of this criterion to the field situation in the case of tracked heavy construction machinery. 'Wet' and 'dry' test plots at three different test sites along an overland gas pipeline construction site were experimentally trafficked with heavy tracked machines used for the construction work. The comparison of samples taken from beneath the tracks with samples taken from non-trafficked areas beside the tracks showed that no significant increase in precompression stress occurred in the subsoil. Comparing calculated vertical stress with precompression stress in the subsoil, only little compaction effects could have been expected. Precompression stress was determined by the Casagrande procedure from confined uniaxial compression tests carried out in the laboratory on undisturbed samples at -6 kPa initial soil water potential. Dye tracer experiments showed little differences between water flow patterns of trafficked and non-trafficked subsoils, in agreement with the results of the precompression stress, bulk density and macroporosity measurements. The results indicate that the existing precompression stress may be a suitable criterion to define the maximum allowable stress in the contact area of a rigid track in order to protect agricultural and forest subsoils against compaction.

3.1 Introduction

Compaction has been recognised as a major threat to soil fertility of large areas of culti-vated land. It is estimated to be responsible for the degradation of an area of $6.8 \times 10^4 \, \text{km}^2$ world-wide, of which $3.3 \times 10^4 \, \text{km}^2$ is located in Europe (Oldeman et al., 1991), adversely affecting crop production as well as environmental quality (Soane and Van Ouwerkerk, 1995). Compaction of subsoils is regarded as particularly problematic because of its per-sistence and the difficulty to remediate it. Natural regeneration can result from activity of soil fauna and flora (von Albertini et al., 1995) as well as from abiotic processes such as drought and frost induced shrinkage. Research reviewed by Håkansson and Reeder (1994) showed that the effectiveness of these processes, however, decrease rapidly with depth beneath the main root zone of the topsoil. Artificial loosening by deep ploughing, on the other hand, may aggravate rather than solve problems. For example Kooistra et al. (1984) reported that secondary soil compaction was even worse than the first compac-tion because subsoil structure had been disrupted and weakened by the loosening opera-tion. Neilsen et al. (1990) found that reduced crop yields due to subsoil compaction were only partially compensated by fertiliser treatment.

The review by Håkansson and Reeder (1994) shows that the risk of subsoil compaction may be considerable for soils with high moisture content under vehicles with high axle loads. Other important factors, apart from axle load and moisture content, are tyre di-mensions, contact stresses, number of passes, soil strength and stress history (Hadas, 1994). While many studies investigated soil compaction caused by wheeled traffic, only a few publications deal with the extent of (sub-)soil compaction in agricultural land due to tracked heavy construction machinery. McKyes (1980) found an increase in bulk density down to 0.3 m depth and a slight decrease in crop yield one year after construction of high voltage transmission lines in Canada. Culley et al. (1982) found that porosity and hydraulic conductivity were reduced and bulk density and penetration resistance were in-creased down to 0.3 m depth in a medium-to-fine grained soil, affected by oil pipeline construction in Ontario, Canada. Moreover, yields of corn, soybeans and cereals were depressed for up to 10 years after the installation of the oil pipeline (Culley and Dow, 1988). Dumbeck (1984) carried out traffic experiments on arable land in Germany with heavy excavators (weighing up to 4.7×10^4 kg, mean stress in the contact area up to 100 kPa) under 'dry' (-30 to -100 kPa soil water potential) and 'wet' ($\approx$ -6 kPa soil water potential) soil conditions. He found a decrease in the amount of macropores down to 0.65 m in the 'dry' and 1 m in the 'wet' soil. Håkansson (personal communication) found a decrease in crop yield of about 35% in the first year and about 5 % from the

third to the fifth year on agricultural land trafficked by machines in the course of gas pipeline construction in Sweden.

In Switzerland, subsoil compaction has raised particular concern because of the use of agricultural land as temporary access way for heavy machinery required in construction work. Apart from road and railway line construction, the construction of overland gas pipelines has become a topical issue in this respect. Tracked vehicles weighing more than 3×10^4 kg are routinely used in this construction work. Even machines weighing more than 6×10^4 kg have been used. In a first study, von Rohr (1996) found changes in bulk density, porosity and pore size distribution down to 0.65 m depth of a soil trafficked with tracked pipeline construction machines weighing up to 3.3×10^4 kg (mean normal stress in the contact area: 73 kPa). While due to the relatively large contact area, the mean normal stress in the contact area is smaller than of some agricultural machines, however the stress reaches deeper into the soil. This was already reported by Söhne (1953; 1958) applying the theory of Boussinesq (1885) and Fröhlich (1934) on traffic induced stress propagation in agricultural soils.

The limited reversibility of subsoil compaction calls for measures to prevent it. That is to avoid stresses exceeding the soil's range of elastic behaviour and thus leading to plastic deformation. Horn (1981; 1988), Horn and Lebert (1994) and Kirby (1991b) proposed to use the precompression stress as a limiting criterion. According to this concept, reloading a soil at a given moisture status up to a stress which it had previously experienced will cause only elastic (i.e. reversible) and no plastic (i.e. non-reversible) compression (e.g. Terzaghi and Peck, 1948 p. 106f). This concept appears to be particularly appropriate for application in setting tolerance limits for the use of tracked construction machinery on agricultural land. These machines drive slowly and exert compression stresses primarily through their weight, which is supported by a rather large contact area compared to wheeled machines. Consequently, precompression stresses determined under static stress conditions, as they occur in confined uniaxial compression tests, were assumed to represent critical stresses under the tracks of such construction machines adequately enough for practical purposes.

While the precompression stress concept is theoretically very appealing, only few investigations have been performed to test its suitability to access soil compaction sensitivity under field conditions (Culley and Larson, 1987; Hammel, 1993; Blunden et al., 1994; Gysi et al., 1999). For example, differences in drainage conditions between field and laboratory experiments were considered as potentially limiting to the validity of laboratory determined precompression stresses. Furthermore, laboratory tests on intact samples cannot reproduce stress conditions of the undisturbed soil under field conditions

exactly as it is not possible to reproduce the field boundary conditions in any detail. Oedometer tests e.g. subjecting a sample to uniaxial compression with lateral extension confined by a steel cylinder, offers different boundary conditions of strain to those experienced by undisturbed soil in the field, which is loaded by a tracked vehicle. Also precompression stress is usually not evident as a sharp bend in the stress-volumetric strain curve but rather an operationally defined point in an often rather gradual transition between recompression curve and virgin compression line, indicating that there is no abrupt change from purely elastic to plastic compression. In addition, precompression stress has to be as sensitive to changes of compactness as bulk density and pore size distribution, and additionally easy to determine under practical conditions.

While the mechanics of water saturated 'engineering' soils (Atkinson and Bransby, 1978 p. 2) has been extensively investigated, much less is known about the more complicated mechanical behaviour of unsaturated agricultural soils, in which structure is predominantly influenced by biological factors, i.e. the activity of organisms and their organic residues. Given these uncertainties about the feasibility of precompression stresses, the validity of this criterion in predicting subsoil compressibility under tracked heavy construction machinery and field conditions has to be demonstrated unequivocally.

To test the applicability of precompression stress as a criterion for susceptibility to compaction under 'real world' conditions, field traffic experiments were performed with tracked machinery in the course of pipeline construction work. For this purpose, wetted and non-wetted test plots of three different soils along the construction site were trafficked under controlled conditions. Precompression stress, bulk density, coarse- and coarse-to-intermediate porosity of samples taken from trafficked soil beneath tracks were compared to reference measurements of non-trafficked soil. In addition, dye tracer experiments were carried out in order to compare the flow patterns of water in the trafficked and non-trafficked subsoils. We expected precompression stress, bulk density and coarse-to-intermediate porosity to increase, coarse porosity to decrease and flow pathways to disappear if the predicted stress in the soil below the tracks exceeded the precompression stress.

3.2 Material and methods

The traffic experiments were performed in autumn 1996 and spring 1997 on the three different sites 'Freienstein', 'Güllenhau' and 'Ruckfeld', which were situated along the gas pipeline TRAWO, running from Zuzgen to Winterthur/Ohringen in northern Switzerland. Soil properties at the three test sites are given in Table 3.1.

Table 3.1.   Soil parameters at the three test sites Freienstein, Güllenhau and Ruckfeld

Site	Depth [m]	Silt[†] [kg kg^{-1}]	Clay[†] [kg kg^{-1}]	Gravel [m^3 m^{-3}]	Organic matter[‡] [kg kg^{-1}]	Bulk density [kg m^{-3}]
Freienstein	0.07–0.17	0.31	0.25	2	0.028	1510
	0.27–0.37	0.34	0.24	< 1	0.012	1620
	0.47–0.57	0.34	0.25	< 1	0.011	1590
	0.67–0.77	0.43	0.32	< 1	0.013	1510
Güllenhau	0.07–0.17	0.52	0.17	8	0.044	1130
	0.27–0.37	0.51	0.20	8	0.010	1330
	0.47–0.57	0.48	0.19	12	0.007	1530
Ruckfeld 'wet' plot	0.07–0.17	0.55	0.14	< 0.01	0.033	1310
	0.27–0.37	0.60	0.12	< 0.01	0.011	1570
	0.47–0.57	0.57	0.17	< 0.01	0.011	1510
	0.67–0.77	0.57	0.18	< 0.01	0.010	1520
Ruckfeld 'dry' plot	0.07–0.17	0.57	0.16	< 0.01	0.031	1360
	0.27–0.37	0.55	0.16	< 0.01	0.025	1530
	0.47–0.57	0.58	0.16	< 0.01	0.015	1540
	0.67–0.77	0.56	0.17	< 0.01	0.012	1610

[†]   Determined with the pipette method

[‡]   Measured as weight loss after oxidation by H_2O_2.

Soil types according to FAO (1990) were an Eutric Cambisol at Freienstein, a Dystric Cambisol at Güllenhau and a Haplic Luvisol at Ruckfeld. The Freienstein and Ruckfeld site were under crop rotation and used as grassland in the year of the experiment. The Güllenhau site was situated in a pine forest.
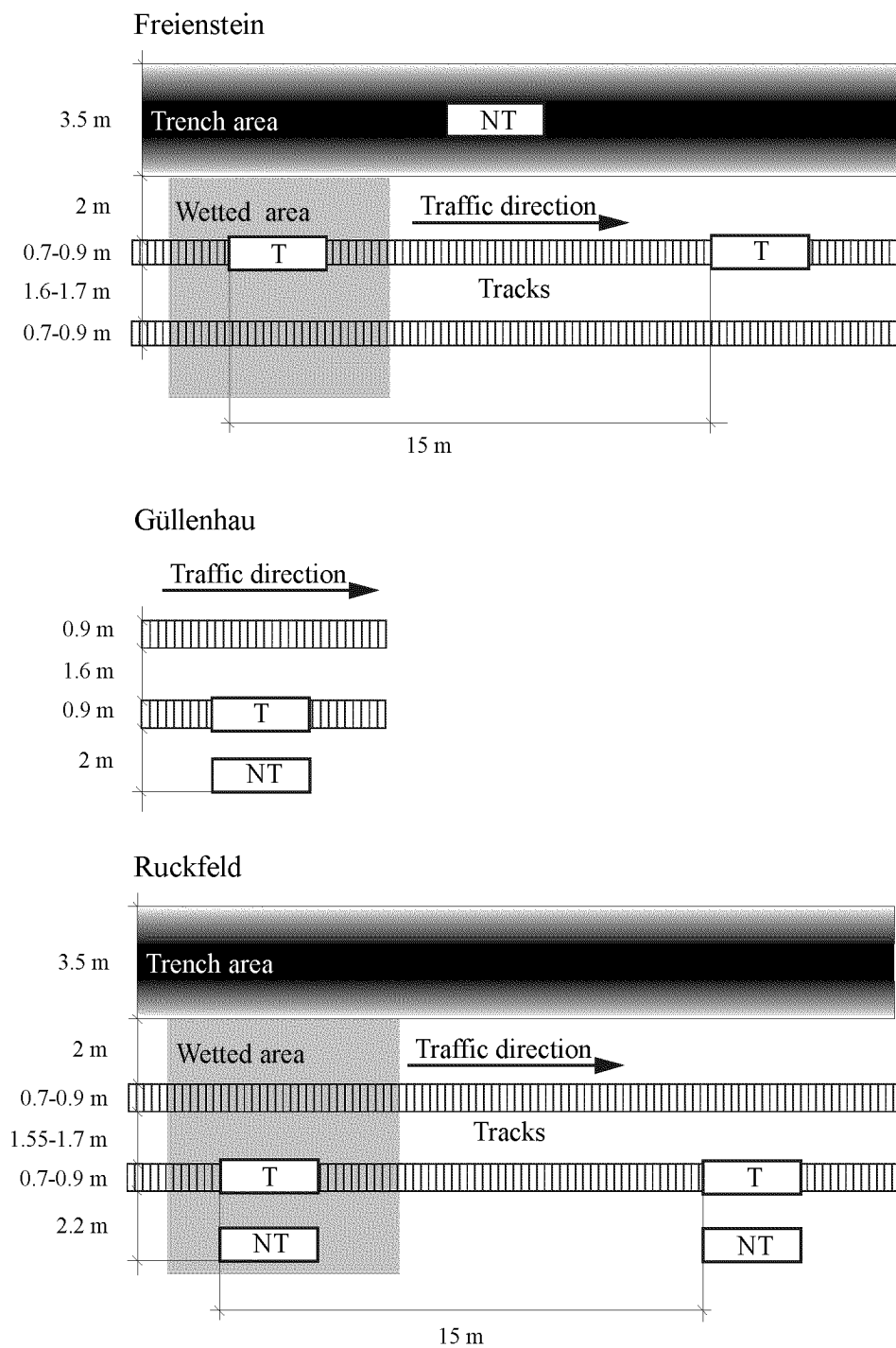
Freienstein

Güllenhau

Ruckfeld

Fig. 3.1.   Situation of the test plots at the three experimental sites with sampling and sprinkling areas: NT non-trafficked, T trafficked.

The situation of the experiments at the three sites is depicted in Fig. 3.1. The experimental trafficking was part of the pipeline construction process, i.e. under 'real-world' conditions.

At Freienstein and Ruckfeld, test plots were wetted prior to trafficking by sprinkling for one day at a rate of 0.1 m d^{-1} at Freienstein and five days at a precipitation rate of 0.1 m d^{-1} at Ruckfeld. Thereafter, the soil was left to redistribute the infiltrated water for one more day. At the forest site of Güllenhau, space allowed only for one trafficked plot. Due to the weather conditions during the experiment, this site was relatively wet. In order to assess compaction effects from all test plots, samples were taken from non-trafficked areas beside the tracks.

Table 3.2.　　Characteristics of the machinery used in the experiments

Machine type	Net machine weight [kg]	Length of the contact area [m]	Width of the contact area (twice track width) [m]	Net mean normal stress in the contact area [kPa]
Fiat FH 300	3.02×10^4	4.0	1.8	42
Fiat Allis PL 40 C	2.56×10^4	3.5	1.4	51
Cat 583	3.8×10^4	3.2	1.5	78

For the traffic experiment, three different types of construction machines were used, as given in Table 3.2. The machinery used in the experiments were Fiat FH 300 excavators and Fiat Allis PL 40 C as well as Cat 583 sidebooms, specially constructed for placing large diameter pipes into trenches. The machines were driving directly on the soil surface without a protecting layer put on top of it. Table 3.3 gives the sequence, duration and mean normal stress in the contact area performed by these machines in the three experiments.

Table 3.3.   Test sequence for the three test sites

Machinery used	'Wet' plot		'Dry' plot	
	Load duration [s]	Mean normal stress in the contact area [kPa]	Load duration [s]	Mean normal stress in the contact area [kPa]
Freienstein				
1st Fiat FH 300	20	42	20	42
1st Fiat Allis PL 40C	20	51	20	51
2nd Fiat Allis PL 40C	20	51	20	51
3rd Fiat Allis PL 40C	20	51	920	86[†]
2nd Fiat FH 300	920	72[†]	920	72[†]
Güllenhau				
Fiat FH 300	40	42	-	-
Ruckfeld				
1st Fiat FH 300	140	42	140	42
Fiat Allis PL 40C	140	51	140	51
Cat 583	140	78	140	78
2nd Fiat FH 300	140	42	140	42

[†] Normal stress under the trench closest track during the placement of pipe.

At the Freienstein site, a Fiat FH 300 followed by three Fiat Allis PL 40 C and a second Fiat FH 300 trafficked slowly over the two plots at a velocity of 0.1-0.2 m s^{-1}. The second Fiat FH 300 stayed for 900 s on each plot while placing the pipe in the trench. The third Fiat Allis PL 40 C stayed for 900 s on the 'dry' plot holding up the pipe. Holding up and placing the pipe leads to an additional load of 4×10^3 kg per excavator or sideboom and increases the mean normal stress in the contact area of the trench closest track up to 72 kPa for the Fiat FH 300 and to 86 kPa for the Fiat Allis PL 40 C.

At Güllenhau, only a Fiat FH 300 was available which trafficked the plot once forward and backward with a velocity of 0.1-0.2 m s^{-1}. The machine did not perform any other working action and also did not carry any additional load during the experiment.

In the experiment at Ruckfeld a Fiat FH 300 was followed by a Fiat Allis PL 40 C, a Cat 583 and a second Fiat FH 300. These machines drove at a velocity of 0.1-0.2 m s^{-1},

stopping on each of the plots for 120 s. Again the machines did not perform any working action and also carried no additional load during the experimental passages.

'Wet' and 'dry' conditions varied considerably between the three sites and between depths as shown by the tensiometer readings taken immediately before the passage of the machines (Table 3.4). In the subsoil of Güllenhau and the wetted plots at the other two sites, water potential was around -7 kPa or higher, while in the subsoils of the non-wetted plots of Freienstein and Ruckfeld they were around -15 kPa or lower down to 0.55 m depth. Below that depth, the subsoils showed the same water potential of around -6 to -7 kPa in both plots at Freienstein, whereas the same difference as in the upper subsoil was also found at 0.7-0.75 m depth at Ruckfeld.

Table 3.4.   Soil water potential of the three test sites at different depths immediately before the passage of the machines

Site	Test plot	Soil water potential [kPa]			
		0.1-0.15 m depth	0.3-0.35 m depth	0.5-0.55 m depth	0.7-0.75 m depth
Freienstein	'dry'	-70.1	-48.3	-14.7	-5.7
	'wet'	-17.3	-6.7	-5.5	-7.2
Güllenhau	'wet'	-3.9	-4.2	-1.7	-0.7
Ruckfeld	'dry'	<-85.0	-85.0	-33.4	-16.3
	'wet'	-5.2	-2.7	-0.7	-0.2

To measure the stress distribution under the vehicle tracks, four Bolling probes (Bolling, 1987) were placed in the centreline of the track at a depth of 0.32 m in the 'wet' test plot at Ruckfeld. Pressure readings were taken electronically every 2 s. In order to compare measurements of different Bolling probes, pressure values were expressed as relative pressure i.e. pressure readings, taken as a function of time, divided by the mean of the pressure readings over the measured time interval.

After trafficking, soil profiles were opened across the plots at right angles to the direction of the passage and soil cores were sampled using sharpened thin-walled metal cylinders. Size and number of the samples used for the determination of precompression stress, bulk density, coarse- and coarse-to-intermediate porosity are given in Table 3.5.

Table 3.5.   Size (D/H: diameter/height) and number of samples of the three test sites

Site	Precompression stress		Bulk density		Coarse porosity		Coarse-to-intermediate porosity	
	D/H [m/m]	No.	D/H [m/m]	No.	D/H [m/m]	No.	D/H [m/m]	No.
Freienstein								
topsoil	0.1/ 0.06	16	0.1/ 0.06	16	0.1/ 0.06	16	-	-
subsoil	0.108/ 0.11	4-6	0.108/ 0.11	4-6	0.05/ 0.02	8	0.05/ 0.02	8
Güllenhau								
topsoil	0.108/ 0.11	8	0.108/ 0.11	8	0.108/ 0.11	3	-	-
subsoil	0.108/ 0.11	8	0.108/ 0.11	8	0.108/ 0.11	3	-	-
Ruckfeld								
topsoil	0.108/ 0.11	6	0.108/ 0.11	6	-	-	-	-
subsoil	0.108/ 0.11	6	0.108/ 0.11	6	0.05/ 0.02	8	0.05/ 0.02	8

Given the asymmetric loading situation at the Freienstein site, trafficked soil was sampled only beneath the track adjacent to the trench. Non-trafficked soil samples were also taken from the trench area between the 'wet' and 'dry' trafficked plot before the traffic experiment took place. At Güllenhau and Ruckfeld trafficked soil beneath the track most removed (distant) from the trench was sampled. Non-trafficked soil samples were taken 2 m at right angles from the centreline of the track farest the trench, in order to avoid influence of the load but also to be as close as possible to minimise the influence of spatial

heterogeneity (see Fig. 3.1). It was not possible to take undisturbed soil cores at Güllenhau beneath 0.4 m depth due to the high gravel content.

For the dye tracer experiment, test plots of 'wet' and 'dry' trafficked and non-trafficked soil were chosen adjacent to the sampling areas of the three test sites. The dye 'Brillant Blue FCF' (Flury and Flühler, 1995) was dissolved in water (4 kg m^{-3}) and sprinkled by a constant rate of 5 mm h^{-1} during 8 h on an area of 1.5 by 1.5 m using the apparatus described by Flury et al. (1994). The sprinkling rate was kept so low in order to avoid dye ponding on the soil surface. For the Freienstein and Güllenhau soil 0.09 m^3 and for the Ruckfeld soil 0.225 m^3 of dye tracer were applied on each test plot. At Freienstein, the topsoil was removed first and then the dye was applied directly on the subsoil surface in 0.2 m depth. At Güllenhau, the dye was applied on the undisturbed topsoil. At Ruckfeld, the topsoil was loosened manually down to 0.3 m depth in order to create similar surface conditions for the application of the tracer on trafficked and non-trafficked soil. One day after sprinkling, a 1.5 m deep trench was dug with the face perpendicular to the border of the sprinkled area. For the trafficked plots, the trench centreline was aligned with the centreline of the track. Between 3 and 10 vertical profiles of 1 by 1 m (0.1 m horizontal distance between the profiles) were prepared at the trench face, exposing the infiltrated dye. Each profile was photographed with a 35-mm camera. The pictures were digitalised, their geometrical distortion and illumination were corrected and the colours adjusted in order to distinguish the dye in the flow paths from the surrounding soil (Forrer et al., 2000). In order to obtain the flow pattern of the whole test plot we laid the resulting 'maps' of the flow paths of each profile on top of each other.

Precompression stress was determined from confined uniaxial compression tests. Prior to the compression test, the samples were conditioned to an initial soil water potential of -6 kPa (values with respect to the sample's centre) by applying a hanging water column. Samples were kept within the coring cylinders which were built into the compression cell and subsequently subjected to stepwise increased stress. Stresses from a range of 8 to 2000 kPa were applied through a piston, which fitted the inner diameter of the cylinders. Each compression step lasted for 1800 s after which the stress was increased to the next level. This stress duration was assumed to represent the duration a machine stays at the same place during normal construction work. Precompression stress was determined from the resulting stress-strain curves using the graphical procedure of Casagrande (1936). After the oedometer test, the samples were dried at 105 °C for at least 24 hours and weighed to determine the dry bulk density.

For the subsoil from Freienstein and Ruckfeld, coarse- (equivalent pore diameter > 5×10^{-5} m) and coarse-to-intermediate (equivalent pore diameter 5×10^{-5}-5×10^{-6} m) porosity was determined using 4×10^{-5} m^3 core samples with a pressure cell apparatus (Richards, 1941; Richards and Fireman, 1941). Because of the higher gravel content, samples to determine coarse porosity taken from Freienstein topsoil and Güllenhau top- and subsoil were larger i.e. of 4.73×10^{-4} m^3 and 10^{-3} m^3 volume, respectively. After saturation, the samples were drained by applying a 0.6 m hanging water column. The drained volume fraction was interpreted as representing the coarse porosity of the sample at -6 kPa soil water potential.

3.3 Results

The comparison of the samples from trafficked and non-trafficked parts of the plots (Fig. 3.2, 3.5 and 3.8) indicates that precompression stress was significantly (P < 0.05) increased by trafficking only in the wetted topsoil of the Ruckfeld site.
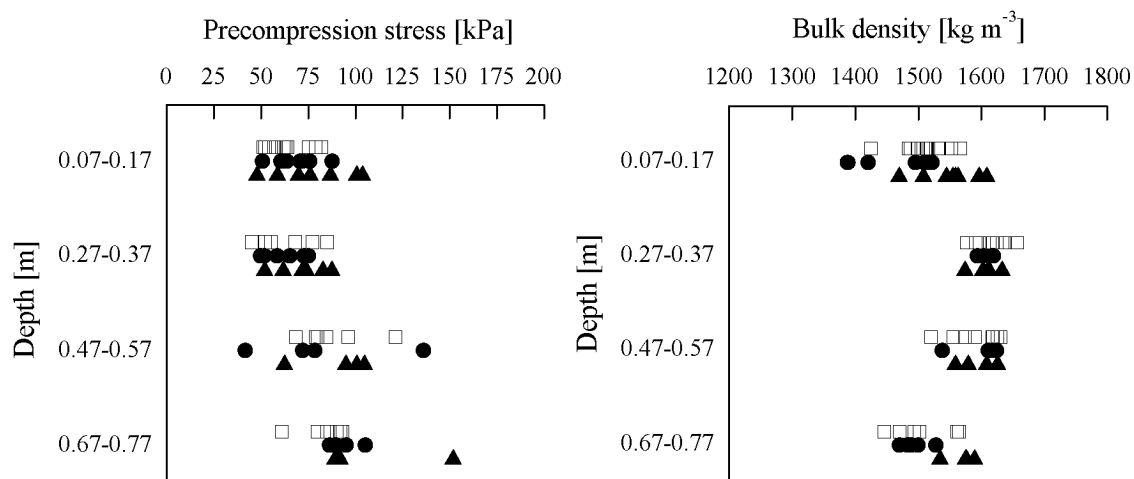

Fig. 3.2. Precompression stress (left) and bulk density (right) of the non-trafficked (□), 'wet'-trafficked (●) and 'dry'-trafficked (▲) Freienstein soil.
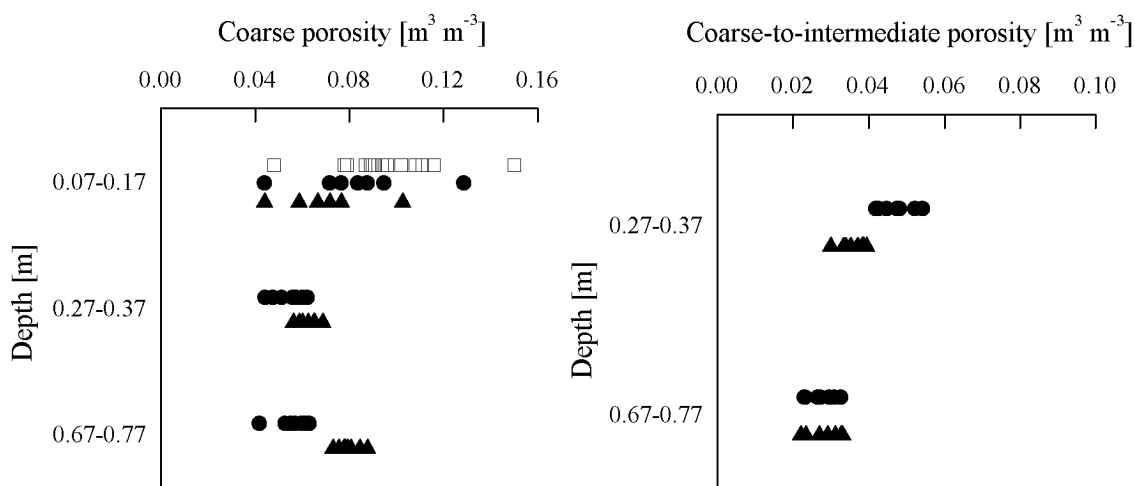

Fig. 3.3. Coarse porosity (left) and coarse-to-intermediate porosity (right) of the non-trafficked (□), 'wet'-trafficked (●) and the 'dry'-trafficked (▲) Freienstein soil.
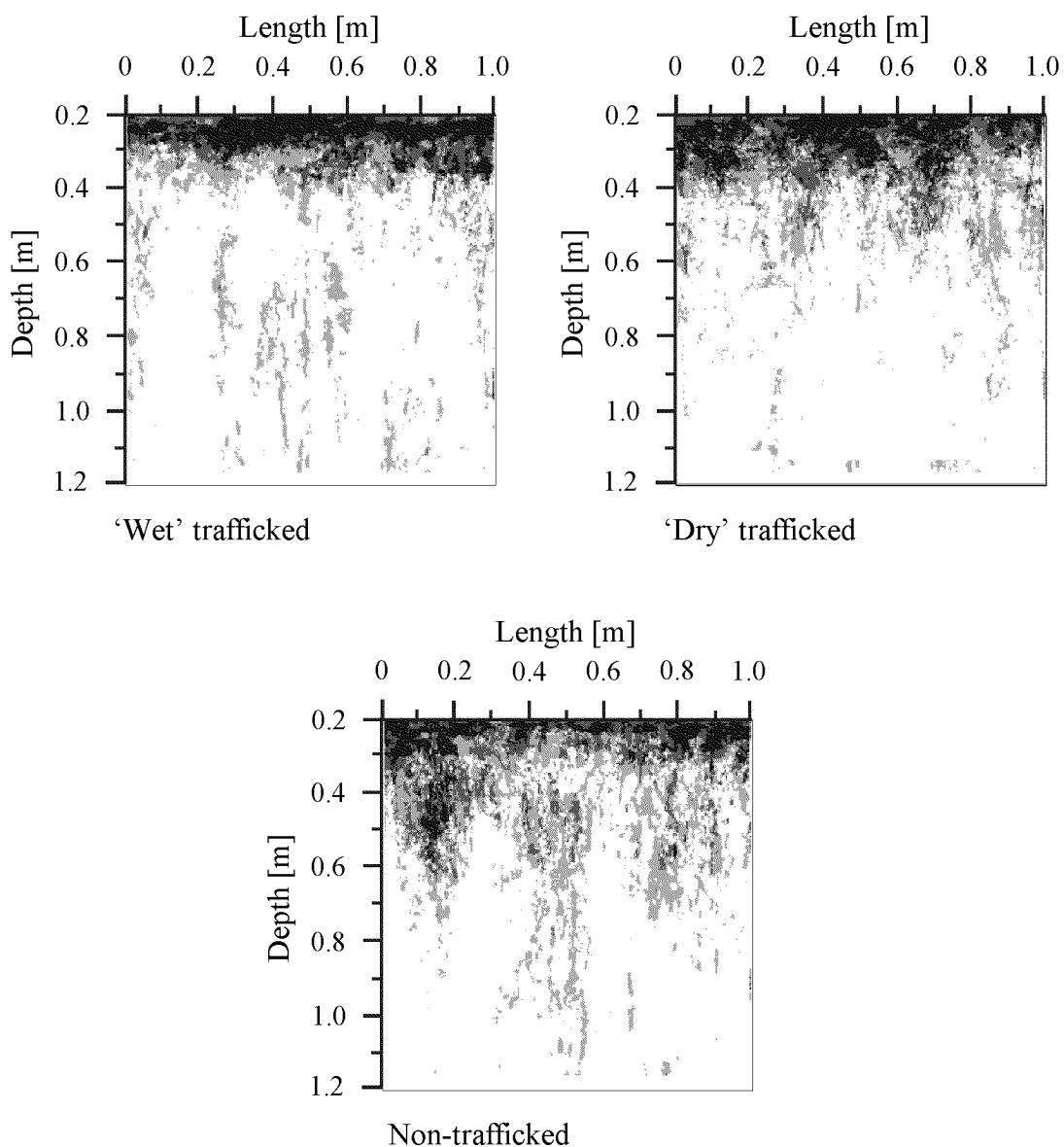
Fig. 3.4. Flow pattern of dye tracer in the 'wet', 'dry' and non-trafficked Freienstein soil.

At Freienstein the subsoil samples of 0.67-0.77 m depth, at Güllenhau the topsoil and subsoil samples (0.07-0.17 m and 0.27-0.37 m depth) and at Ruckfeld the samples of the 'dry' subsoil (0.47-0.57 m depth) from the trafficked plot tended to have higher precompression stresses than the samples from the non-trafficked plot. However, these differences were not significant (P < 0.05).
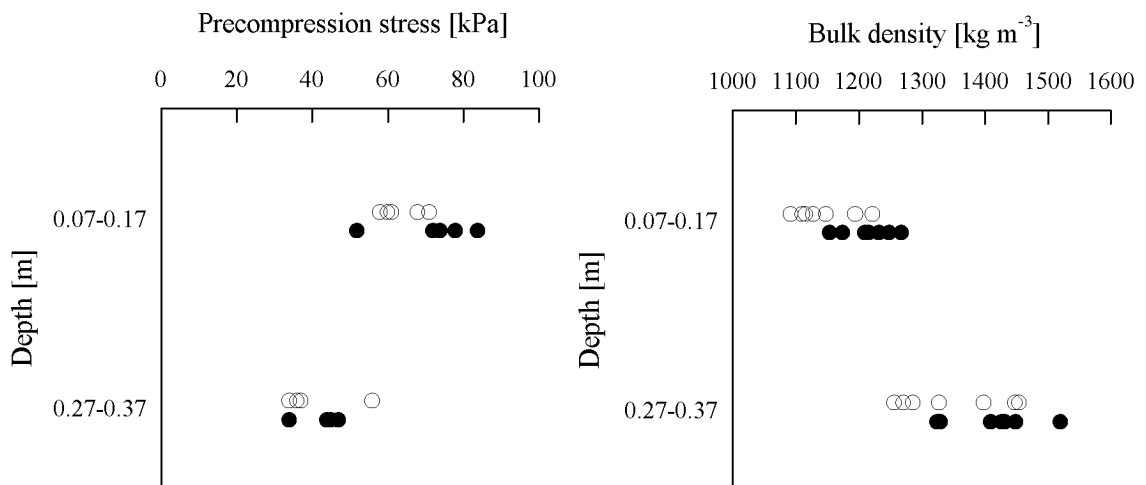
Fig. 3.5. Precompression stress (left) and bulk density (right) of the trafficked (●) and the non-trafficked (○) Güllenhau soil.
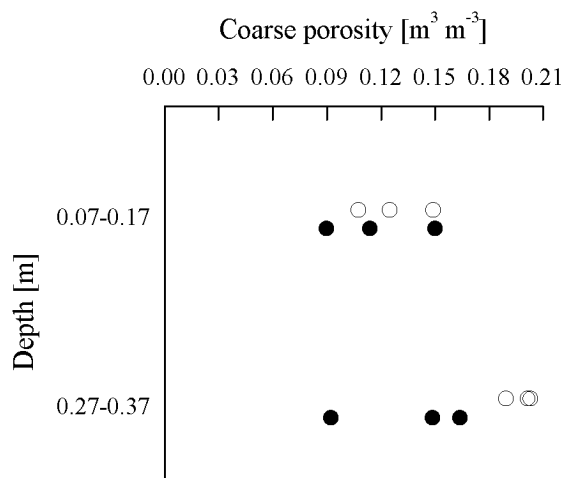

Fig. 3.6. Coarse porosity of the trafficked (●) and non-trafficked (○) Güllenhau soil.

Statistically significant differences in bulk density between trafficked and non-trafficked soil were found at Freienstein in 0.07-0.17 m and 0.67-0.77 m depth of the 'dry' plot, in the topsoil of Güllenhau and in the wetted plot of Ruckfeld in 0.07-0.17 and 0.47-0.57 m depth. In 0.27-0.37 m depth at Güllenhau, bulk densities tended to be higher in the trafficked than in the non-trafficked plot. The increased bulk density in the topsoil of the 'wet' Ruckfeld plot and the absence of a similar increase in the 'dry' plot agree with the corresponding effects on precompression stress.
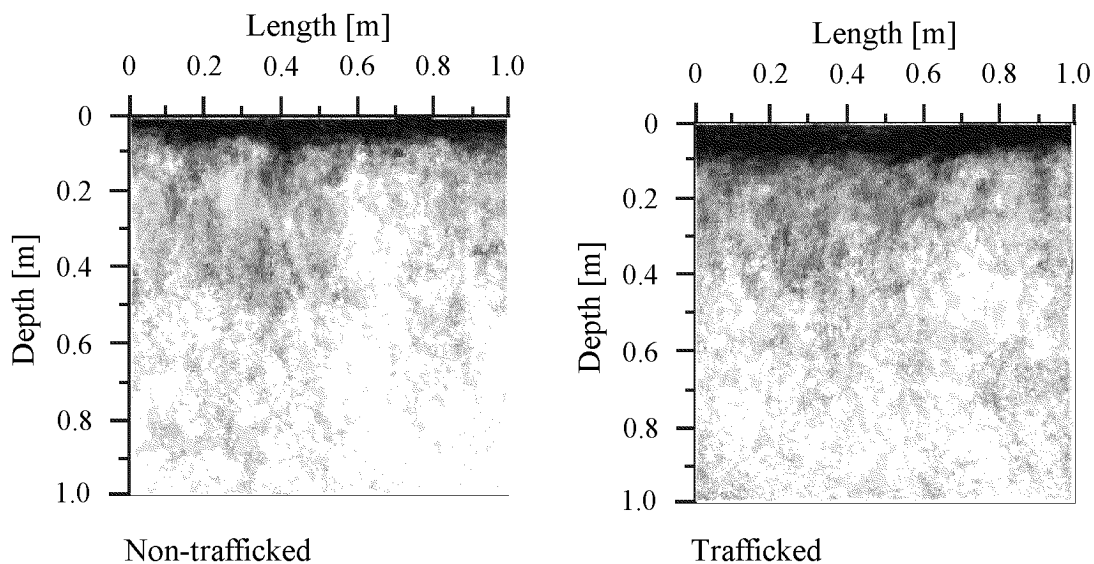
41

Fig. 3.7.   Flow pattern of dye tracer in the trafficked and non-trafficked Güllenhau soil.

At Freienstein, we found significantly (P < 0.05) decreased coarse porosity in the 'dry' trafficked compared with the non-trafficked topsoil (0.07-0.17 m) and higher coarse porosity values in the 'dry' compared with the 'wet' trafficked subsoil (0.27-0.37 and 0.67-0.77 m depth). Also at Güllenhau, coarse porosity was significantly lower in the trafficked than the non-trafficked subsoil (0.27-0.37 m). In contrast, coarse-to-intermediate porosity was significantly higher (P < 0.05) in the 'wet' than in the 'dry' trafficked subsoil (0.27-0.37 m) at Freienstein and higher in the 'dry' trafficked than in the non-trafficked subsoil (0.27-0.37 m) at Ruckfeld. No significant effects on coarse porosity were found, however, in the topsoil at Güllenhau and in the 'wet' plot at Freienstein. It may therefore be questioned whether the before mentioned differences in the subsoil of Güllenhau and the 'dry' plot of Freienstein were caused by trafficking or rather represented pre-existing differences between the plots. A comparison between the non-trafficked reference plots at Ruckfeld shows that such differences must be taken into account (Fig. 3.8). The absence of effects on the precompression stress in these cases also suggests such an interpretation of the apparent inconsistency of porosity and density effects in this pattern.

Further support derives from the analysis of the flow patterns. We found less flow paths in 0.4-0.6 m depth of the 'wet' trafficked and below 0.6 m of the 'dry' trafficked Freienstein subsoil compared with the flow pattern of the non-trafficked soil. Neither in the Güllenhau nor in the Ruckfeld subsoil we did observe differences in flow patterns between trafficked and non-trafficked plots. The pattern in the 'wet' trafficked was

slightly more distinct than in the 'dry' and the non-trafficked subsoil at Ruckfeld, due to the higher moisture content which allowed more dye to flow from coarser into finer pores. The absence of significant effects on flow pattern and precompression stress agrees well.
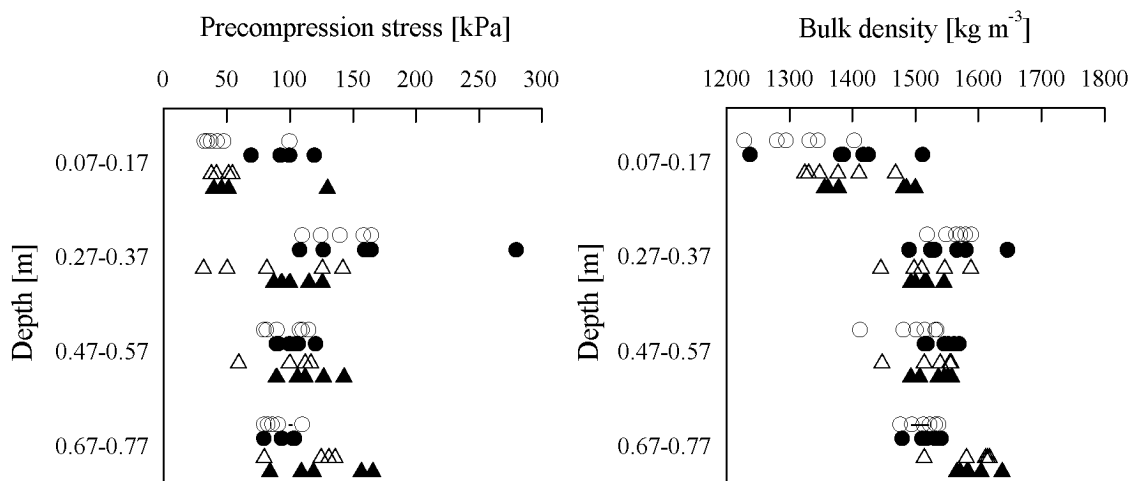

Fig. 3.8.   Precompression stress (left) and bulk density (right) of the 'wet' trafficked (●), 'dry' trafficked (▲), 'wet' non-trafficked (○) and 'dry' non-trafficked (△) Ruckfeld soil.
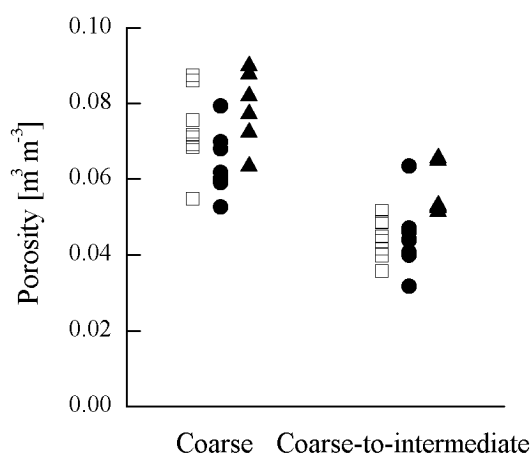

Fig. 3.9.   Porosity of the non-trafficked (□), 'wet' trafficked (●) and 'dry' trafficked (▲) Ruckfeld subsoil at 0.27-0.37 m depth.

Lack of statistical significance does not mean that compaction effects can be entirely excluded. Minor effects may have been concealed by the rather large scatter of the measured values, which was primarily due to a high degree of short-range spatial variability of these parameters.
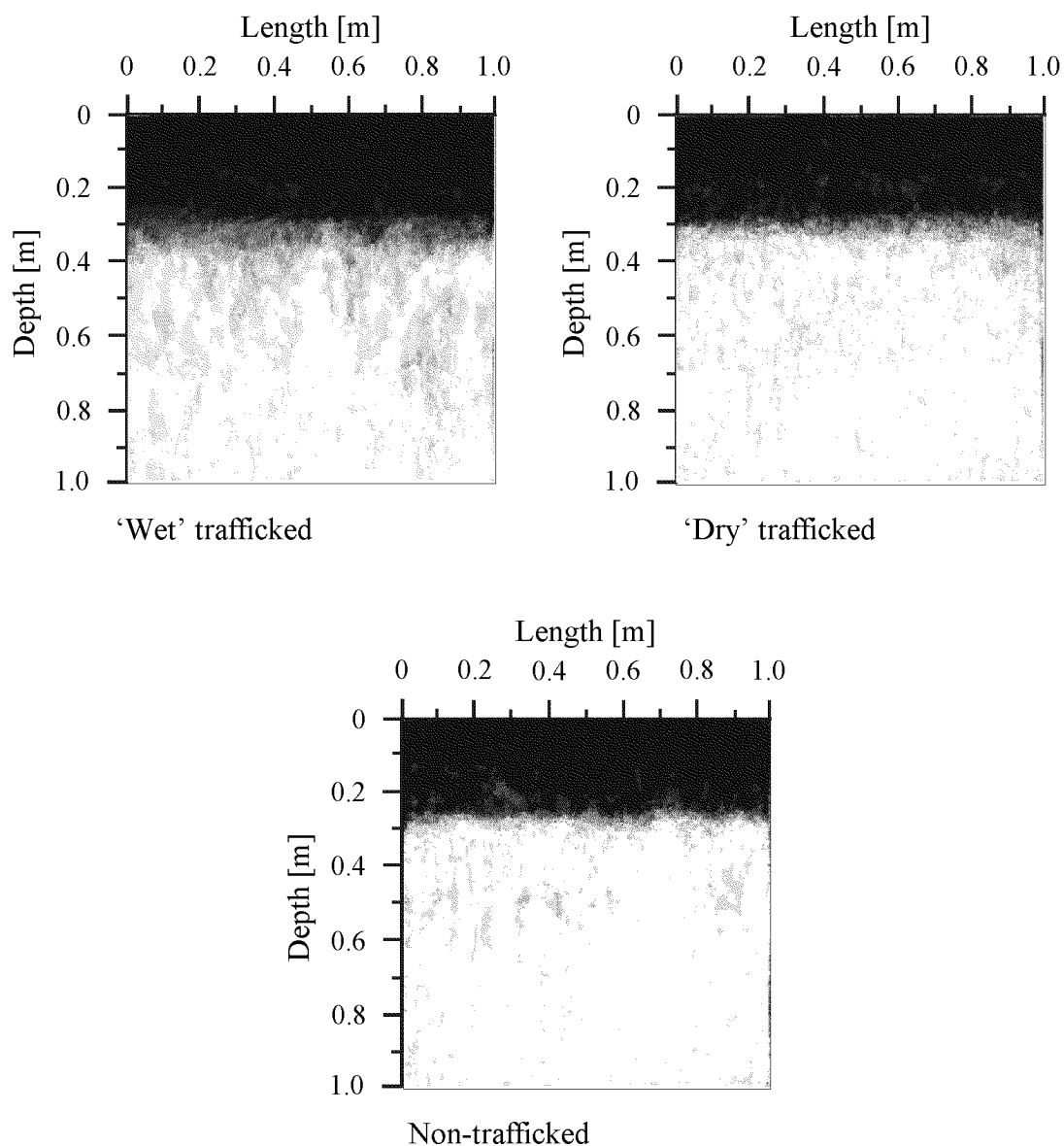
Fig. 3.10. Flow pattern of dye tracer in the 'wet', 'dry' and non-trafficked Ruckfeld soil.

The total variation between samples from the same horizon and site was much larger than the analytical error e.g. in respect of the determination of bulk density. The variation coefficient of bulk density measurements in this study was larger than 1.3% while the analytical error was smaller than 0.7%. Likewise the differences in bulk density and porosity of the subsoils described above may simply represent spatial variability at longer range. For example at 0.67-0.77 m depth of the Ruckfeld site, the difference between bulk density of the 'wet' and 'dry' plot is larger than between the values of trafficked and non-trafficked plot. From a strictly objective point of view, however, it also cannot be

excluded that spatial variability instead of traffic influence is the reason for the significant effects in precompression stress and bulk density in the 'wet'-trafficked topsoil at Ruckfeld.

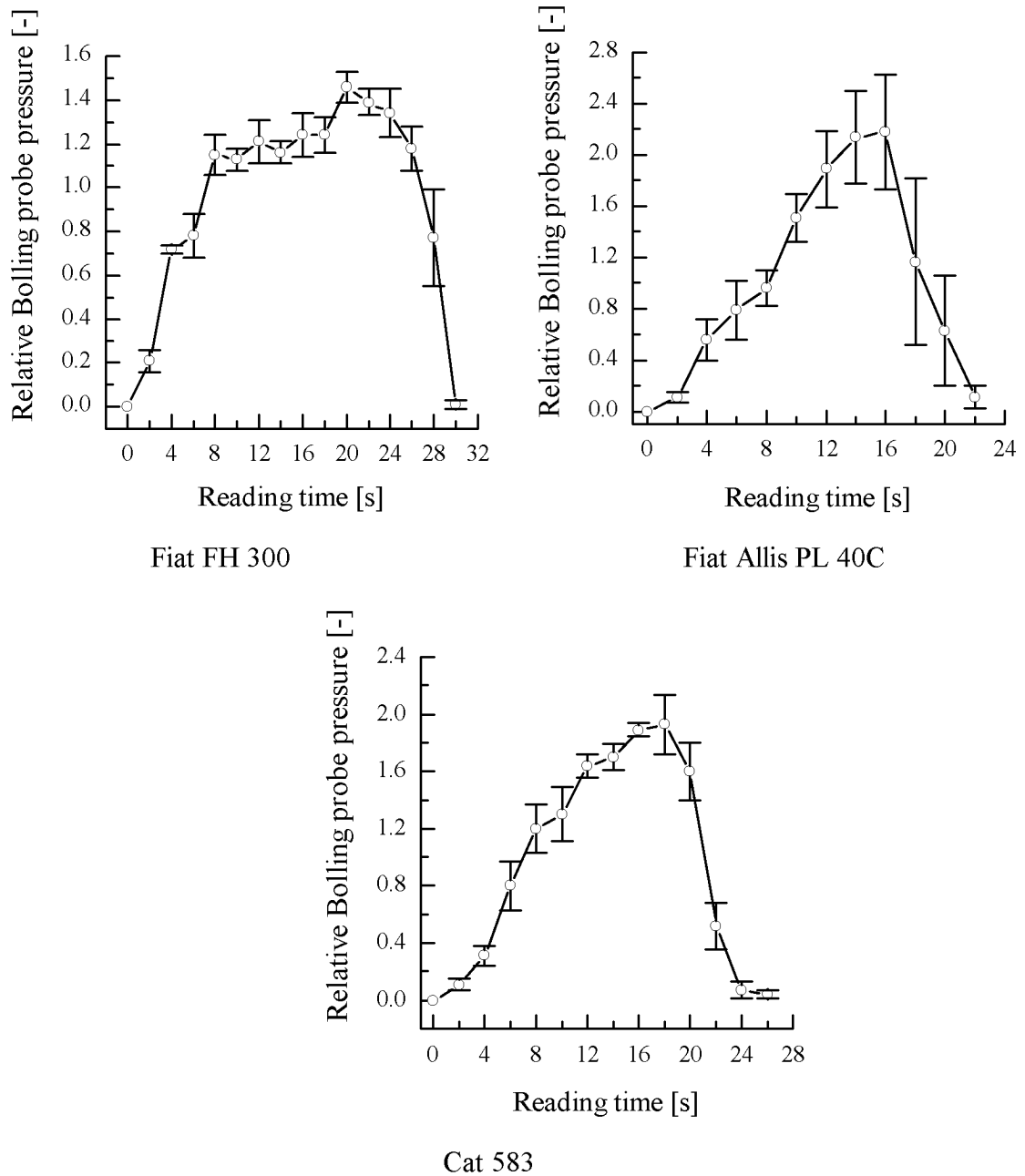Fiat FH 300

Fiat Allis PL 40C

Cat 583

Fig. 3.11.   Relative Bolling probe pressure (pressure readings as a function of time divided by the mean of the pressure readings over the measured time interval) determined at 0.32 m depth of the 'wet' plot at Ruckfeld under the tracks of the machinery used for the traffic experiment. The error bars indicate standard errors.

Relative Bolling probe pressure showed that stress at 0.32 m depth along the track centreline was rather 'triangularly' than 'rectangularly' distributed over time (Fig. 3.11). The relative pressures of the Fiat Allis PL 40 C and the Cat 583 showed a distinct maximum. This maximum was under the Fiat FH 300 1.5, under the Fiat Allis PL 40 C 2.2 and under the Cat 583 1.9 times the measured mean relative pressure. Koolen and Kuipers (1983) stated that for tracked machinery under practical conditions the maximum stress in the contact area is 1.4 to 3.0 times the mean normal pressure.

3.4 Discussion and conclusions

The results show that no consistent compaction effects were observed in the subsoil (Table 3.6). The only clear compaction, which was likely due to the trafficking, occurred in the wetted topsoil at Ruckfeld. At Güllenhau, a similar topsoil effect was likely but the evidence was less constant.

While these scarcity of significant and consistent compaction effects may partially be due to the large spatial variability of soil properties within and between plots, it also does not contradict expectations, if we compared the measured precompression stresses with estimates of the normal stresses exerted by the trafficking machines. Since stress is not homogeneously distributed beneath the track centreline (Fig. 3.11), peak rather than mean stress in the contact area could govern compaction.

To check for this, we compared two contact stress scenarios. In the 'best case' scenario, the normal stress in the contact area was taken to be the mean normal stress, i.e. the weight of machine and load divided by the total contact area (Table 3.3). In the 'worst case' scenario the normal stress in the contact area was assumed to be 2.2 times the mean normal stress for the Fiat Allis PL 40 C, 1.5 times for the Fiat FH 300 and 1.9 times for the Cat 583. We assumed that the Fiat FH 300 for the 'wet' and the Fiat Allis PL 40 C for the 'dry' Freienstein plot, the Fiat FH 300 for Güllenhau and the Cat 583 vehicle for the Ruckfeld site was likely to govern compaction. In both scenarios, soil-vehicle interaction was simplified as a plane strain problem. Stress propagation in the soil was modelled according to Fröhlich (1934) with the track idealised as an infinite strip load with homogeneous contact stress distribution on 'dry' (concentration factor $v = 4$) and 'wet' (concentration factor $v = 5$) soil. In addition to traffic induced stress, vertical stress due to the weight of the overlying soil at each depth was considered.

The calculated total vertical stresses in the soil below the track centreline were compared with the precompression stresses in the respective depths of 0.12, 0.32, 0.52 and 0.72 m. The median of precompression stress values depicted in Fig. 3.2, 3.5, and 3.8 were chosen in order to calculate the vertical stress/precompression stress ratio. Since precompression stress depends on soil moisture conditions (e.g. Culley and Larson, 1987; Horn, 1988; Kirby, 1991a), its values in the field were assumed to be higher or lower than the measured values at -6 kPa initial water potential if water potentials in the field were lower or higher than -6 kPa, respectively. Compaction effects were expected if the total vertical stress/precompression stress ratio exceeded 1 and the soil water potential in the field experiment was above -6 kPa and vice versa. In all other cases compaction effects were considered as 'possible'. The results are given separately for the three sites in Table 3.7, 3.8 and 3.9.

Table 3.6. Effects found at the three test sites for 'wet' and 'dry' trafficked plots compared with non-trafficked plots (-: no effect, (+): trend, +: significant effect, n.d.: not determined)

Site	Depth [m]	Precompression stress		Bulk density		Coarse porosity		Coarse-to-inter-mediate porosity		Flow pattern	
		'wet'	'dry'	'wet'	'dry'	'wet'	'dry'	'wet'	'dry'	'wet'	'dry'
Freienstein	0.07-0.17	-	-	-	+	(+)	+	n.d.	n.d.	n.d.	n.d.
	0.27-0.37	-	-	-	-	n.d.	n.d.	n.d.	n.d.	-	-
	0.47-0.57	-	-	-	-	n.d.	n.d.	n.d.	n.d.	(+)	-
	0.67-0.77	(+)	(+)	-	+	n.d.	n.d.	n.d.	n.d.	-	(+)
Güllenhau	0.07-0.17	(+)	n.d.	+	n.d.	-	n.d.	n.d.	n.d.	-	n.d.
	0.27-0.37	(+)	n.d.	(+)	n.d.	+	n.d.	n.d.	n.d.	-	n.d.
Ruckfeld	0.07-0.17	+	-	+	-	n.d.	n.d.	n.d.	n.d.	n.d.	n.d.
	0.27-0.37	-	-	-	-	-	-	-	+	-	-
	0.47-0.57	-	(+)	+	-	n.d.	n.d.	n.d.	n.d.	-	-
	0.67-0.77	-	-	-	-	n.d.	n.d.	n.d.	n.d.	-	-

Table 3.7. Effects expected at the Freienstein sites for 'wet' and 'dry' trafficked compared with non-trafficked plots under the assumption of a minimum ('best case') and maximum ('worst case') normal stress at the soil surface

Scenario	Depth [m]	Total vertical stress [kPa]		Total vertical stress/pre-compression stress [-]		Compaction effect expected	
		'wet'	'dry'	'wet'	'dry'	'wet'	'dry'
Best case[†]	0.12	74	88	1.18	1.39	possible	possible
	0.32	76	84	1.22	1.35	possible	possible
	0.52	73	74	0.89	0.90	possible	no
	0.72	69	66	0.79	0.75	no	possible
Worst case[‡]	0.12	107	185	1.7	2.94	possible	possible
	0.32	108	172	1.74	2.78	possible	possible
	0.52	102	147	1.25	1.80	yes	possible
	0.72	95	126	1.08	1.43	possible	yes

[†]   'best case': Normal stress = net mean stress + stress due to pipe weight under the trench closer track of Fiat FH 300 for the 'wet' and Fiat Allis PL 40 C for the 'dry' plot.

[‡]   'worst case': Normal stress = (net mean stress + stress due to pipe weight under the trench closer track of Fiat FH 300 for the 'wet' and Fiat Allis PL 40 C for the 'dry' plot) × 1.5 (Fiat FH 300), 1.9 (Cat 583) or 2.2 (Fiat Allis PL 40 C) for maximum stress along the track.

Table 3.8. Effects expected at Güllenhau for the trafficked compared with the non-trafficked plot for a minimum ('best case') and maximum ('worst case') normal stress at the soil surface

Scenario	Depth [m]	Total vertical stress [kPa]	Total vertical stress/pre-compression stress [-]	Compaction effect expected
Best case[†]	0.12	44	0.72	possible
	0.32	46	1.25	yes
Worst case[‡]	0.12	63	1.04	yes
	0.32	65	1.75	yes

[†]   'best case': Normal stress = net mean stress in the contact area of Fiat FH 300.

[‡]   'worst case': Normal stress = net mean stress × 1.5 (Fiat FH 300) for the maximum stress along the track.

Table 3.9.   Effects expected at Ruckfeld for 'wet' and 'dry' trafficked compared with non-trafficked plots for a minimum ('best case') and maximum ('worst case') normal stress at the soil surface

Scenario	Depth [m]	Total vertical stress [kPa]		Total vertical stress/pre-compression stress [-]		Compaction effect expected	
		'wet'	'dry'	'wet'	'dry'	'wet'	'dry'
Best case[†]	0.12	80	80	1.95	1.70	yes	possible
	0.32	79	77	0.53	0.70	possible	no
	0.52	74	70	0.75	0.74	possible	no
	0.72	68	62	0.80	0.49	possible	no
Worst case[‡]	0.12	153	152	3.72	3.24	yes	possible
	0.32	148	144	0.99	1.39	possible	possible
	0.52	135	126	1.36	1.26	yes	possible
	0.72	119	109	1.40	0.85	yes	no

[†]   'best case': Normal stress = net mean stress in the contact area of Cat 583.

[‡]   'worst case': Normal stress = net mean stress × 1.9 (Cat 583) for the maximum stress along the track.

Comparing expected (according to the scenario analysis, Table 3.7-3.9) with observed effects (Table 3.6), it emerges that the 'worst case' expectations did not agree better with observed effects in the subsoil than the 'best case' scenario. The 'worst case' scenario predicted compaction in the subsoil of the 'wet' plot in 0.27-0.37 and 0.67-0.77 m depth at Ruckfeld, although no effect was found. For the 'best case' scenario, the increased bulk density in the 'dry' Freienstein plot at 0.67-0.77 m depth and the 'wet' Ruckfeld plot at 0.47-0.57 m depth (Table 3.6) disagreed with expectations. The increased bulk density in the 'wet' Ruckfeld plot at 0.47-0.57 m depth, however, was inconsistent with the lack of an increase in precompression stress or an effect on the flow pattern. As pointed out already in the results, this inconsistency may have been due to natural variability.

In summary, the 'best case' scenario tended to underestimate while the 'worst case' scenario overestimated subsoil compaction. Under the investigated experimental conditions, it appears to be adequate to estimate the effective normal stress in the contact area under the tracks as about 1.5-times the mean normal stress. For the prediction of topsoil compaction, however, the inhomogeneity of the load distribution may not be negligible. An indication for this are the results observed at Güllenhau where only the 'worst case' scenario clearly predicted such compaction whereas it could not necessarily have been expected according to the 'best case' scenario.

As discussed before, such interpretations should be taken with caution. Inconsistency may also have arisen from factors such as the natural heterogeneity between the plots and sites which is not captured by replicate measurements within plots. Differences in the experimental conditions between field and laboratory are other factors of uncertainty and possible inconsistency within the results. Taking these limitations into account as well as reservations concerning the exact physical meaning of the precompression stress as determined by the procedure of Casagrande (1936), the agreement between expectations and measurements is surprisingly good. Therefore, we conclude that the precompression stress may provide a useful and practical criterion for assessing the compaction sensitivity of soils under field conditions.

3.5 References

Atkinson, J.H. and Bransby, P.L., 1978. The Mechanics of Soils: An Introduction to Critical State Soil Mechanics. McGraw-Hill University Series in Civil Engineering. McGraw-Hill Book Company, 375 pp.

Blunden, B.G., McBride, R.A., Daniel, H. and Blackwell, P.S., 1994. Compaction of an earthy sand by rubber tracked and tyred vehicles. Australian Journal of Soil Research, 32: 1095-1108.

Bolling, I., 1987. Bodenverdichtung und Triebkraftverhalten bei Reifen - Neue Mess- und Rechenmethoden. PhD Thesis, Forschungsbericht Agrartechnik des Arbeitskreises Forschung und Lehre der Max-Eyth-Gesellschaft (MEG), Technische Universität München, München, 274 pp.

Boussinesq, M.J., 1885. Applications des potentiels à l'étude de l'equilibre et du mouvement des solides élastiques. Gauthier-Villars, Paris, 721 pp.

Casagrande, A., 1936. The determination of pre-consolidation load and its practical significance. 1st International Conference on Soil Mechanics and Foundation Engineering, Harvard University, Cambridge, Massachusetts. pp. 60-64.

Culley, J.L.B. and Dow, B.K., 1988. Long-term effects of an oil pipeline installation on soil productivity. Canadian Journal of Soil Science, 68(Feb.): 177-181.

Culley, J.L.B., Dow, B.K., Presant, E.W. and MacLean, A.J., 1982. Recovery of productivity of Ontario soils disturbed by an oil pipeline intallation. Canadian Journal of Soil Science, 62(May): 267-279.

Culley, J.L.B. and Larson, W.E., 1987. Susceptibility to compression of a clay loam Haplaquoll. Soil Science Society of American Journal, 51: 562-567.

Dumbeck, G., 1984. Einfluss aussergewöhnlicher Druckbelastung auf das Bodengefüge und die Durchwurzelung. Mitteilungen der Deutschen Bodenkundlichen Gesellschaft, 40: 61-62.

FAO, 1990. FAO-Unesco Soil Map of the World, Food and Agriculture Organisation of the United Nations (FAO), Revised Legend, Rome.

Flury, M. and Flühler, H., 1995. Tracer characteristics of Brillant Blue FCF. Soil Science Society of America Journal, 59(1): 22-27.

Flury, M., Flühler, H., Jury, W.A. and Leuenberger, J., 1994. Susceptibility of soils to preferential flow of water: A field study. Water resources research, 30(7): 1945-1954.

Forrer, I., A., P., Kasteel, R., Flühler, H. and Luca, D., 2000. Quantifying dye tracers in soil profiles by image processing. European Journal of Soil Science, 51(June): 313-322.

Fröhlich, O.K., 1934. Druckverteilung im Baugrunde mit besonderer Berücksichtigung der plastischen Erscheinungen. Verlag von Julius Springer, Wien, 185 pp.

Gysi, M., Ott, A. and Flühler, H., 1999. Influence of single passes with high wheel load on a structured , unploughed sandy loam soil. Soil & Tillage Research, 52: 141-151.

Hadas, A., 1994. Soil compaction caused by high axle loads - review of concepts and experimental data. Soil & Tillage Research, 29: 253-276.

Håkansson, I. and Reeder, R.C., 1994. Subsoil compaction by vehicles with high axial load - extend, persistence and crop response. Soil & Tillage Research, 29: 277-304.

Hammel, K., 1993. Spannungsverteilung und Bodenverdichtung unter profilierten Reifen am Beispiel zweier Böden unter Grünland. PhD Thesis, Institut für Bodenkunde und Standortlehre, Universität Hohenheim, Stuttgart, 141 pp.

Horn, R., 1981. Eine Methode zur Ermittlung der Druckbelastung von Böden anhand von Drucksetzungsversuchen. Zeitschrift für Kulturtechnik und Flurbereinigung, 22(1): 20-26.

Horn, R., 1988. Compressibility of arable land. In: J. Drescher, R. Horn and M. De Boodt (Editors). Impact of Water and External Forces on Soil Structure, Catena Supplement 11. Catena-Verlag, Cremlingen-Destedt, pp. 53-71.

Horn, R. and Lebert, M., 1994. Soil compactibility and compressibility. In: B.D. Soane and C. van Ouwerkerk (Editors). Soil Compaction in Crop Production. Elsevier, Amsterdam, pp. 45-69.

Kirby, J.M., 1991a. Critical-state soil mechanics parameters and their variation for Vertisols in eastern Australia. Journal of Soil Science, 42: 487-499.

Kirby, J.M., 1991b. Strength and deformation of agricultural soil: measurement and practical significance. Soil Use and Management, 7: 223-229.

Kooistra, M.J., Bouma, J., Boersma, O.H. and Jager, A., 1984. Physical and morphological characterisation of undisturbed and disturbed ploughpans in a sandy loam soil. Soil & Tillage Research, 4: 405-417.

Koolen, A.J. and Kuipers, H., 1983. Agricultural Soil Mechanics. Advanced Series in Agricultural Sciences 13. Springer-Verlag, Berlin, 241 pp.

McKyes, E., Stemshorn, E. and Bousquet, R., 1980. Damage to agricultural fields by construction traffic. Transactions of the American Society of Agricultural Engineers, 23(6): 1388-1391.

Neilsen, D., MacKenzie, A.F. and Stewart, A., 1990. The effect of burried pipeline installation on fertilizer treatments on corn productivity on three eastern Canadian soils. Canadian Journal of Soil Science, 70(May): 169-179.

Oldeman, L.R., Hakkeling, R.T.A. and Sombroeck, W.G., 1991. World Map of the Status of Human-Induced Soil Degradation: An Explanatory Note, International Soil Reference and Information Centre (ISRIC), Wageningen.

Richards, L.A., 1941. A pressure-membrane extraction apparatus for soil solution. Soil Science, 51: 377-386.

Richards, L.A. and Fireman, M., 1941. A pressure-plate apparatus for measuring moisture sorption and transmission by soils. Soil Science, 56: 395-404.

Soane, B.D. and Van Ouwerkerk, C., 1995. Implications of soil compaction in crop production for the quality of the environment. Soil & Tillage Research, 35: 5-22.

Söhne, W., 1953. Druckverteilung im Boden und Bodenverformung unter Schlepperreifen. Grundlagen der Landtechnik, 5: 49-63.

Söhne, W., 1958. Fundamentals of pressure distribution and soil compaction under tractor tires. Agricultural Engineering, May: 276-291.

Terzaghi, K. and Peck, R.B., 1948. Soil Mechanics in Engineering Practice. John Wiley and Sons, New York, 566 pp.

von Albertini, N., Leuenberger, J., Läser, H.P. and Flühler, H., 1995. Regeneration der Bodenstruktur eines verdichteten Ackerbodens unter Kunstwiese. Aktuelle Bodenforschung in der Schweiz. Bodenkundliche Gesellschaft er Schweiz, St. Gallen. pp. 10-16.

von Rohr, G., 1996. Auswirkungen des Rohrleitungsbaus auf bodenphysikalische Kenngrössen. Diploma Thesis, Geographisches Institut der Univerität Bern, Bern, 108 pp.

4

Moisture dependence of compressibility of a Haplic Luvisol

M. Berli, W. Attinger, J.M. Kirby, S.M. Springman, H. Flühler, R. Schulin

Abstract

Efficient protection of agricultural and forest soils against compaction requires knowledge of the mechanical behaviour and properties of structured unsaturated soils and, in particular, their dependence on soil moisture. In this study, we performed confined uniaxial compression tests on undisturbed top- and subsoil samples from a silt loam Haplic Luvisol in Switzerland at five different initial water potentials between -1 and -32 kPa.

We found a positive correlation between the precompression stress and the logarithms of negative soil water potential, a negative correlation between precompression stress and water content and no correlation between precompression stress and degree of water saturation of the samples. The influence of soil moisture was much stronger in the sub- than in the topsoil. For the compression index we found a small positive correlation to initial water potential but no correlation to water content and saturation degree. The re-compression index slightly decreased with decreasing water potential but no correlation was found with water content and saturation degree. Initial void ratio was strongly correlated with the compression index but weakly correlated with precompression stress and recompression index.

4.1 Introduction

Compaction of agricultural soil due to heavy vehicle traffic has been recognised as a major threat to soil fertility world-wide. Efficient protection against compaction requires knowledge of the mechanical behaviour and properties of the affected soils. Compared to water-saturated soils, an additional complication in the understanding of the mechanics of unsaturated soils arises from the fact that these properties may strongly depend on soil moisture. Already in the 1950s, Söhne (1953; 1958) emphasised the influence of moisture conditions on the compressibility of agricultural soils. He observed that in order to compact an undisturbed soil sample to a specific porosity, increasing stress had to be applied with decreasing moisture content.

The influence of soil moisture on compression characteristics was investigated by a number of authors for disturbed unsaturated engineering (Jennings and Burland, 1962; Matyas and Radhakrishna, 1968; Maâtouk et al., 1995; Wheeler and Sivakumar, 1995) and agricultural (Larson et al., 1980; Stone and Larson, 1980; Leeson and Campbell, 1983; Hettiaratchi and O'Callaghan, 1985; Petersen, 1993; O'Sullivan et al., 1994; Adams and Wulfsohn, 1997) soils. Soil susceptibility to compression strongly depends on its structure and stress history (Dexter and Tanner, 1974; Horn et al., 1994). This means that measurements of mechanical properties of disturbed samples are of limited value for the prediction of soil compaction of undisturbed soils under field conditions. Nonetheless, except for the early work of Söhne (1953; 1958), only a few researchers analysed undisturbed samples. Culley and Larson (1987) determined the effects of various tillage systems and wheel traffic loads on stress-compression curves at -5, -10, -20, and -40 kPa initial matric potential for a clay loam Haplaquoll topsoil. They found increasing precompression stresses but no clear trend of the slopes of virgin and recompression lines for decreasing water potential. Horn (1988), Lebert (1989) and Semmel (1993) measured higher precompression stress values at lower water content of a variety of German soils at two different initial soil water potentials (-6.3 and -31.6 kPa). Kirby (1991) investigated the influence of initial soil moisture conditions on critical state soil mechanical parameters of 18 Vertisols in Eastern Australia. He found a negative correlation between moisture content and precompression stress, but no correlation with compression and rebound index. O'Sullivan and Robertson (1996) measured higher precompression stresses and higher slopes of the rebound and virgin compression lines for dry than for wet samples of a sandy loam Eutric Cambisol and a clay loam Gleysol in Scotland. Panayiotopoulos (1996) found that Young's modulus increased by about two orders of magnitude as water potential was decreased from -1 to -10^5 kPa in three Greek Alfisols.

A more detailed knowledge of the moisture-dependence of the mechanical behaviour of agricultural soils is desirable for various reasons. In particular, mathematical modelling of compaction under variable moisture conditions requires that these dependencies are defined quantitatively. Furthermore, knowledge of the moisture dependence of soil mechanical characteristics may also be important from the regulatory point of view. Pre-compression stress, i.e. the yield point between elastic and plastic compression behaviour, has recently been proposed as a key criterion in the regulation of allowable mechanic loads on agricultural soils in Switzerland (BEW, 1997).

The objective of this study was to determine the influence of soil moisture on the stress-compression curves of undisturbed samples of a Haplic Luvisol, a common soil type found as arable land in Switzerland. For this purpose, confined uniaxial compression tests were performed with undisturbed samples conditioned to different initial moisture content. Following Kirby (1989) we used total instead of effective stress to represent the results. The reason is that primarily the effective stress concept, as it is used for saturated soils, has no thermodynamic meaning under unsaturated conditions as it depends on constitutive assumptions. Secondly, to use total instead of effective stresses is quicker, easier and more useful in practice. The use of total stress as a stress state variable has been discussed and experimentally verified by Hettiaratchi and O'Callaghan (1985) and Hettiaratchi (1987).

4.2 Material and methods

Soil samples were taken from a Haplic Luvisol (FAO, 1990) in Switzerland. The site was an agricultural field in the 'Ruckfeld', a plateau area in the north-west of Zurich. Reflecting the parent material, i.e. loess deposited in the forefield of a glacier during the Riss glaciation, the soil was a loamy silt (see Table 4.1) with less than 1% gravel content. In the season preceding sampling, potatoes had been grown on the field.

Table 4.1.   Soil parameters of the test plot

Depth [m]	Sand [kg kg^{-1}]	Silt [kg kg^{-1}]	Clay [kg kg^{-1}]	Organic matter [kg kg^{-1}]	Mineral density [kg m^{-3}]
0.07-0.17	0.28	0.59	0.13	0.028	2600
0.27-0.37	0.31	0.56	0.13	0.023	2610
0.47-0.57	0.29	0.58	0.13	0.008	2630
0.67-0.77	0.23	0.59	0.18	0.007	2640

Samples were collected on the 16th October 1998 after harvesting. The soil had freely drained in the days before and approached conditions of field capacity as monitored by tensiometers installed at various depth (Table 4.2).

Table 4.2.   Soil water potential in the field at the sampling date with standard errors

Depth of tensiometer cup [m]	Soil water potential [kPa] Average	Standard error
0.12	-6.9	0.16
0.32	-4.4	0.22
0.52	-4.0	0.31
0.72	-3.1	0.15

Between 25 and 30 replicate soil samples were taken from 0.07-0.17, 0.27-0.37, 0.47-0.57 and 0.67-0.77 m depth each, by coring with sharpened 10^{-1} m^3 steel cylinders (0.108 m inner diameter and 0.11 m height). In order to minimise disturbance, the samples were kept in these cylinders throughout the following preparation procedures and compression tests. For transport and storage, the cylinders were sealed with plastic caps and tightly packed into plastic bags to avoid loosening of the soil and water losses.

Prior to the compression tests, the samples were first saturated with water for at least 24 h and then conditioned to soil water potential of -1, -3, -6, -16 and -32 kPa, applied at the bottom of the samples by hanging water columns through sand and kaolin tension tables. The above water potentials spanned the range of values measured in the subsoil of the sampling site between April and June in the year before. In the topsoil, water potentials occasionally were below -85 kPa during that period. The conditioned samples were trimmed to 0.11 m height, weighed and than built into the compression cell (Fig. 4.1).
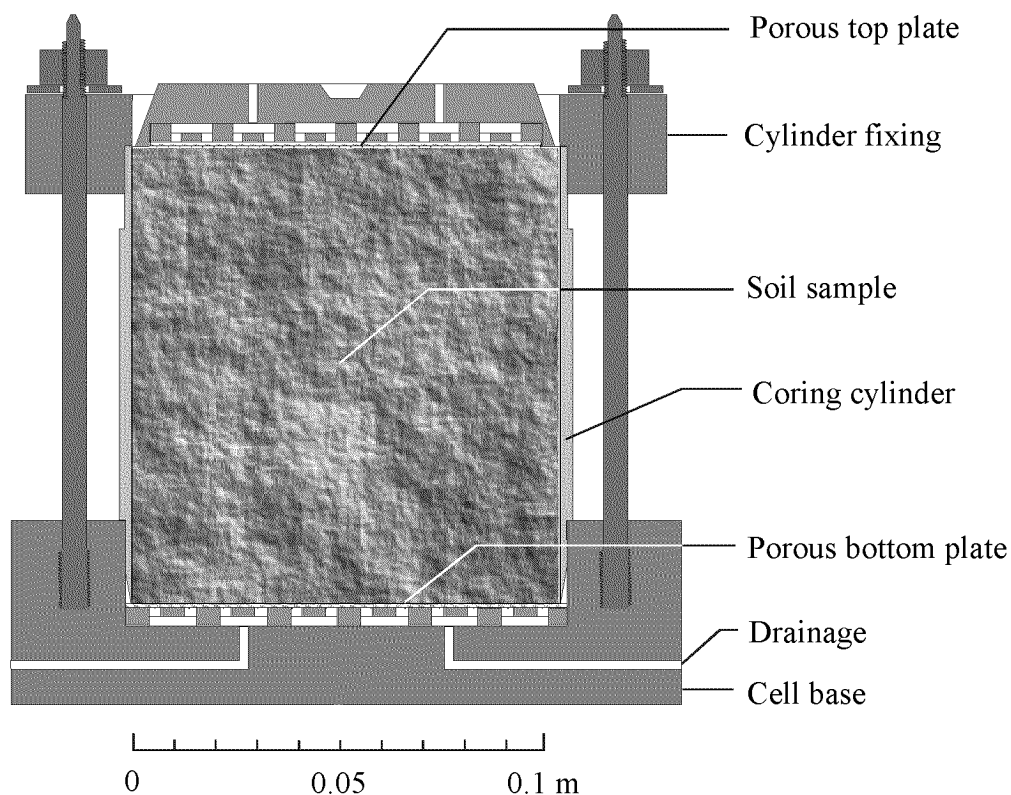
Fig. 4.1.   Cross section of the compression cell used for the uniaxial compression test.
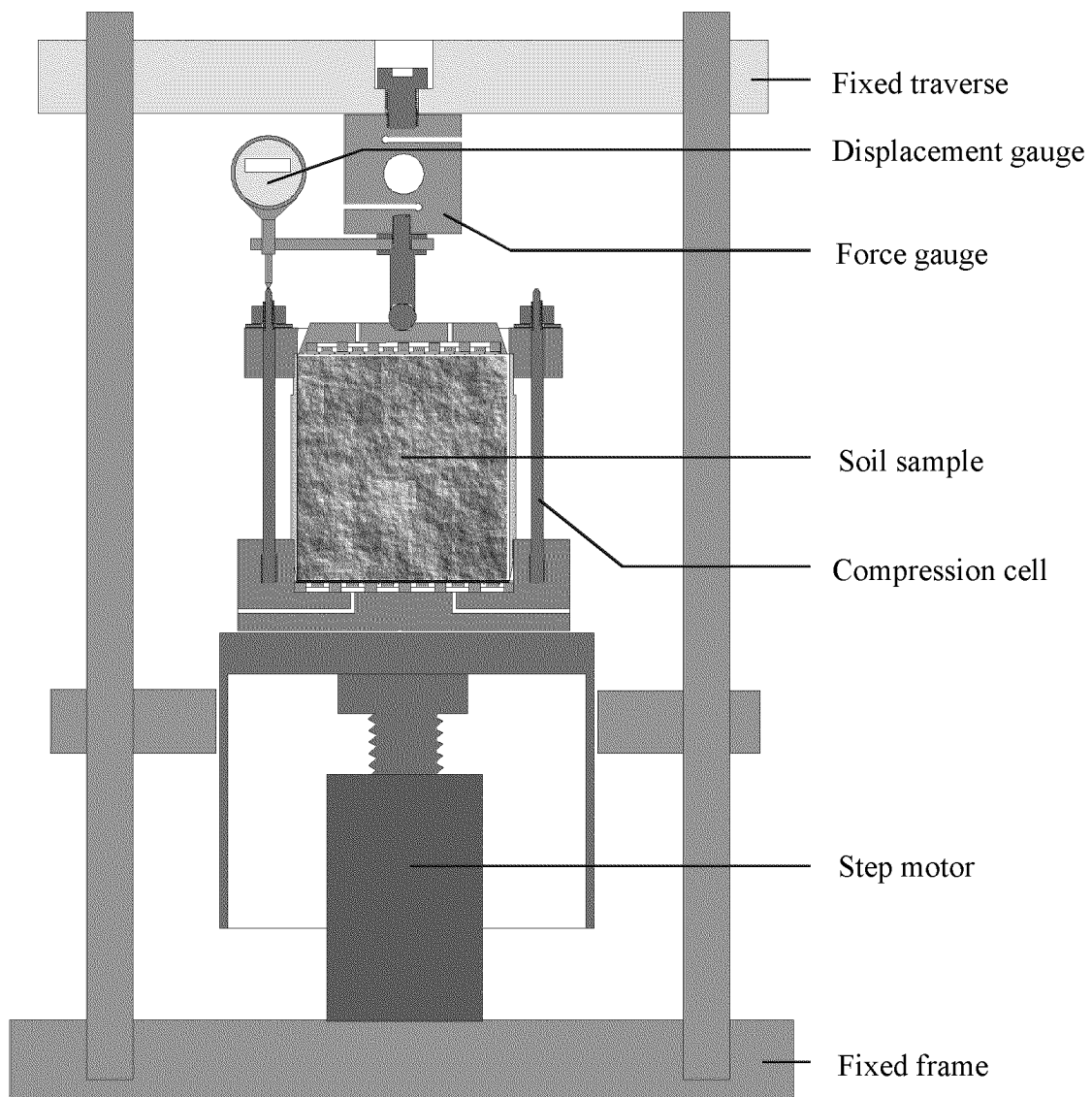
Fig. 4.2. Cross section of the compression apparatus used for the uniaxial compression test (not to scale).

Stress were subsequently increased stepwise from 8 to 2000 kPa between the cell base and the top plate, which fitted the internal diameter of the cylinders (Fig. 4.2). Each compression step lasted for 1800 s, then the stress was increased to the next level. During the compression test, water and air were allowed to drain freely through the top and bottom plate of the compression cell (see Fig. 4.1).
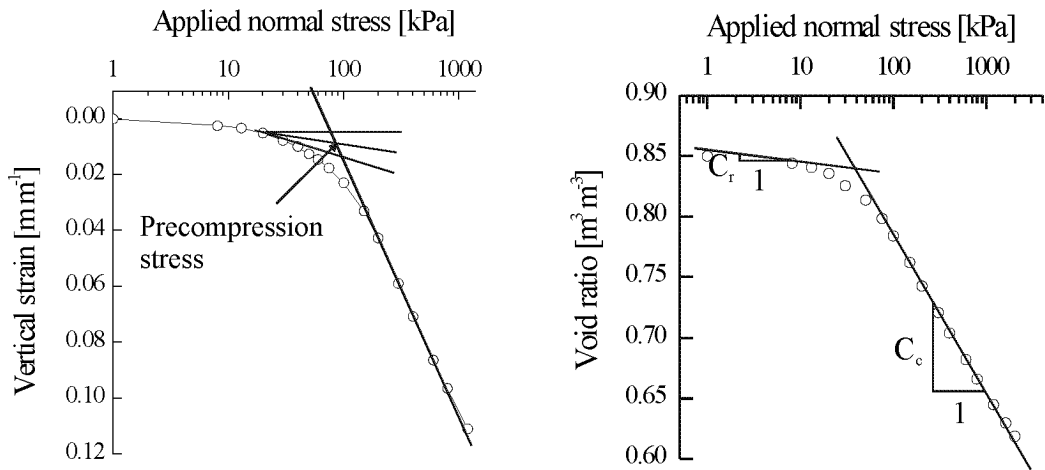
Fig. 4.3. Definition of precompression stress (left graph), compression index C_c and recompression index C_r (right graph).

Precompression stress was determined from the resulting applied normal stress-vertical strain curves using the graphical procedure of Casagrande (1936). In addition, we evaluated the slope of the virgin compression line, denoted as compression index C_c and the gradient of the curve at 8 kPa, denoted as recompression index C_r (see Fig. 4.3). Relative void ratio was defined as the ratio of the void ratio after a compression step to the initial void ratio of the sample at the beginning of the test. After the compression tests, the samples were dried at 105 °C for at least 24 hours and weighed to determine their dry bulk density.

4.3 Results

The dry bulk density of the topsoil samples (0-07-0.17 m depth) was significantly smaller than that of the subsoil samples in 0.27-0.37, 0.47-0.57 and 0.67-0.77 m depth (Table 4.3).

Table 4.3.   Initial values of soil water conditions and dry bulk density of the samples used for the compaction experiment (standard errors in parentheses)

Depth [m]	No. of samples	Water potential [kPa]	Water content [m m^{-3}]	Saturation degree[†) [m m^{-3}]	Dry bulk density [kg m^{-3}]
0.07-0.17	-	0	0.449 (0.004)	1.000	-
	5	-1	0.393 (0.003)	0.900 (0.010)	1465 (13)
	5	-3	0.370 (0.002)	0.828 (0.009)	1438 (10)
	5	-6	0.370 (0.005)	0.822 (0.015)	1428 (29)
	5	-16	0.366 (0.007)	0.798 (0.012)	1406 (23)
	4	-32	0.337 (0.001)	0.743 (0.016)	1418 (24)
0.27-0.37	-	-0	0.405 (0.003)	1.000	-
	5	-1	0.365 (0.003)	0.920 (0.008)	1573 (18)
	5	-3	0.340 (0.002)	0.834 (0.013)	1547 (15)
	5	-6	0.325 (0.003)	0.816 (0.018)	1567 (16)
	4	-16	0.319 (0.004)	0.772 (0.021)	1530 (21)
	5	-32	0.294 (0.005)	0.724 (0.022)	1546 (22)
0.47-0.57	-	0	0.396 (0.002)	1.000	-
	5	-1	0.336 (0.002)	0.859 (0.014)	1601 (18)
	5	-3	0.311 (0.001)	0.793 (0.007)	1598 (7)
	9	-6	0.300 (0.002)	0.750 (0.007)	1579 (6)
	5	-16	0.286 (0.003)	0.716 (0.011)	1579 (5)
	6	-32	0.260 (0.013)	0.666 (0.033)	1602 (11)
0.67-0.77	-	-0	0.418 (0.002)	1.000	-
	5	-1	0.357 (0.001)	0.857 (0.004)	1539 (6)
	5	-3	0.335 (0.003)	0.810 (0.013)	1548 (13)
	5	-6	0.318 (0.001)	0.752 (0.006)	1522 (7)
	5	-16	0.309 (0.002)	0.731 (0.006)	1524 (5)
	5	-32	0.289 (0.012)	0.699 (0.020)	1550 (23)

[†] Water content at saturation (0 kPa water potential) was assumed to be equal to porosity.
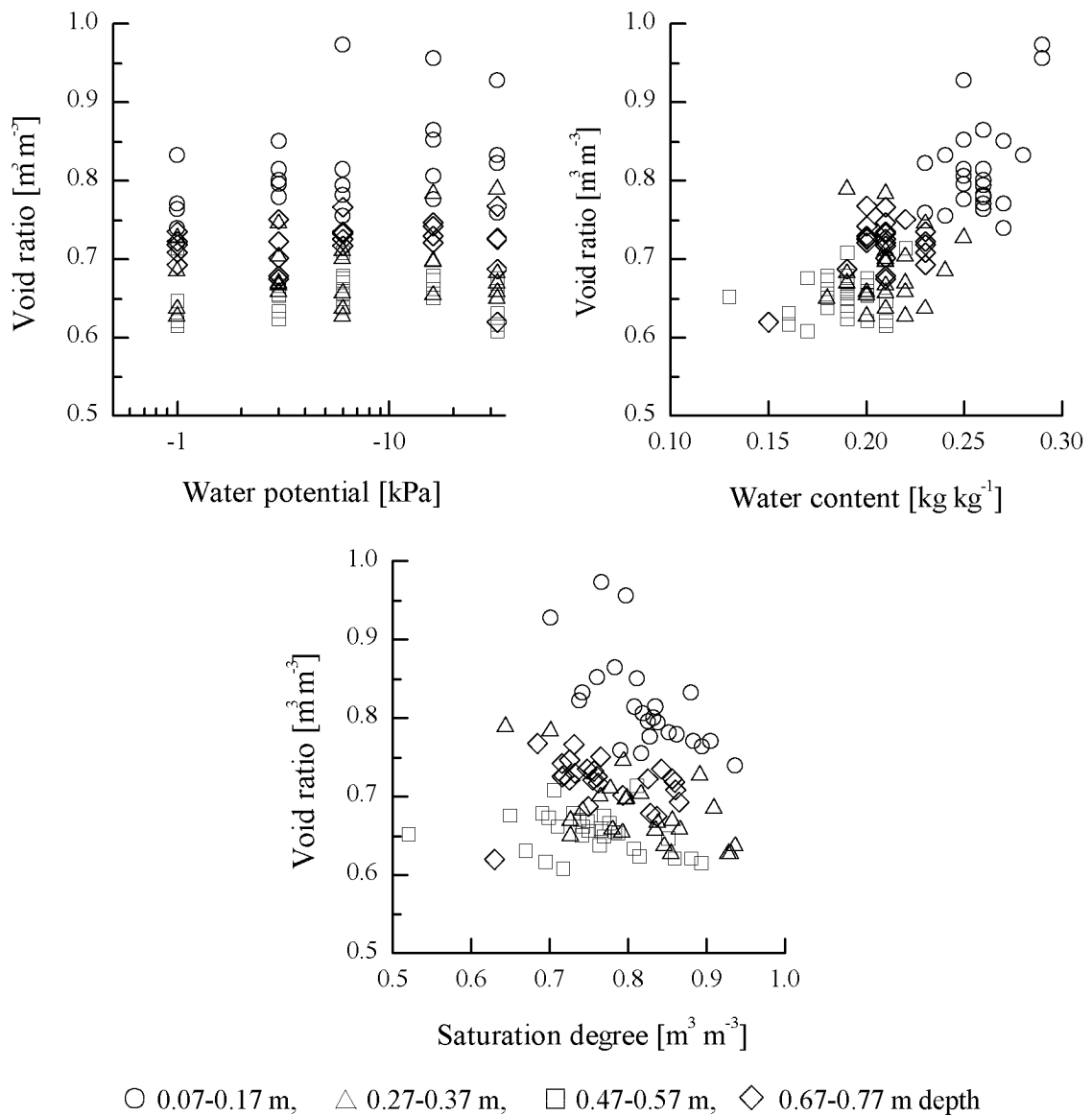
Fig. 4.4.   Void ratio versus initial water potential, water content and saturation degree of the investigated samples.

There was no significant difference in dry bulk density between subsoil samples of different depth, whereas macroporosity, defined as the pore volume drained at a water potential of -6 kPa, clearly increased with depth in the subsoil.

We found higher void ratios related to higher initial water content but no relationship between void ratio and initial soil water potential or saturation degree although the initial moisture conditions of the samples were controlled by soil water potential (Fig. 4.4).

To allow a better comparison, stress-compression curves were plotted in terms of relative void ratio (Fig. 4.5).

0.07-0.17 m depth

0.27-0.37 m depth

0.47-0.57 m depth

0.67-0.77 m depth

——— -1 kPa,   - - - - -3 kPa,   ········ -6 kPa,   - · - · - -16 kPa,   - · · - · · - -32 kPa initial water potential
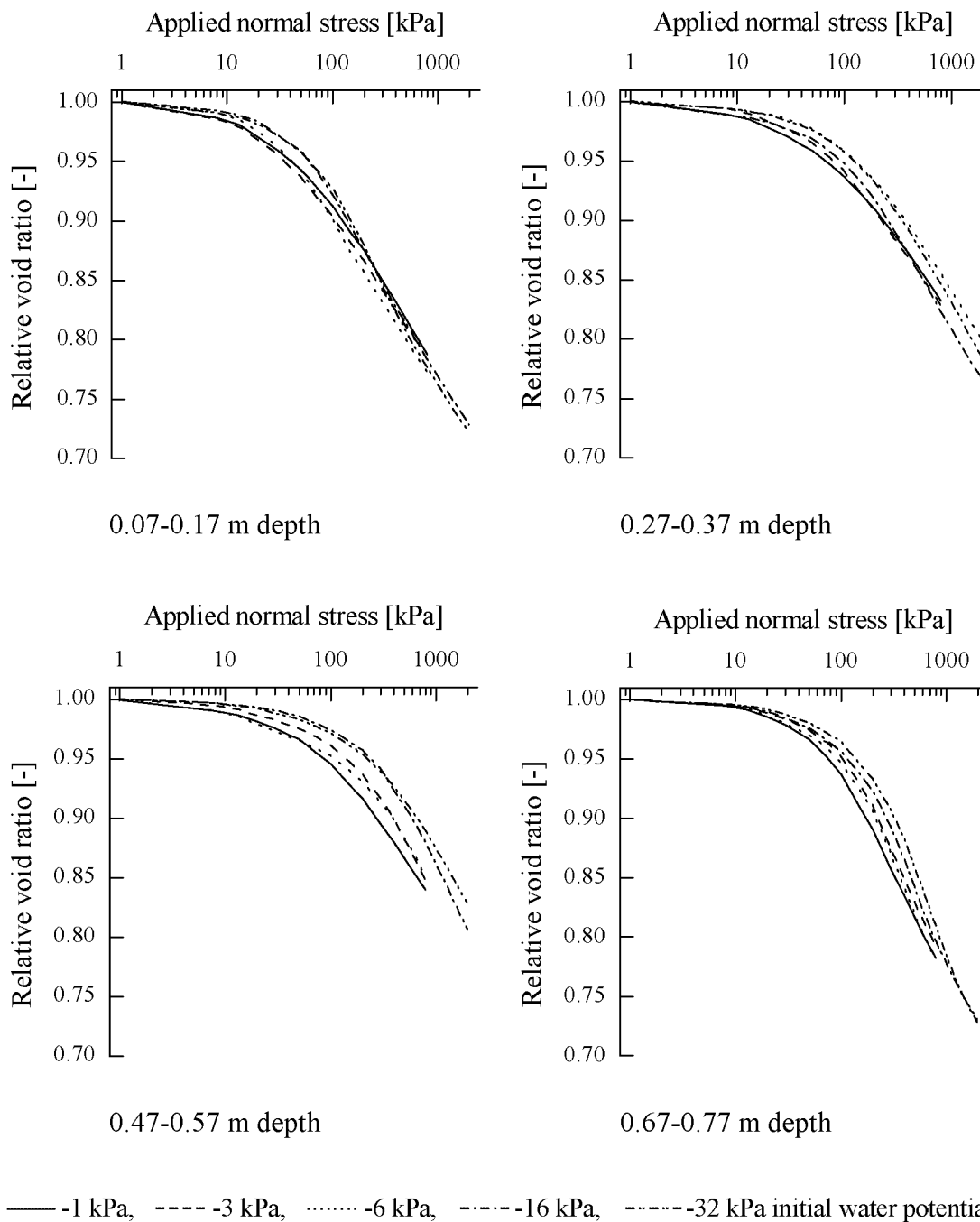
Fig. 4.5.   Applied normal stress-void ratio-curves at -1, -3, -6, -16 and -32 kPa initial water potential. Each curve represents the average of 4 to 9 replicate samples as specified in Table 4.3.

In general, the stress-compression curves tend to be shifted to the right, i.e. to higher stresses with decreasing water content. The same behaviour was reported by Greacen (1960), Larson et al. (1980) and Adams and Wulfson (1997) for disturbed and by Söhne (1953; 1958) for undisturbed samples. This trend was clearer in the lower subsoil, in particular for 0.47-0.57 and 0.67-0.77 m depth. Differences were comparably small for the upper two depths. While a decrease in moisture content tended to shift the stress-compression curves towards higher stresses, it also tended to increase the slope of the virgin compression line with the result that the curves tended to converge with increasing stress. The change of slope was particularly apparent in the transition from -1 to -3 kPa initial water potential. This indicates that compression was increasingly limited by drainage as the initial water content approached saturation. These observations are sub-stantiated if we consider the indicated parameters characterising the stress-compression curve, i.e. precompression stress, compression index and recompression index. All curves show a very gradual transition from the recompression to the virgin compression line. However, because they are also very smooth, precompression stresses could be de-termined very precisely by the Casagrande method (Casagrande, 1936). The relationship between precompression stress and moisture variables reflects the shifts in position with changing initial moisture conditions described above (Fig. 4.5).
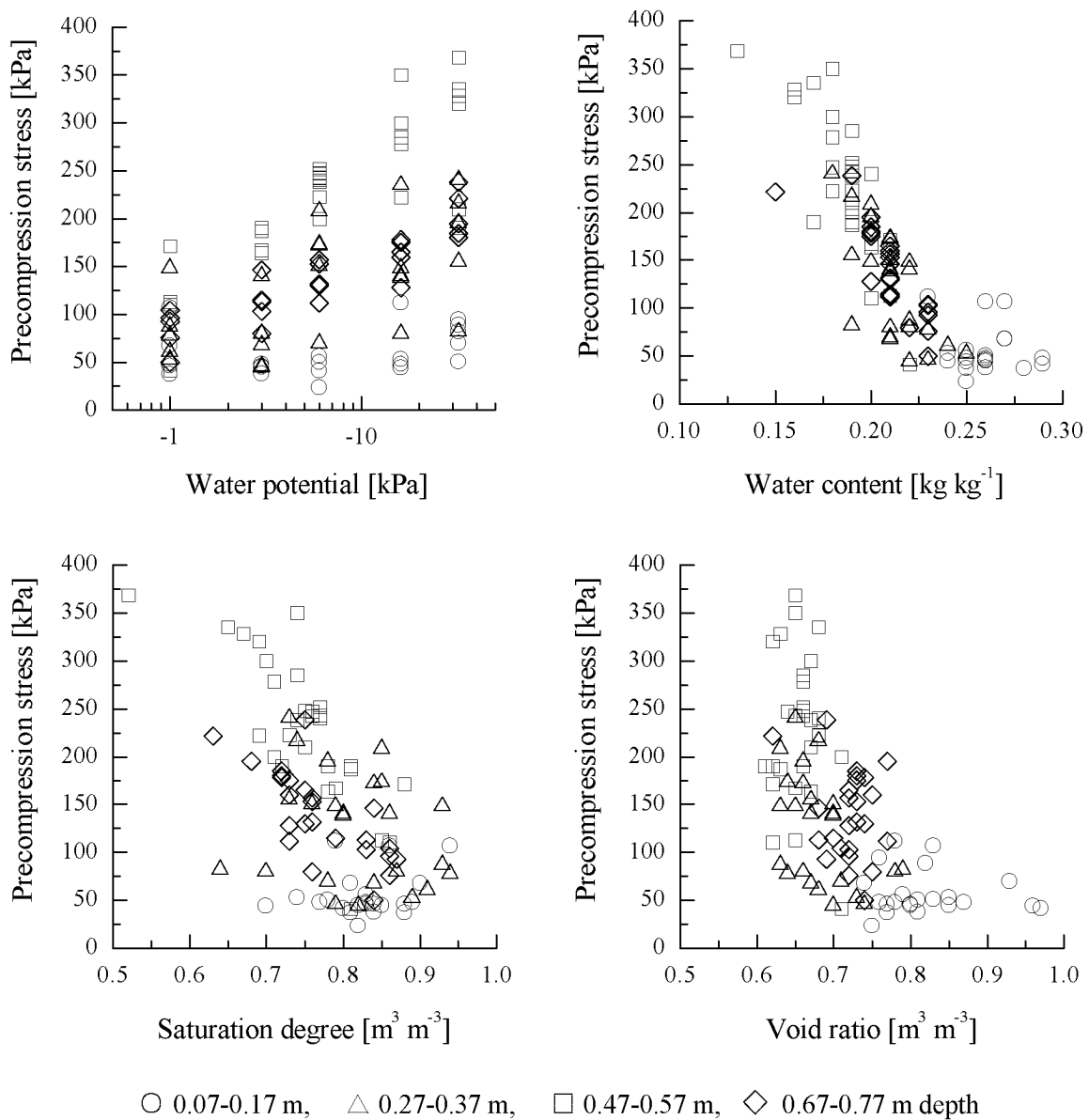
Fig. 4.6. Precompression stress versus initial values of water potential, water content, saturation degree and void ratio.

The subsoil samples of the lower two depths (0.47-0.57 and 0.67-0.77 m) showed a clear and strong increase in precompression stress with decreasing water potential or water content (Fig. 4.7 and 4.8). For these depths, linear relationships were found between precompression stress and the initial water content and the logarithm of the water potential, respectively.
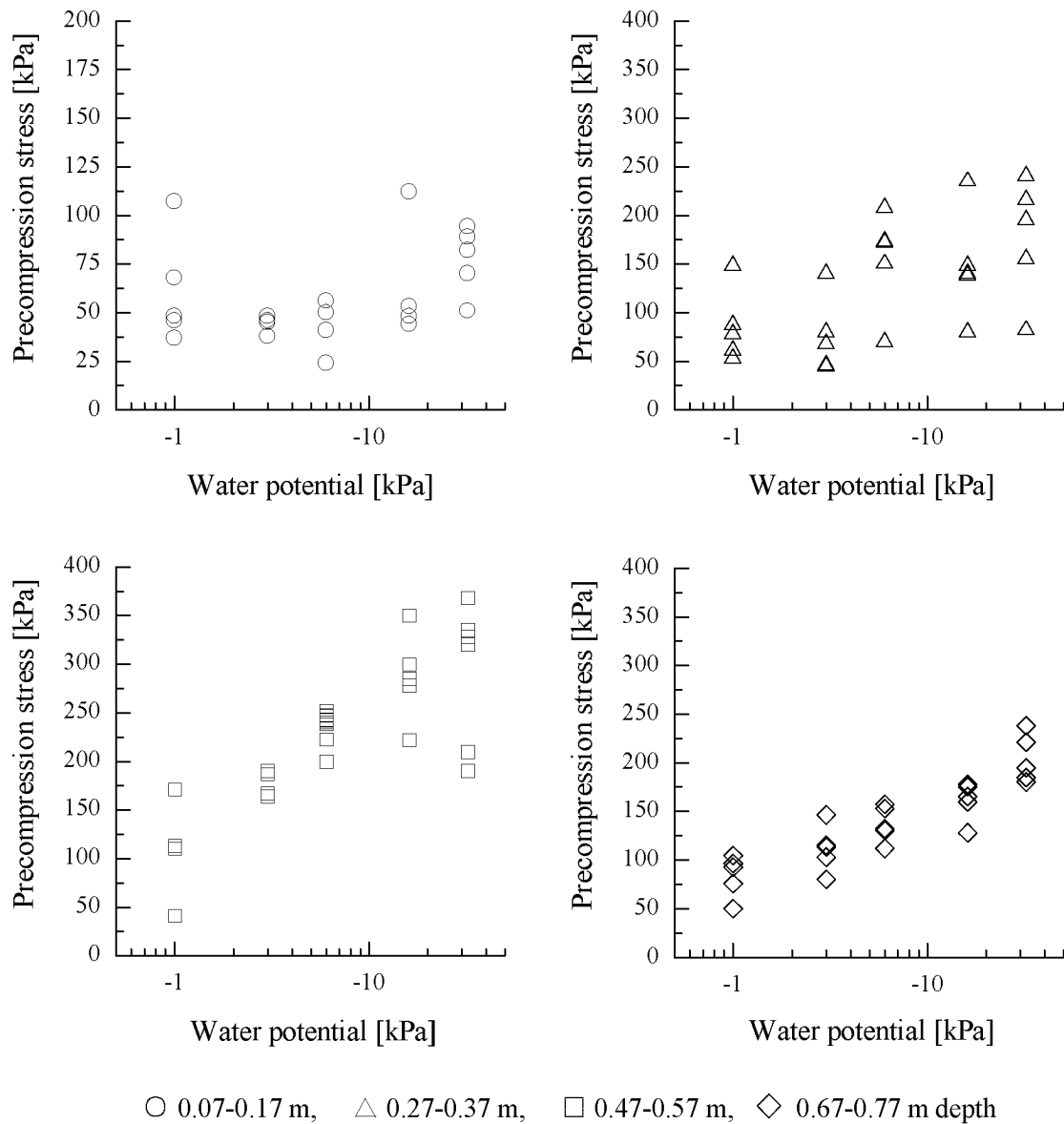
Fig. 4.7.   Precompression stress versus initial water potential determined from samples of 0.07-0.17, 0.27-0.37, 0.47-0.57 and 0.67-0.77 m depth.

In the topsoil samples (0.07-0.17 m depth), no clear trend is visible, while the upper subsoil samples (0.27-0.37 m depth) show a weak trend and thus a behaviour in between topsoil and lower subsoil. Interestingly, in the case of the upper subsoil (0.27-37 m depth) precompression stress was more closely related to water content (Fig. 4.8) than to water potential (Fig. 4.7). However, no relationship was found between saturation degree and precompression stress for any depth. Also void ratio showed no relationship with precompression stress for individual depths (Fig. 4.6).
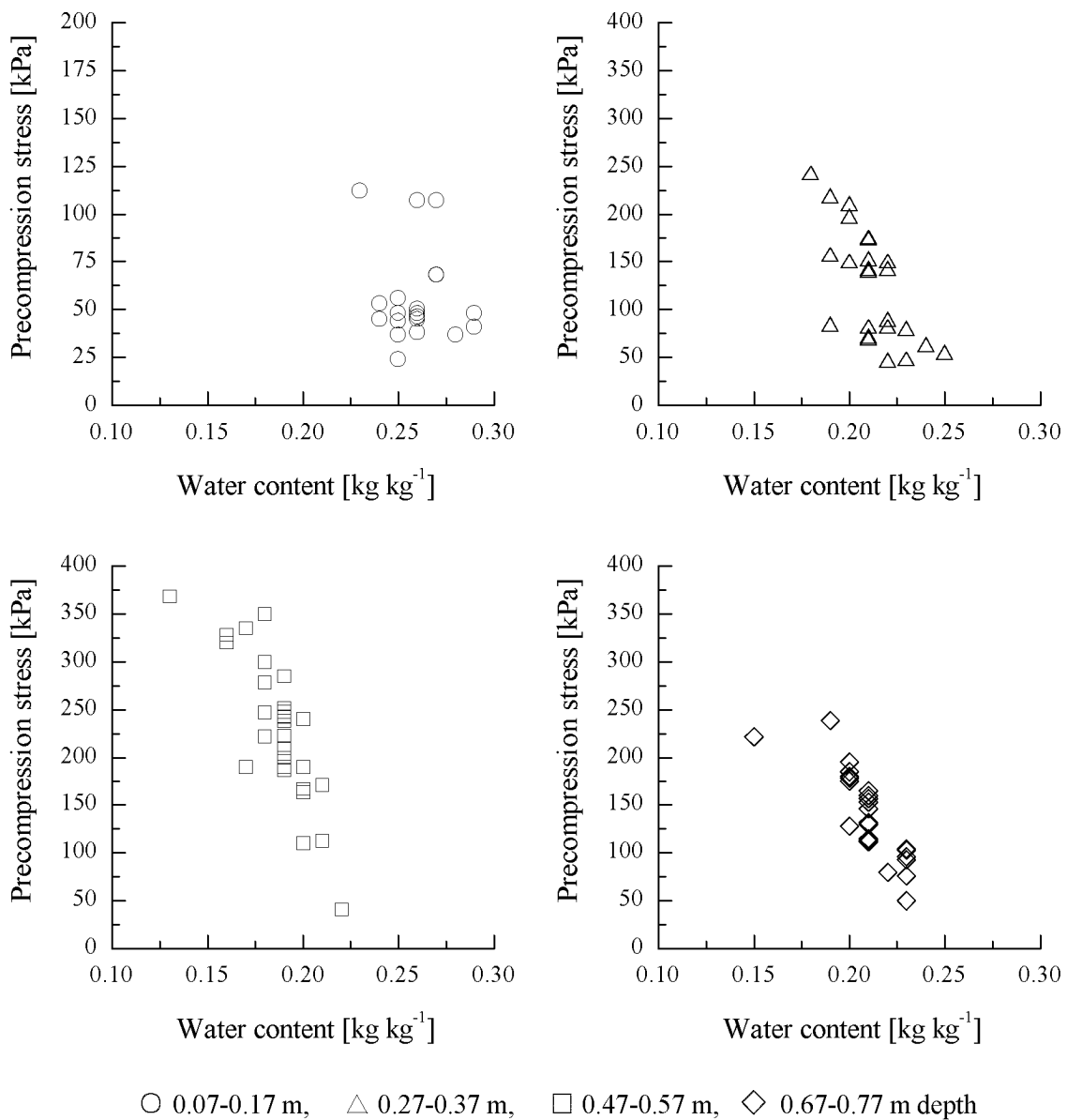
Fig. 4.8.   Precompression stress versus initial water content determined from samples of 0.07-0.17, 0.27-0.37, 0.47-0.57 and 0.67-0.77 m depth.

The increase in precompression stress was much larger than the corresponding decrease in water potential. With an decrease in water potential of 29 kPa from -3 to -32 kPa, precompression stress increased from 180 to 312 kPa for 0.47-0.57 m depth and from 111 to 204 kPa for 0.67-0.77 m depth (Fig. 4.7). In terms of effective stress, the influence of water potential on precompression stress would be even stronger.
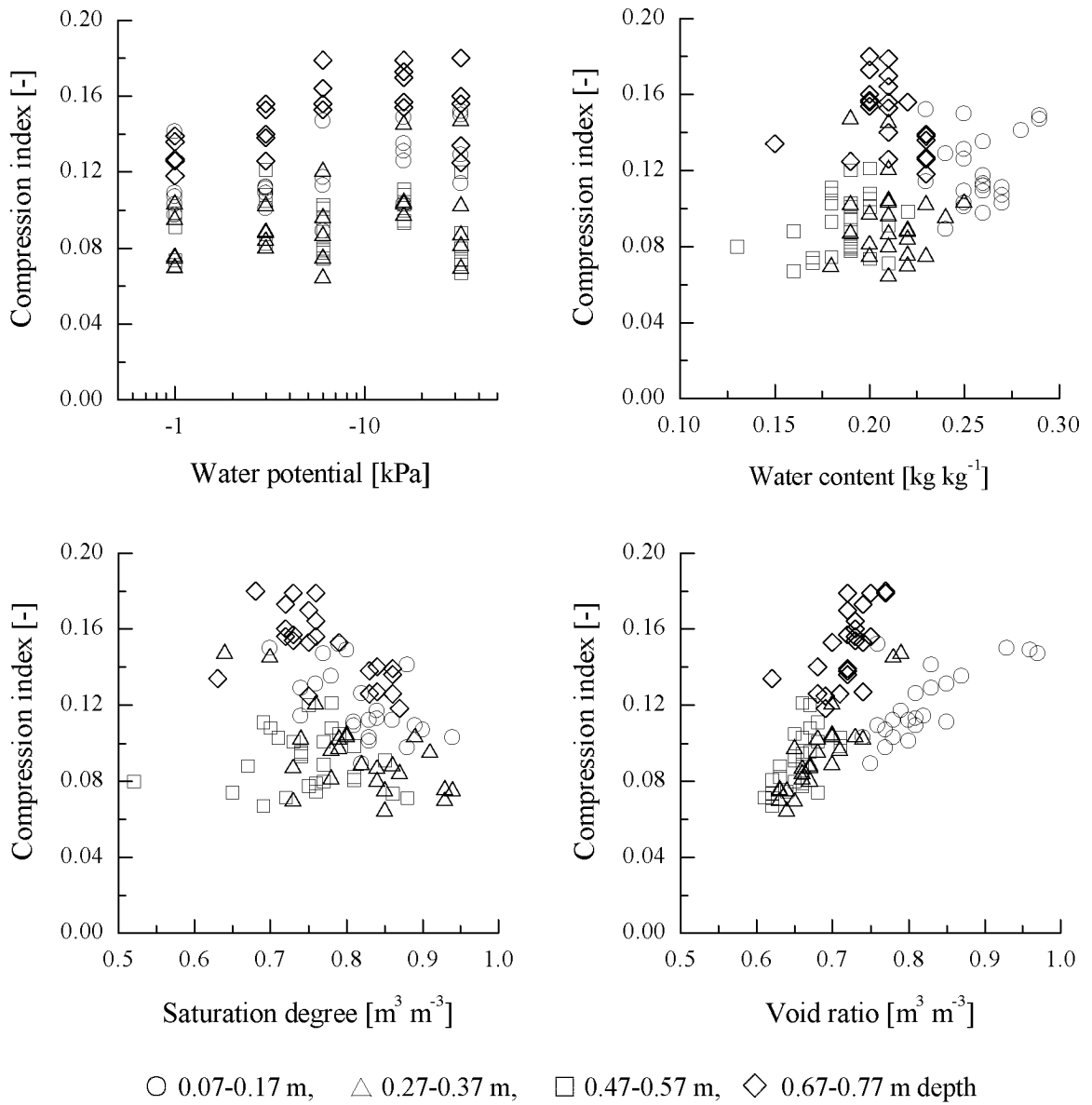
Fig. 4.9.   Compression index C_c versus initial values of water potential, water content, saturation degree and void ratio.

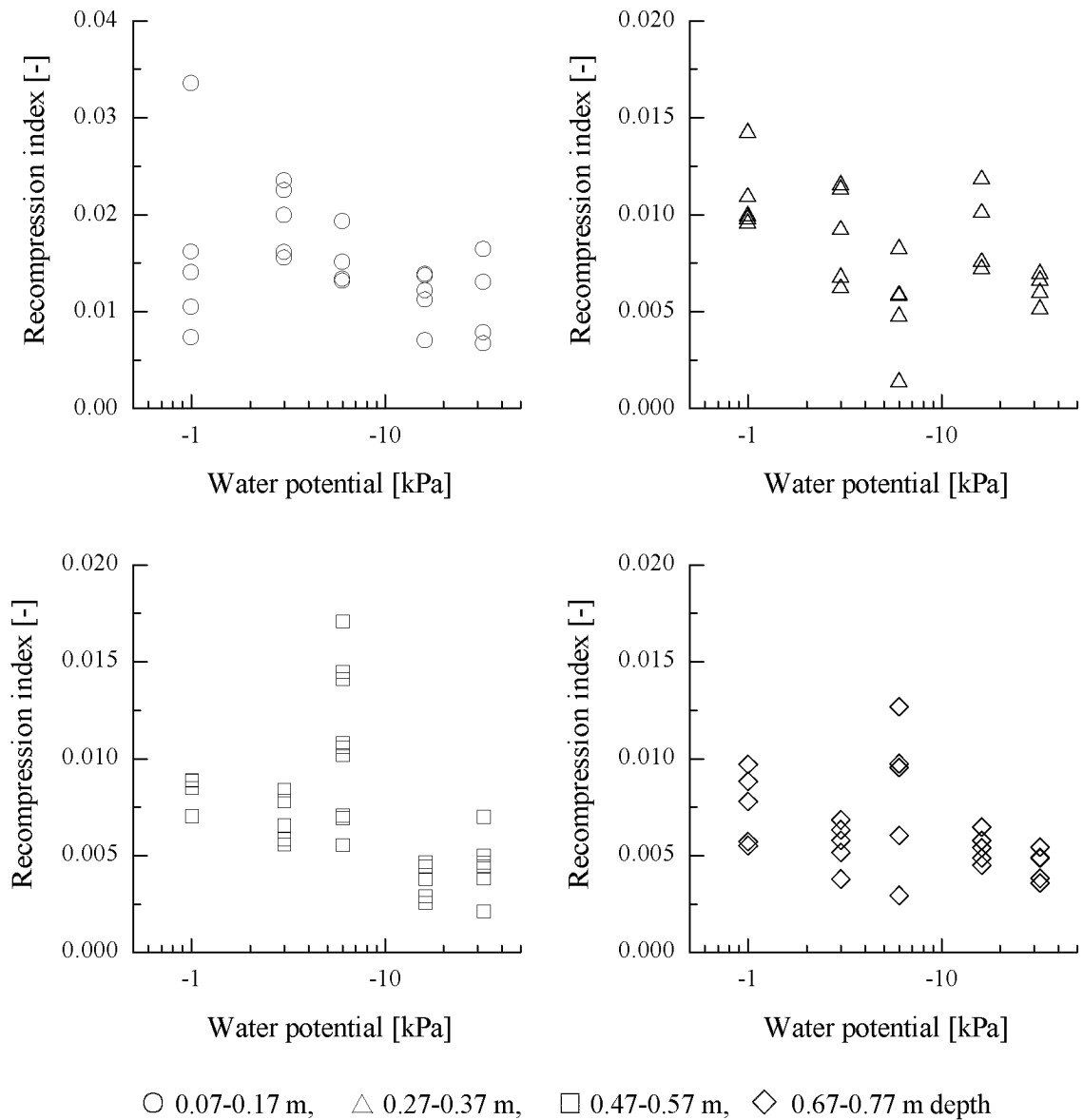O 0.07-0.17 m,   △ 0.27-0.37 m,   □ 0.47-0.57 m,   ◇ 0.67-0.77 m depth
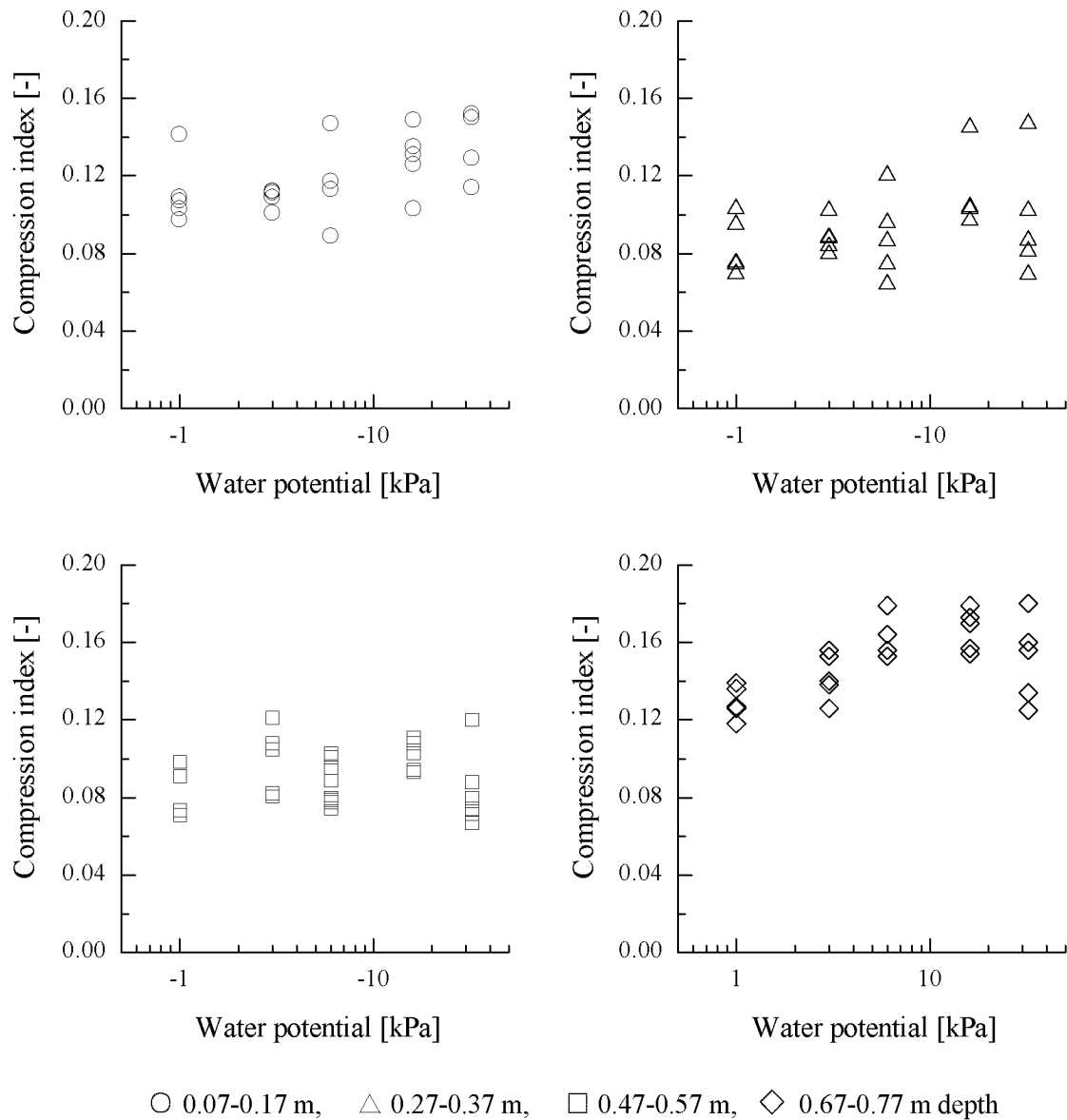
Fig. 4.10.   Compression index C_c versus initial water potential determined from samples of 0.07-0.17, 0.27-0.37, 0.47-0.57 and 0.67-0.77 m depth.

The compression index showed only a slight tendency to decrease with decreasing water potential and no correlation at all with initial water content and saturation degree (Fig. 4.9 and 4.10).

$\bigcirc$ 0.07-0.17 m, $\triangle$ 0.27-0.37 m, $\square$ 0.47-0.57 m, $\diamondsuit$ 0.67-0.77 m depth
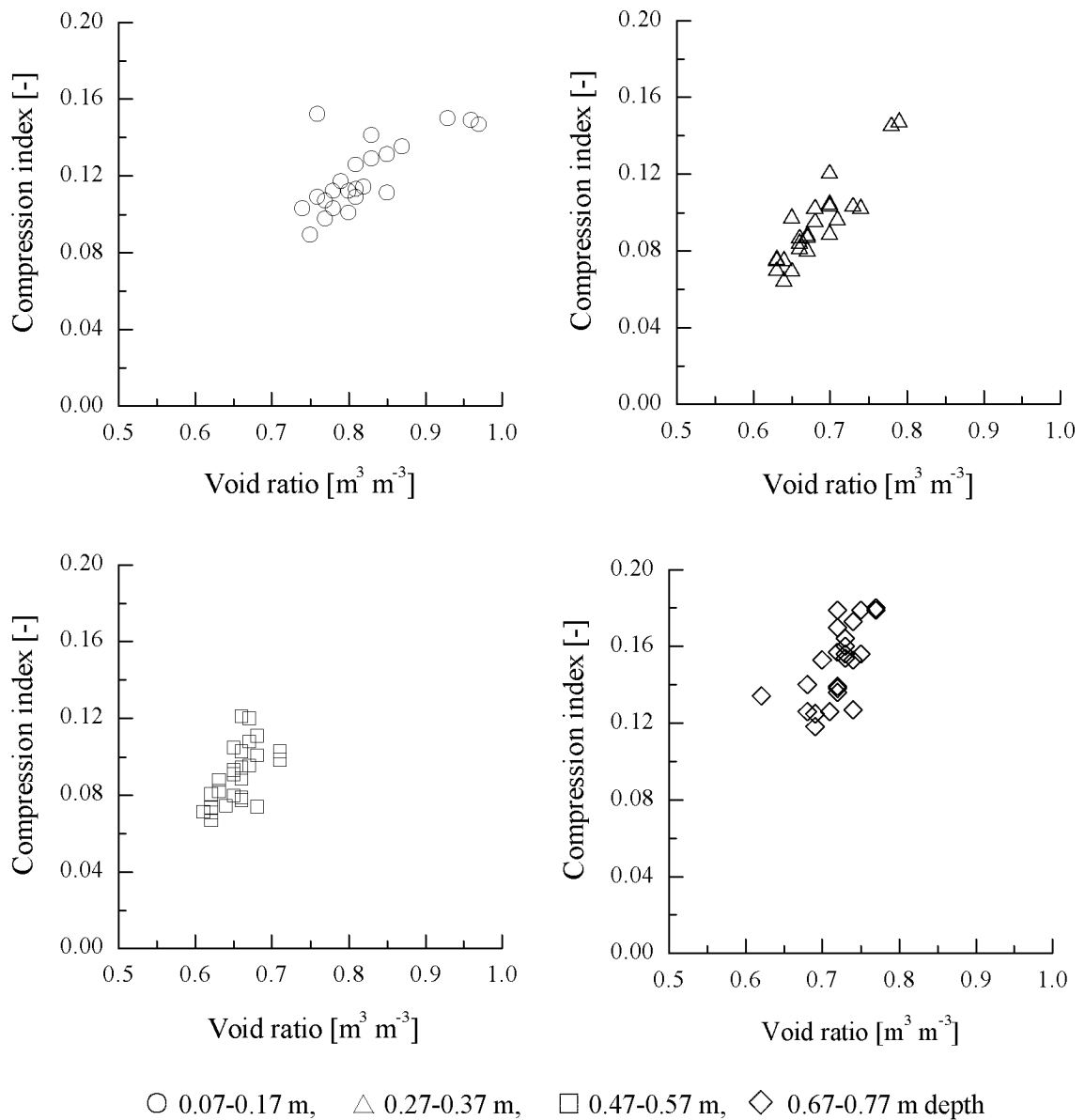
Fig. 4.11.   Compression index C_c versus initial void ratio determined from samples of 0.07-0.17, 0.27-0.37, 0.47-0.57 and 0.67-0.77 m depth.

The compression index was strongly correlated with initial void ratio (Fig. 4.11). Combining the samples of the lower two subsoil depths (0.47-0.57 and 0.67-0.77 m), they fall approximately on the same line, while the topsoil samples (0.07-0.17 m depth) follow a line with a much smaller slope. The upper subsoil samples (0.27-0.37 m depth) lie in between the other two relationships (Fig. 4.11).
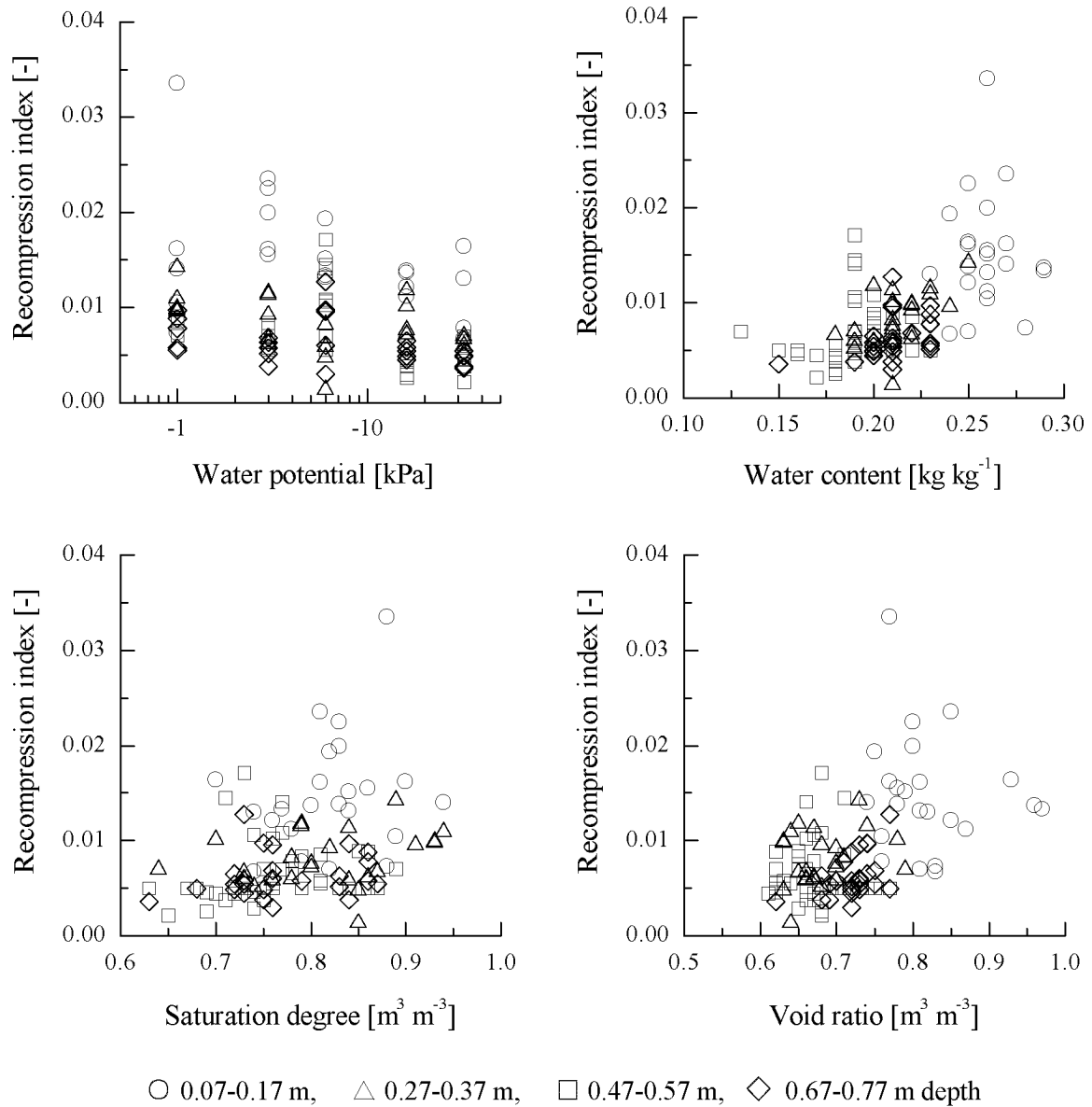
Fig. 4.12. Recompression index C_r versus initial values of water potential, water content, saturation degree and void ratio.

Fig. 4.13. Recompression index C_r versus initial water potential determined from samples of 0.07-0.17, 0.27-0.37, 0.47-0.57 and 0.67-0.77 m depth.

The only relationship found between recompression index and moisture variables was a slight tendency to decrease with decreasing water potential (Fig. 4.13). No correlation was found between recompression index and initial water content, saturation degree and void ratio (Fig. 4.12).

4.4 Discussion and conclusions

In summary precompression stress was distinctly dependent on initial water conditions (Table 4.4). Compression and recompression index, however, correlated only partially with the initial water conditions.

Table 4.4.   Correlation between initial negative water potential, gravimetric water content, saturation degree, void ratio and precompression stress, compression and recompression index (++: strong positive correlation, +: weak positive correlation, --: strong negative correlation, -: weak negative correlation, 0: no correlation)

	Depth	Precompression stress	Compression index	Recompression index
	[m]	[kPa]	[-]	[-]
Negative water	0.07-0.17	+	+	-
potential	0.27-0.37	+	+	-
[kPa]	0.47-0.57	++	0	-
	0.67-0.77	++	+	-
Water content	0.07-0.17	0	0	0
[kg kg^{-1}]	0.27-0.37	--	0	+
	0.47-0.57	--	0	0
	0.67-0.77	--	0	0
Saturation degree	0.07-0.17	0	0	0
[m^3 m^{-3}]	0.27-0.37	0	0	+
	0.47-0.57	-	0	0
	0.67-0.77	-	0	0
Void ratio	0.07-0.17	0	++	0
[m^3 m^{-3}]	0.27-0.37	-	++	0
	0.47-0.57	0	++	0
	0.67-0.77	0	++	0

To describe changes in compression characteristics due to various moisture conditions, water potential is the most sensitive parameter since it was correlated to more compression parameters than other explanatory variables (see Table 4.4). An interesting point was that the compression index was stronger correlated with the initial void ratio than with moisture conditions although the former was in a rather small range and could not be varied systematically. This indicates that not only soil moisture but also soil density conditions, e.g. expressed as void ratio or dry bulk density, are required to explain changes in compression characteristics.

The correlation between precompression stress and moisture content of undisturbed samples found in this study agree well with the results reported by Culley and Larson (1987), Horn (1988), Lebert (1989), Kirby (1991), Semmel (1993) and O'Sullivan and Robertson (1996). For the compression and rebound index of undisturbed samples, however, O'Sullivan and Robertson (1996) reported increasing compression and rebound indices with decreasing water content which contradicts the current findings. The results of O'Sullivan and Robertson (1996) are probably due to the higher initial density of the wet compared with the dry soil. Culley and Larson (1987) also found slightly increasing compression indices with decreasing water potential. Kirby (1991) reported that the compression index was clearly related to void ratio and saturation degree but only weakly to moisture content. Between recompression line and initial water content Culley and Larson (1987) as well as Kirby (1991) found no clear trend which agrees with the current results.

An explanation of the observed compression behaviour may be that compression and yielding are the macroscopic manifestation of microscopic particle movements. In unsaturated soil, the particles are forced together by the action of water menisci around grain contacts. These act as a normal force at the contact, additional to any applied force, and comprise both a water surface tension component and an applied suction component. Compression (and other deformations) occur as slippage at the contact when the transverse (shear) force there exceeds the resistance to movement: this resistance is related to the normal force by a Coulomb like friction law. Changing water potential changes this normal contact force, and hence the resistance to slippage. The gradual transition from elastic to plastic compression arises because there are many contacts, with many orientations, contact areas, mineral composition, etc. The weakest contacts slip first, followed by progressively more resistant contacts until finally all contacts slip. Macroscopically, we see the gradual transition. Burland (1965) and Newland (1965) provide a more detailed discussion of these issues. In very wet (saturated or near satu-

rated) soil, contact slippage can occur but unless the water can escape in the time available, there is no overall compression. This is the conventional explanation for an observation of consolidation in civil engineering soil mechanics. The lack of overall compression we interpret in the total stress approach as a small compression index. The dependence of compression behaviour on the void ratio (or density) arises because at smaller void ratio there are more particle contacts. A greater applied stress is required to supply the force required to cause slippage at each particle contact.

It can be concluded from the present study that moisture was an important factor governing the mechanical properties of the subsoil. But, at least in the range we investigated, it was much less important for the topsoil. The different parts of the stress-compression curve were each most closely related to initial soil moisture or density status. The closest relationships were found between precompression stress and initial water potential or water content, and between compression index and initial void ratio. Linear relationships were found between precompression stress and the initial water content or the logarithm of water potential. From a practical point of view, the finding of a strong dependence of the precompression stress on the initial moisture status means that this factor should be considered in setting limits for the allowable trafficability in order to protect the subsoil against compaction.

Acknowledgement

4.5 References

Adams, B.A. and Wulfsohn, D., 1997. Variation of the critical-state boundaries of an agricultural soil. European Journal of Soil Science, 48: 739-748.

BEW, 1997. Richtlinien zum Schutze des Bodens beim Bau unteririsch verlegter Rohrleitungen, Bundesamt für Energiewirtschaft (BEW), Bern.

Burland, J.B., 1965. Some aspects of the mechanical behaviour of partly saturated soils. Moisture Equilibria and Moisture Changes Beneath Covered Areas. Butterworths, Sydney, pp. 270-278.

Casagrande, A., 1936. The determination of pre-consolidation load and its practical significance. 1st International Conference on Soil Mechanics and Foundation Engineering, Harvard University, Cambridge, Massachusetts. pp. 60-64.

Culley, J.L.B. and Larson, W.E., 1987. Susceptibility to compression of a clay loam Haplaquoll. Soil Science Society of American Journal, 51: 562-567.

Dexter, A.R. and Tanner, D.W., 1974. Time dependence of compressibility for remoulded and undisturbed samples. Journal of Soil Science, 25: 153-164.

FAO, 1990. FAO-Unesco Soil Map of the World, Food and Agriculture Organisation of the United Nations (FAO), Revised Legend, Rome.

Greacen, E.L., 1960. Water content and soil strength. Journal of Soil Science, 11(2): 313-333.

Hettiaratchi, D.R.P., 1987. A critical state soil mechanics model for agricultural soils. Soil Use and Manangement, 3(3): 94-105.

Hettiaratchi, D.R.P. and O'Callaghan, J.R., 1985. The mechanical behaviour of unsaturated soils. International Conference on Soil Dynamics, Auburn, Alabama. pp. 266-281.

Horn, R., 1988. Compressibility of arable land. In: J. Drescher, R. Horn and M. De Boodt (Editors). Impact of Water and External Forces on Soil Structure, Catena Supplement 11. Catena-Verlag, Cremlingen-Destedt, pp. 53-71.

Horn, R., Taubner, H., Wuttke, M. and Baumgartel, T., 1994. Soil physical properties related to soil structure. Soil & Tillage Research, 30: 187-216.

Jennings, J.E.B. and Burland, J.B., 1962. Limitations of the use of effective stresses in partially saturated soils. Géotechnique, 12(1): 125-144.

Kirby, J.M., 1989. Measurements of the yield surfaces and critical state of some unsaturated agricultural soils. Journal of Soil Science, 40: 167-182.

Kirby, J.M., 1991. Critical-state soil mechanics parameters and their variation for Vertisols in eastern Australia. Journal of Soil Science, 42: 487-499.

Larson, W.E., Gupta, S.C. and Useche, R.A., 1980. Compression of agricultural soils from eight soil orders. Soil Science Society of America Journal, 44: 450-457.

Lebert, M., 1989. Beurteilung und Vorhersage der mechanischen Belastbarkeit von Ackerböden. PhD Thesis, Fakultät für Biologie, Chemie und Geowissenschaften, Universität Bayreuth, Bayreuth, 131 pp.

Leeson, J.J. and Campbell, D.J., 1983. The variation of soil critical state parameters with water content and its relevance to the compaction of two agricultural soils. Journal of Soil Science, 34: 33-44.

Maâtouk, A., Leroueil, S. and La Rochelle, P., 1995. Yielding and critical state of collapsible unsaturated silty soil. Géotechnique, 45(3): 465-477.

Matyas, E.L. and Radhakrishna, H.S., 1968. Volume change characteristics of partially saturated soils. Géotechnique, 18: 432-448.

Newland, P.L., 1965. The behaviour of soils in terms of two kinds of effective stress. Engineering Effects of Moisture Changes in Soils. Texas A&M, Texas, pp. 78-92.

O'Sullivan, M.F., Campbell, D.J. and Hettiaratchi, D.R.P., 1994. Critical state parameters derived from constant cell volume triaxial tests. European Journal of Soil Science, 45: 249-256.

O'Sullivan, M.F. and Robertson, E.A.G., 1996. Critical state parameters from intact samples of two agricultural topsoils. Soil & Tillage Research, 39: 161-173.

Panayiotopoulos, K.P., 1996. The effect of matric suction on stress-strain relation and strength of three Alfisoils. Soil & Tillage Research, 39: 45-59.

Petersen, C.T., 1993. The variation of critical-state parameters with water content for two agricultural soils. Journal of Soil Science, 44: 397-410.

Semmel, H., 1993. Auswirkungen kontrollierter Bodenbelastungen auf das Druckfortpflanzungsverhalten und physikalisch-mechanische Kenngrössen von Ackerböden. PhD Thesis, Institut für Pflanzenernährung und Bodenkunde, Christian-Albrechts-Universität, Kiel, 183 pp.

Söhne, W., 1953. Druckverteilung im Boden und Bodenverformung unter Schlepperreifen. Grundlagen der Landtechnik, 5: 49-63.

Söhne, W., 1958. Fundamentals of pressure distribution and soil compaction under tractor tires. Agricultural Engineering, May: 276-291.

Stone, J.A. and Larson, W.E., 1980. Rebound of five one-dimensionally compressed unsaturated granular soils. Soil Science Society of America Journal, 44: 819-822.

Wheeler, S.J. and Sivakumar, V., 1995. An elasto-plastic critical state framework for unsaturated soil. Géotechnique, 45(1): 35-53.

5

Modelling compaction of agricultural subsoils by tracked heavy construction machinery under various moisture conditions

M. Berli, J.M. Kirby, S.M. Springman and R. Schulin

Abstract

In recent years, agricultural land in Switzerland has been increasingly used as temporary access ways for heavy machinery in road and pipeline construction operations. The Swiss soil protection law requires that measures are taken to prevent soil compaction in such operations, but gives no criteria to determine tolerable loads. We studied the compaction sensitivity of a loess soil (Haplic Luvisol) at different soil moisture conditions in a field traffic experiment and by a numerical model on the computer using finite element analysis. Two plots, one wetted by sprinkling and one left 'dry' (no sprinkling), were traversed by heavy caterpillar vehicles during construction of a large overland gas pipe-line. Compaction effects were determined by comparing precompression stresses of samples taken from trafficked and non-trafficked soil. A finite element model with a constitutive relation, based on the concept of critical state soil mechanics, was used to interpret the outcome of the field trials.

We found significantly higher precompression stresses in the trafficked (median 97 kPa) compared with the non-trafficked (median 41 kPa) topsoil of the 'wet' plot. No effect was evident in the topsoil of the 'dry' plot as well as in the subsoils of the 'wet' and the 'dry' plot. The observed compaction effects were in agreement with the model predictions if the soil was assumed to be partially drained but disagreed for the 'wet' subsoil, if fully drained conditions were assumed. Agreement between model and experimental results also required that the moisture dependence of the precompression stress was taken into account.

5.1 Introduction

In recent years, Swiss agricultural land has become increasingly affected by temporary use as access ways for heavy machinery in the course of overland gas pipeline construction.

Fig. 5.1.   Placement of sections of pipeline.

A typical construction sequence consists of the removal of the topsoil in the trench area, excavation of a trench 2-3 m deep, placement of the pipes (see Fig. 5.1) and the refilling of the trench followed by recultivation of the trench area. Many of the excavators weigh more than 4×10^4 kg, some even more than 6×10^4 kg unloaded. The tracked machinery for placing the pipes is in general also very heavy, weighing 3×10^4 kg and more without load. Trafficking agricultural land with such heavy machines inevitably will increase the risk of undesired compaction of the subsoil.

To characterise the sensitivity of a soil for compaction, Horn (1988), Horn and Lebert (1994) and Kirby (1991b) proposed using the precompression stress. Compaction leads to increase of the soil strength, and the precompression stress can therefore be a useful measure of strength. The slow moving, heavy construction equipment with wide, rigid steel tracks is expected to compact the soil and increase the precompression stress. Blunden et al. (1994) showed that compaction by tracked and tyred vehicles significantly affected the precompression stress of an earthy sand at 4 % moisture content. Kirby et al. (1997) simulated the results of Blunden et al. (1994) using a critical state, finite element model. They concluded that, while the simulated results agreed with the measurements, the latter had a large range and the comparison was not useful. Kirby et al. (1997) also

simulated the results of several soil bin tests, and concluded that agreement between measurement and model was poor, because the precompression stress varied greatly over small distances (due to the gradient of compacting stresses beneath the tyre) and samples taken for precompression stress were too large to observe these changes. Apart from the problem of dealing with the spatial heterogeneity, a major difficulty in the application of such models to practical field situations with variably saturated soil arises from the dependence of precompression stress on soil moisture content.

Addressing these problems, an opportunity was presented during the course of the construction of a gas pipeline to carry out a field experiment with the heavy machinery used in that work. Our aim was to measure the compaction caused by the machinery, and to investigate whether the precompression stress was a useful indicator of the likely compaction.

The experiment was performed on two plots immediately adjacent to the trench. One plot was artificially wetted by sprinkling, the other was kept 'dry'. One part of each plot was mechanically stressed by the heavy machinery used to place the tubes into the trench (Fig. 5.1). The idea of the experiment was to compare the precompression stress of the soil under the tracks with the precompression stress of non-affected soil beside the tracks, in order to assess compaction effects. Measured precompression stresses were compared with vertical stresses calculated with the critical state soil mechanics model 'Modified Cam Clay' (Britto and Gunn, 1987).

5.2 Material and methods

The experimental site was an arable field, located on the 'Ruckfeld', a loess plain in the north-west of Zurich, Switzerland.

Table 5.1.   Soil parameters of the 'wet' plot

Depth [m]	Sand [kg kg^{-1}]	Silt [kg kg^{-1}]	Clay [kg kg^{-1}]	Gravel [m^3 m^{-3}]	Organic matter [kg kg^{-1}]	Bulk density [kg m^{-3}]
0.07-0.17	0.31	0.55	0.14	< 0.01	0.033	1310
0.27-0.37	0.28	0.60	0.12	< 0.01	0.011	1570
0.47-0.57	0.26	0.57	0.17	< 0.01	0.011	1510
0.67-0.77	0.25	0.57	0.18	< 0.01	0.010	1520

Table 5.2.   Soil parameters of the 'dry' plot

Depth [m]	Sand [kg kg^{-1}]	Silt [kg kg^{-1}]	Clay [kg kg^{-1}]	Gravel [m^3 m^{-3}]	Organic matter [kg kg^{-1}]	Bulk density [kg m^{-3}]
0.07-0.17	0.23	0.57	0.16	< 0.01	0.031	1360
0.27-0.37	0.22	0.55	0.16	< 0.01	0.025	1530
0.47-0.57	0.22	0.58	0.16	< 0.01	0.015	1540
0.67-0.77	0.25	0.56	0.17	< 0.01	0.012	1610

Data on soil texture, organic matter content and bulk density are given in Table 5.1 and 5.2. Gravel content was less than 1 % by volume over the entire profile. Soil type was a Haplic Luvisol (FAO, 1990). The field was under crop rotation and was covered by grass during the season of the experiment.
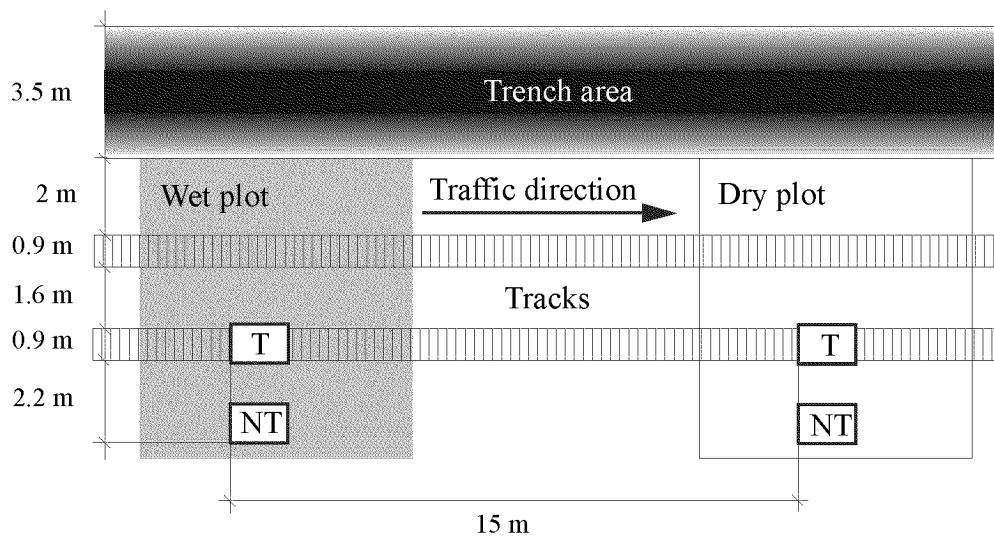
Fig. 5.2. Situation of the field experimental site with sampling areas: NT non-trafficked, T trafficked.

The two test plots were chosen adjacent to the trench (Fig. 5.2). The plot to be wetted was sprinkled during five days at a rate of 0.1 m d^{-1}. After that, the soil was left to redistribute the infiltrated water for one more day. Soil water potentials were monitored in the 'wet' and in the 'dry' plot by tensiometers set at depths of 0.12, 0.32, 0.52 and 0.72 m (mean depth of ceramic cup, 3 replicates per depth). Three different construction machines were used. Relevant characteristics are given in Table 5.3.

Table 5.3. Machinery used for the experiment

Machine type	Net machine weight [kg]	Length of the contact area [m]	Width of the contact area (twice track width) [m]	Net mean normal stress in the contact area [kPa]
Fiat FH 300	3.02×10^4	4.0	1.8	42
Fiat Allis PL 40 C	2.56×10^4	3.5	1.4	51
Cat 583	3.8×10^4	3.2	1.5	78

In the experiment, a Fiat FH 300 was followed by a Fiat PL 40 C, a Cat 583 and a second Fiat FH 300. These machines drove at speeds between 0.1 and 0.2 m s^{-1}, stopping on each of the plots for 120 s. They did not perform any 'work' relating to the pipeline construction, carrying no load during these passages. The contact stresses are similar to

those experienced in agricultural operations using low ground stress tyres (e.g. Vermeulen and Perdok, 1994) or tracks (e.g. Kirby and Blunden, 1992).

After the vehicle pass, soil profiles were opened across the plots at right angles to the direction of the pass, and soil cores of 10^{-3} m^3 volume were sampled using sharpened metal cylinders of 0.11 m height and 0.108 m inner diameter. We took samples from 'wet' and 'dry' trafficked and non-trafficked soil from 0.07-0.17, 0.27-0.37, 0.47-0.57 and 0.67-0.77 m depth (6 replicates per treatment and depth) and conditioned them to -6 kPa initial soil water potential. Uniaxial compression tests were performed on them and precompression stress was estimated from these tests. We were thus able to compare the precompression stress of trafficked and non-trafficked soil at the same initial soil water potential. The large sample volume was used in order to adequately represent the macrostructure of the soil. The representative elementary volume of a soil must be expected in general to be much larger for undisturbed field soils than for remoulded, fine grained 'engineering' soils. In preliminary experiments, we performed confined uniaxial compression tests with undisturbed samples of 0.03 and 0.11 m height (0.1 and 0.108 m inner diameter, respectively) and found no significant difference in compression behaviour. Other samples of non-trafficked soil from 0.07-0.17, 0.27-0.37, 0.47-0.57 and 0.67-0.77 m depth were brought to a range of initial soil water potentials between -1 and -32 kPa (5-9 replicates per soil water potential and depth). Uniaxial compression tests were performed from which the precompression stresses at different initial soil water potentials were determined. We were thus able to derive a quantitative relationship between soil water potential and precompression stress. With this relationship we could estimate the precompression stress in the field, immediately before the machinery trafficked the soil, this value being required for use in the finite element model.

For the confined uniaxial compression tests, samples were kept within the coring cylinders, built into the compression cell and subsequently subjected to stepwise increased stress. Stress was applied through a piston, which fitted the opening of the cylinders. Each compression step lasted for 1800 s after which the stress was increased to the next level. A maximum duration of 1800 s for each compression step was chosen because this represented the time of a machine staying at the same place during normal construction work. Precompression stress was determined from the resulting stress-strain curves using the graphical procedure of Casagrande (1936).

Soil-vehicle interaction calculations were performed on the continuum with the finite element program „Sage Crisp" Version 4.02 using the constitutive model 'Modified Cam Clay' to describe the mechanical behaviour of the soil in terms of critical state soil mechanics (Britto and Gunn, 1987). The experiment was modelled as a plane strain problem

with the rigid track acting as an infinite strip load. Symmetry required only half the problem domain to be modelled, which was chosen to be 2 m wide and 2.8 m deep (Fig. 5.3). The finite element mesh comprised 420 triangular elements ranging in size from 0.05 by 0.05 m near the track to 0.2 by 0.6 m in the corner farthest away from the track. The load exerted by the rigid steel track onto the soil surface was considered to be uniformly distributed over the entire contact area. The load was assumed to be a normal stress of 78 kPa applied on a 0.75 m wide strip, which is equivalent to the mean normal stress and the width of the contact area under the heaviest machine used for the experiment. Shear tractions at the surface were ignored, because the vehicles were either standing still or moving slowly without draft, and so shear tractions were probably small.
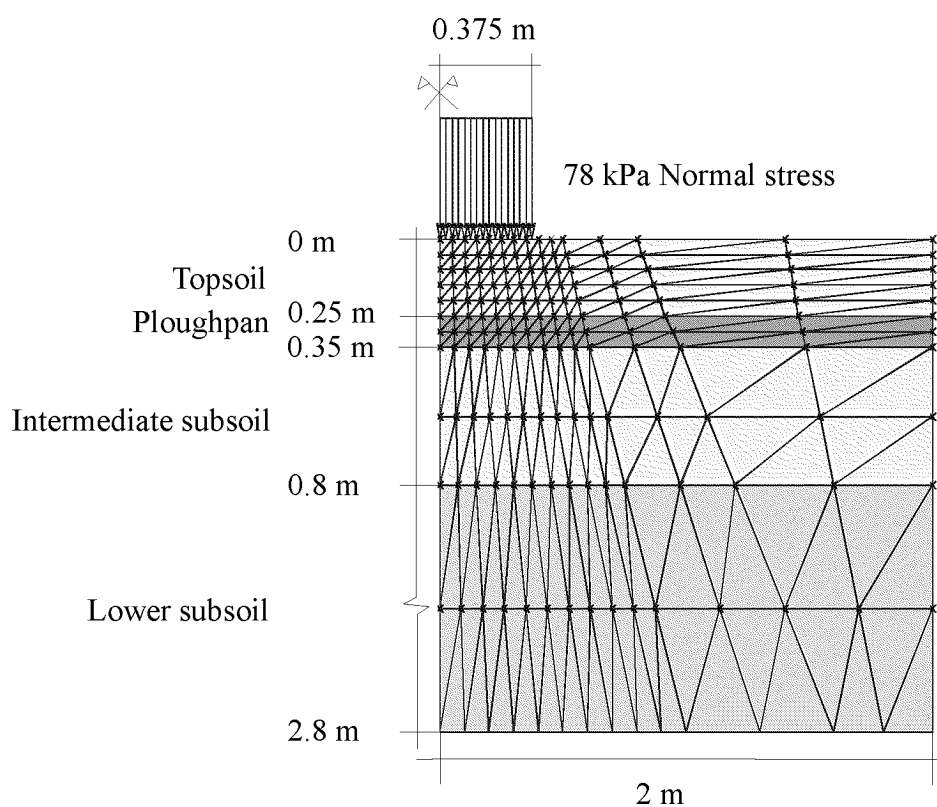
Fig. 5.3.   The finite element mesh chosen for the calculation.

The finite element mesh was divided into four layers with different critical state stress-strain soil properties. For the topsoil (0-0.25 m), the ploughpan (0.25-0.35 m) and the intermediate subsoil (0.35-0.8 m), the slope of the normal consolidation line, λ, the slope of the reload line, κ, and the initial void ratio on the critical state line, e_{cs}, were determined from the stress-strain relationships obtained from the uniaxial compression tests on samples from the non-trafficked 'wet' and 'dry' plots described above. The slope of the critical state line, M, was determined by direct shear tests for these layers, measured

separately on samples from non-trafficked soil. These tests were carried out with undisturbed samples (0.02 m thick, 0.1 m diameter) taken from non-trafficked soil from 0.07-0.17, 0.27-0.37, 0.47-0.57 and 0.67-0.77 m depth and also conditioned to an initial soil water potential of -6 kPa in the laboratory by applying a hanging water column. After consolidation for 1800 s, the samples were sheared in a direct shear box with a constant shear velocity of 5×10^{-7} m s^{-1}. During consolidation and shearing, a constant normal stress was imposed on the samples. The shear tests were carried out under normally consolidated conditions which means that the normal stress applied to the sample was higher than the precompression stress. The angle of internal friction ϕ was determined graphically as the slope of the Mohr-Coulomb failure line. The slope of the critical state line, M, was calculated according to Britto and Gunn (1987 p 173) from the angle of internal friction ϕ with equation (5.1)

$$M = \frac{6 \sin \phi}{3 - \sin \phi}$$ (5.1)

The mechanical properties of the lower subsoil (0.8-2.8 m) were taken from triaxial and oedometer tests carried out by Rosal (1997) for the same site and were assumed to be the same for both plots. Poisson's ratio v was assumed to be 0.3 for the whole soil profile of both plots.

For the continuum calculation, the critical state soil properties M, λ, and κ were assumed to be constant during the traffic experiments. The initial precompression stress was calculated from the experimentally determined relationship between precompression stress and soil water potential (see Fig. 5.4) for the actual soil water potentials measured immediately before the passage of the machines (Table 5.4). The resulting precompression stress values are given in Table 5.5. The initial in situ vertical stress was considered to be the weight of the overlying soil. To calculate the initial horizontal stress, the initial vertical stress was multiplied by the initial coefficient of earth pressure at rest K_o. K_o was assumed to be 0.55 for the whole profile of the 'wet' and the 'dry' plot based on a simplified version of Jaky's empirical formula (Britto and Gunn, 1987, p. 180) considering measured angles of internal friction ϕ of 26° for the topsoil, 27° for the ploughpan and the intermediate subsoil and 28° for the lower subsoil.

For the 'dry' plot, vertical stress was calculated under fully drained conditions. Since in the 'dry' plot, soil water potentials were much lower than field capacity (= -6 kPa, see Table 5.4), air was assumed to be the continuous mobile phase 'draining' freely under compaction. For the 'wet' plot, two scenarios were compared with the simulations. In the first scenario, fully drained conditions were assumed, whereas in the second scenario, conditions were assumed to be partially drained. To calculate fully drained conditions,

we used an uncoupled model, meaning one in which only the solid stress-strain was considered, and there was no fluid in it all. By a partially drained model we used a coupled model, in which both the solid stress-strain and the fluid pressure-flow were considered. At all boundaries we used a constant fluid pressure boundary and set the excess fluid pressure to zero. That is, these boundaries could drain perfectly freely. At the part of the boundary (top surface) representing the track, we put on a normal stress of 78 kPa. For the fully drained analysis this stress was applied in one step whereas for the partially drained analysis, the normal stress was applied in 20 steps of 3.9 kPa lasting for 1 s each followed by a constant stress of 78 kPa lasting for 120 s. Since the track had gaps, and also the grass would act as a drainage zone, we also set it to a constant pressure boundary with zero excess fluid pressure. This had the effect of generating a fluid pressure, which dissipated as the air and water drained away, at a rate controlled by the air and water conductivity, and the pressure was transferred to the solid matrix. Because the time (120 s) was insufficient for all the excess water pressures to dissipate, we called this a partially drained simulation. Air was also assumed to be mobile in the second scenario for the topsoil, whereas air was assumed to be immobile and water mobility was considered to control compaction for the ploughpan, the intermediate and the lower subsoil. For the continuum calculation, air and water conductivity were assumed to be constant. Air and water conductivity values required for the calculations under partially drained conditions were estimated from Richard and Lüscher (1983, Lokalform 'Riedhof') (Table 5.4).

5.3 Results and Discussion

Immediately before the passage of the machines, the soil water potential was between saturation and field capacity (= -6 kPa) in the 'wet' plot and from field capacity down to more than -85 kPa in the 'dry' plot (Table 5.4). As the water potential in the topsoil of the 'dry' plot was out of the measurement range of tensiometers (-70 to -85 kPa), a conservative estimate of -100 kPa was taken, based on extrapolation of the observed trend in the time beforehand. Soil moisture conditions of the lower subsoil (> 0.8 m) were estimated to be at field capacity for the 'dry' condition and at saturation for the 'wet' plot.

Table 5.4. Soil water potential of the 'dry' and 'wet' plot and estimated air and water conductivity (Richard and Lüscher, 1983) of the 'wet' plot immediately before the passage of the machines

Depth [m]	Soil water potential of the 'dry' plot [kPa]	Soil water potential of the 'wet' plot [kPa]	Air (a) and water (w) conductivity of the 'wet' plot [m s^{-1}]
0.12	-100.0 [†]	-5.2	5×10^{-4} (a)
0.32	-85.0	-2.0	5×10^{-8} (w)
0.52	-33.4	-0.7	5×10^{-7} (w)
0.72	-16.3	-0.2	5×10^{-7} (w)
> 0.80	-6.0	0	3×10^{-6} (w)

[†] Estimated value

Precompression stress increased approximately linearly with the logarithm of negative soil water potential (Fig. 5.4). The dependence was stronger in the subsoil than in the topsoil. At soil water potentials close to saturation, measured precompression stresses did not further decrease but rather tended to increase with increasing water potential for the topsoil. Since we suspected that this was an artefact due to insufficient drainage and because water potentials were far outside the range encountered in the field trials, we omitted these values from the regression analysis. Only measurements of the precompression stress at water potentials of -6 kPa and below were taken into account for this depth.
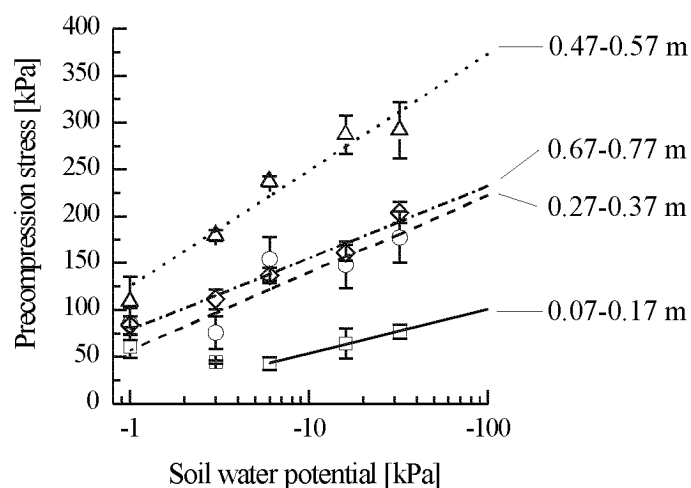
Fig. 5.4. Dependence of precompression stress on soil water potential (experimental data and regression lines). Points represent mean values of 4 to 9 replicate measurements, error bars are standard errors.

Table 5.5 shows that the calculated values of the precompression stresses obtained for the 'dry' plot were mostly two to three times higher than those of the 'wet' plot.

Table 5.5. Calculated precompression stresses and 95 % confidence interval of the two test plots immediately before the passage of the machines

Depth [m]	Average precompression stress of the 'wet' plot [kPa]	95 % confidence interval of the pre-compression stress of the 'wet' plot [kPa]	Average precompression stress of the 'dry' plot [kPa]	95 % confidence interval of the pre-compression stress of the 'dry' plot [kPa]
0.12	47	± 24	107	± 17
0.32	97	± 16	178	± 91
0.52	55	± 9	139	± 39
0.72	51	± 7	146	± 51

Despite considerable variability within each plot, the differences between the 'dry' and 'wet' plots were significant except for 0.32 m depth. The precompression stresses of the 'wet' ploughpan (0.32 m depth) and the entire 'dry' plot were larger than the mean normal stress in the contact area of the heaviest machine used for the traffic experiment.

Table 5.6.   Critical state soil properties of the 'wet' and the 'dry' plots determined at -6 kPa initial water potential, assumed to be independent of soil moisture

Critical state soil properties	Topsoil 0-0.25 m depth	Ploughpan 0.25-0.35 m depth	Intermediate subsoil 0.35-0.8 m depth	Lower subsoil 0.8-2.8 m depth [†]
'Wet' plot				
Slope of the virgin compression line, λ [-]	8.6×10^{-2}	4.0×10^{-2}	6.7×10^{-2}	4.8×10^{-2}
Slope of the recompression line, κ [-]	1.2×10^{-2}	2.9×10^{-3}	3.4×10^{-3}	1.2×10^{-2}
Initial void ratio on the critical state line at $\ln(p' = 1$ kPa$)$, e_{cs} [-]	1.21	0.82	0.99	0.80
'Dry' plot				
Slope of the virgin compression line, λ [-]	7.8×10^{-2}	4.6×10^{-2}	5.9×10^{-2}	4.8×10^{-2}
Slope of the recompression line, κ [-]	8.4×10^{-3}	3.6×10^{-3}	3.6×10^{-3}	1.2×10^{-2}
Initial void ratio on the critical state line at $\ln(p' = 1$ kPa$)$, e_{cs} [-]	1.11	0.86	0.91	0.80
Slope of the critical state line, M [-]	1.02	1.07	1.07	1.11

[†] Values according to Rosal (1997)

For the intermediate subsoil, the λ, κ, and e_{cs} values given in Table 5.6 are the arithmetic means of λ, κ, and e_{cs} determined from samples from 0.47-0.57 and 0.67-0.77 m depth. For the ploughpan and intermediate subsoil, the slopes of the normal consolidation line λ and the reload line κ of both plots were similar. While for the topsoil, the slopes of the normal consolidation line λ were also similar the slope of the reload line κ of the 'dry' plot was smaller than that of the 'wet' plot, although the samples were conditioned at the same initial soil water potential. The κ value of the lower subsoil was much smaller than

for the ploughpan and the intermediate subsoil. The values of κ are from 4 (lower subsoil) to about 20 times (intermediate subsoil of the 'wet' plot) smaller than λ. Kirby (1991a) found the same range of values for λ and κ and that the values for κ are about 20 times smaller than those for λ for various Vertisols in Australia.
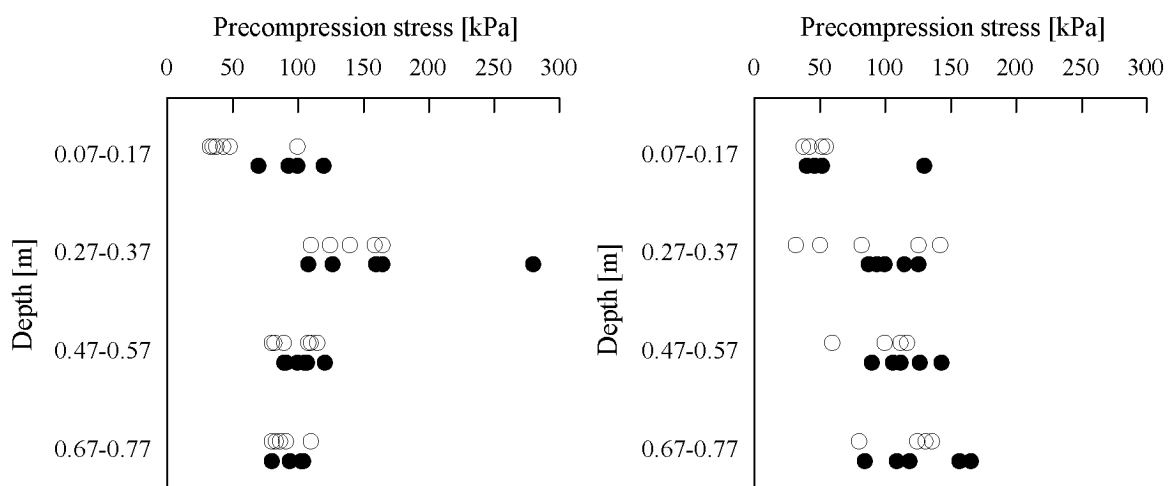
Fig. 5.5. Precompression stress of the trafficked (black circles) and non-trafficked soil (open circles) of the 'wet' (left graph) and 'dry' plot (right graph) determined at -6 kPa initial soil water potential.
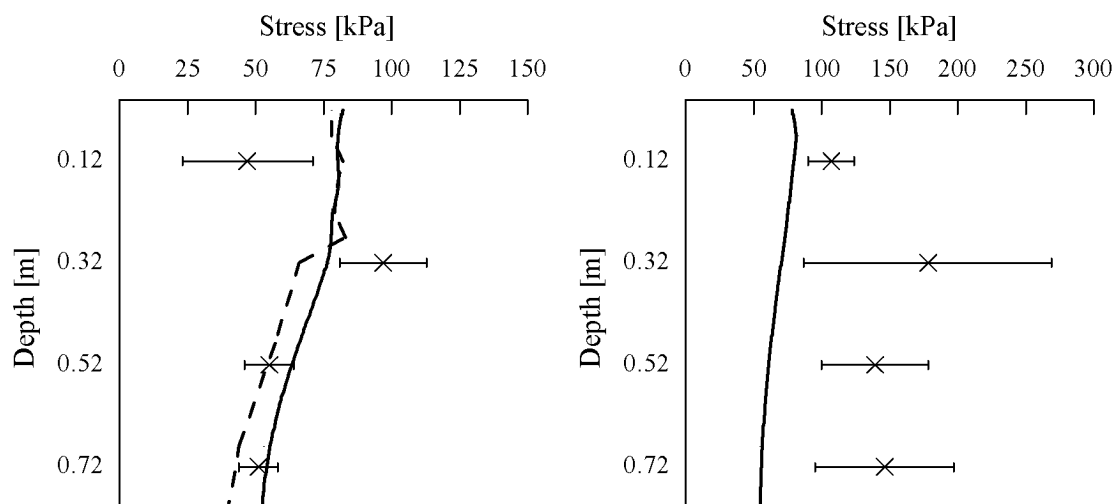
Fig. 5.6. Calculated precompression stresses (crosses with 95% error bars, accounting for sample variability but not for the uncertainty of transforming precompression stresses measured at -6 kPa to actual field soil water potential) from laboratory tests in comparison to effective vertical stresses calculated under fully (solid line) and partially (dashed line) drained conditions of the 'wet' (left graph) and 'dry' plot (right graph).

In the topsoil of the 'wet' plot we found a significant difference between the precompression stress of the non-trafficked soil (median 41 kPa) and the trafficked soil beneath the centre line of the tracks (median 97 kPa), while no such effect was evident in the topsoil of the 'dry' plot. In the subsoil, neither the 'wet' nor the 'dry' plot showed a significant effect of trafficking on precompression stress.

The calculated vertical stress acting on the 'wet' topsoil (0.12 m depth) was larger than the estimated precompression stress, while the estimated precompression stresses of the non-trafficked 'wet' ploughpan (0.32 m depth) and the entire 'dry' plot were larger than the calculated vertical stresses. For the intermediate subsoil of the 'wet' plot, the stresses predicted by the model exceeded the estimated precompression stresses by about 8 kPa at 0.52 m and were about equal at 0.72 m depth. The predicted stresses were within the 95% error bars at both depths. It therefore appears likely that the measured precompression stress would not have changed significantly (bearing in mind the statistical variability in the parameters) at 0.52 m or perhaps not at all at 0.72 m. Furthermore, the fully drained analysis gives the maximum stresses that could have compacted the soil. In fact, the pore water pressure in the soil probably increased when the vehicle drove over the soil, and then dissipated slowly due to drainage. The resulting effective stresses (i.e. those transmitted via and related to the compression of the solid skeleton) would be less than those predicted by the fully drained analysis. The partially drained analysis modelled this situation. Fig. 5.6 shows that the effective vertical stresses predicted by the partially drained analysis were indeed less than those of the fully drained case. It appears likely from this analysis that the measured precompression stress would not have changed at all. It was found experimentally that the precompression stresses of the trafficked and non-trafficked 'wet' subsoils were not significantly different. This agrees with the more probable, partially drained analysis, and with the 'worst case', drained analysis.

According to Koolen and Kuipers (1983 p. 179) peak stress can be between 1.4 and 3 times as high as the mean normal stress in the contact area of caterpillar tracks. Our results suggest that peak stresses under the machinery we used were at the lower end of this range. A significant increase of precompression stress was only found in the 'wet' topsoil and also this effect was rather small. With larger peak stresses we would have expected larger changes in precompression stress.

It should be noted that transformation of the precompression stress values measured at -6 kPa initial soil water potential to the actual water potentials observed in the field was crucial to obtain this good agreement between model and experiment. In contrary to the transformed values, precompression stresses measured at -6 kPa initial water potential were clearly exceeded by the stress predictions at 0.07-0.17 m depth for the 'dry' plot although no compaction effect was observed. This demonstrates the need to take the moisture dependence of precompression stress into account in predicting compaction.

5.4 Conclusion

Heavy, tracked machinery used to construct pipelines in Switzerland exerts stresses on agricultural soils of a similar magnitude to those commonly experienced in agriculture using low ground pressure tyres or tracks (Gysi, 2000). Experiments showed that a 'dry' plot in a loess soil was not compacted by the vehicles, whereas a wetted plot in the same soil was compacted in the topsoil but not in or below the ploughpan. Both direct measurement and modelling (using a critical state finite element model) showed that the 'dry' soil was strong enough to resist compaction. The 'wet' topsoil was too weak to resist compaction but the 'wet' subsoil did not show visible compaction effects although peak stresses may have slightly exceeded the precompression stresses as determined with the Casagrande method (Casagrande, 1936). The observed compaction effects were in agreement with the model predictions if the soil was assumed to be partially drained but disagreed if for the 'wet' subsoil fully drained conditions were assumed. Agreement between model and experimental results also required that the moisture dependence of the precompression stress was taken into account.

5.5 References

Blunden, B.G., McBride, R.A., Daniel, H. and Blackwell, P.S., 1994. Compaction of an earthy sand by rubber tracked and tyred vehicles. Australian Journal of Soil Research, 32: 1095-1108.

Britto, A.M. and Gunn, M.J., 1987. Critical State Soil Mechanics via Finite Elements. Ellis Horwood, Chichester, 488 pp.

Casagrande, A., 1936. The determination of pre-consolidation load and its practical significance. 1st International Conference on Soil Mechanics and Foundation Engineering, Harvard University, Cambridge, Massachusetts. pp. 60-64.

FAO, 1990. FAO-Unesco Soil Map of the World, Food and Agriculture Organisation of the United Nations (FAO), Revised Legend, Rome.

Gysi, M., 2000. Soil compaction due to heavy agricultural wheel traffic. PhD Thesis, Institute of Terrestrial Ecology (ITOe), Swiss Federal Institute of Technology (ETH), Zurich, 94 pp.

Horn, R., 1988. Compressibility of arable land. In: J. Drescher, R. Horn and M. De Boodt (Editors). Impact of Water and External Forces on Soil Structure, Catena Supplement 11. Catena-Verlag, Cremlingen-Destedt, pp. 53-71.

Horn, R. and Lebert, M., 1994. Soil compactibility and compressibility. In: B.D. Soane and C. van Ouwerkerk (Editors). Soil Compaction in Crop Production. Elsevier, Amsterdam, pp. 45-69.

Kirby, J.M., 1991a. Critical-state soil mechanics parameters and their variation for Vertisols in eastern Australia. Journal of Soil Science, 42: 487-499.

Kirby, J.M., 1991b. Strength and deformation of agricultural soil: measurement and practical significance. Soil Use and Management, 7: 223-229.

Kirby, J.M. and Blunden, B.G., 1992. Avoiding compaction: Soil strength more important than vehicle ground pressure. The Australian Cotton Grower, 13(2): 48-50.

Kirby, J.M., Blunden, B.G. and Trein, C.R., 1997. Simulating soil deformation using a critical-state model: II. Soil compaction beneath tyres and tracks. European Journal of Soil Science, 48: 59-70.

Koolen, A.J. and Kuipers, H., 1983. Agricultural Soil Mechanics. Advanced Series in Agricultural Sciences 13. Springer-Verlag, Berlin, 241 pp.

Richard, F. and Lüscher, P., 1983. Physikalische Eigenschaften von Böden der Schweiz, Band 3. Eidgenössische Anstalt für das forstliche Versuchswesen, Birmensdorf.

Rosal, C., 1997. Drucksondierungen in Loess, Ruckfeld. Diploma Thesis, Institut für Geotechnik (IGT), Eidgenössische Technische Hochschule (ETHZ), Zürich, 36 pp.

Vermeulen, G.D. and Perdok, U.D., 1994. Benefits of low ground pressure tyre equipment. In: B.D. Soane and C. van Ouwerkerk (Editors). Soil Compaction in Crop Production. Elsevier, Amsterdam, pp. 447-478.

6

Conclusions

In all three field experiments, significant compaction effects were found where they were expected, i.e. where the vertical stress, calculated according to Fröhlich (1934), exceeded the precompression stress of the soil. Assuming the normal stress in the contact area as the machine weight divided by the total contact area (i.e. the mean normal stress), the observed effects were partially underestimated. On the other hand, compaction effects were overestimated in most cases where they were predicted by a 'worst case' scenario, assuming a maximum instead of the mean normal stress in the contact area. Additionally, for one field experiment changes in precompression stress were interpreted by comparing them with calculated stresses using a critical-state finite element program. The parameters needed for the model were determined by independent laboratory tests.

The lack of distinct and consistent compaction effects in the subsoil does not mean, however, that no compaction occurred. They may have simply remained insignificant in comparison to the rather large background variability of the parameters used to assess the compaction effects. This background variability was primarily due to 'natural' spatial variability and only to a small degree to analytical variability. Considering the likelihood of heterogeneity in soil properties and load situations, different experimental conditions in the field and laboratory, the uncertainty in stress propagation calculations and reservations concerning the exact physical meaning of the precompression stress as determined by the procedure of Casagrande (1936), I concluded that the agreement between expectations and measurements is good. In summary, the results of these investigations show that precompression stress indeed provides a useful and practical concept for setting tolerance limits of allowable loads for tracked construction machines trafficking agricultural land.

Spatial variability could be one of the major problems in practical application of any parameter, not only precompression stress, used to define soil sensitivity to compaction. For precompression stress, this is a larger obstacle with respect to practical applicability than for parameters which are less time-consuming and costly to determine. On the other hand, precompression stress bears the advantage of direct physical meaning with respect

to compressibility. When talking about the physical meaning of this parameter, one should not forget, however, that transition from elastic to plastic deformation in reality occurs always over a rather large stress range. The precompression stress value determined by the Casagrande (1936) method just represents an operationally defined intermediate state. This means that slight compaction damage may already be expected below this value. This is also the case for cyclic loading, which reaches the precompression stress but does not exceed it (Kirby, 1994). Micro-scale plastic shear deformation already occurs before the macroscopically defined precompression stress is reached. In practice, setting a safety margin between experimentally determined precompression stress and tolerance limit could take account of this deviation from 'ideal' behaviour. Irrespective of such corrections, still a number of limitations should be observed in applying the precompression criterion to regulate allowable weights and contact stress of machines used on agricultural land.

The results clearly show that soil moisture conditions also have to be taken into account in applying precompression stress as a criterion to prevent compaction damages by excessive mechanical loading. The sensitivity of the soil to compression can, however, vary considerably even with depth in the same soil profile. To be able to account for this dependence adequately without being over-restrictive, knowledge would be required which allows this dependence to be inferred for a given soil from easily measurable general soil parameters. For this purpose it would be useful to develop a constitutive theory describing the relationship between soil mechanical parameters, associated with general soil properties such as structure, texture, organic matter content etc. and soil hydraulic variables (e.g. Gräsle et al., 1995; Wheeler and Sivakumar, 1995; Klubertanz et al., 1997).

The precompression concept, as it was investigated in this study, is strictly valid only under static stress conditions in which the normal stresses (i.e. compression stresses) are considerably larger than the shear stresses acting on a soil element. This is approximately the case for a subsoil in the centre under a wide contact area of a slowly moving vehicle with negligible dynamic impacts (e.g. vibrations). Shear stresses may in principle also be taken into account by generalising the precompression stress concept in terms of the yield surface as it is defined by the critical-state soil mechanics (Schofield and Wroth, 1968; Wood, 1990, p. 69). A different approach, however, is required for dynamic stresses. This will in general be the case for mechanical stresses exerted by agricultural machines on the topsoil and also by conventional tillage activities on the ploughpan (Or and Ghezzehei, 2001). Furthermore, bulk compaction in the topsoil is in general not the most critical damage because loosening by technical methods or due to natural regenera-

tion is quite feasible. The main problem here is the destruction of the aggregate structure (Horn et al., 1995) which can be effectively regenerated only through biological processes. This requires time in which no intensive use is possible and during which risks of further deterioration e.g. by soil erosion are greatly increased.

Thus I conclude that precompression stress may not be the primary criterion for preventing compaction and structural damage of topsoils by agricultural use. I recommend it, however, as a primary criterion for the prevention of subsoil compaction by quasi-static compression stresses exerted by heavy machines with wide contact areas.

Further work to establish the concept of critical state soil mechanics in general and of precompression stress in particular in physical soil protection should include:

- Traffic experiments using vehicles with mean contact stress considerably higher than the precompression stress of the subsoil.

- An improved description and understanding of the stress distribution in the contact area between soil and tracks or wheels. Constant strain rather than constant stress boundary condition should be investigated as a model for rigid steel tracks on the soil surface.

- Further validation of the critical state soil mechanics model. In addition to comparing calculated vertical stress with measured precompression stress, modelled strain and displacement should be compared with corresponding measurements in the field. The outcome of the coupled two-phase (solid-fluid) model used for the partially saturated soil in this study should be validated with a coupled three-phase (solid-water-air) analysis.

- Investigations on the influence of compression and shearing on soil physical properties as water and air conductivity.

- Model analysis of other scenarios and experimental studies in order to identify potentially critical soil usage in advance.

References

Casagrande, A., 1936. The determination of pre-consolidation load and its practical significance. 1st International Conference on Soil Mechanics and Foundation Engineering, Harvard University, Cambridge, Massachusetts. pp. 60-64.

Fröhlich, O.K., 1934. Druckverteilung im Baugrunde mit besonderer Berücksichtigung der plastischen Erscheinungen. Verlag von Julius Springer, Wien, 185 pp.

Gräsle, W., Baumgartel, T., Horn, R. and Richards, B.G., 1995. Interaction between soil mechanical properties of structured soils and hydraulic process - Theoretical fundamentals of a model. In: E.E. Alonso and P. Delage (Editors). First International Conference on Unsaturated Soils, Paris, France. pp. 719-724.

Horn, R., Domzal, H., Slowinska-Jurkiewicz, A. and van Owerkerk, C., 1995. Soil compaction processes and their effects on the structure of arable soils and the environment. Soil & Tillage Research, 35: 23-36.

Kirby, J.M., 1994. Simulating soil deformation using a critical-state model: I. Laboratory tests. European Journal of Soil Science, 45: 239-248.

Klubertanz, G., Laloui, L. and Vulliet, L., 1997. Numerical modeling of unsaturated porous media as a two and three phase medium: A comparison. In: J. Yuan (Editor). 9th International Conference on Computer Methods and Advances in Geomechanics, Wuhan, China. pp. 1302-1314.

Or, D. and Ghezzehei, T.A., 2001. Modeling post tillage structural dynamics in aggregated soils: a review. Soil & Tillage Research (in press).

Schofield, A.N. and Wroth, C.P., 1968. Critical State Soil Mechanics. McGraw-Hill, London, 310 pp.

Wheeler, S.J. and Sivakumar, V., 1995. An elasto-plastic critical state framework for unsaturated soil. Géotechnique, 45(1): 35-53.

Wood, D.M., 1990. Soil Behaviour and Critical State Soil Mechanics. Cambridge University Press, Cambridge, 462 pp.

List of Figures

List of Tables

Appendix A1

Influence of sample size on compression behaviour of structured soil

M. Berli, W. Attinger, M. Gysi, S.M. Springman and R. Schulin
Prepared for Publication in Soil and Tillage Research

A1.1 Introduction

The confined uniaxial compression test in an oedometer is a simple and therefore widely used way to measure the compression behaviour of soil samples in the laboratory. In geotechnical engineering, standard sample sizes range from of 0.05 to 0.1 m inner diameter and 0.01 to 0.02 m height for oedometer tests on fine-grained material. For fine-grained undisturbed agricultural or forest soils, built up of aggregates of particles (or 'peds' in clays), the representative elementary volume must be expected, in general, to be much larger than for natural or remoulded 'engineering' soils. Large samples with a diameter to height ratio of approximately 1 not only represent the macrostructure of the soil more adequately than smaller or thinner samples but also enable sampling to be carried out on soil with a higher gravel content. While sample quality and hence, the quality of the obtained compression parameters increase with increasing diameter, quality can decrease with increasing sample height due to friction of the soil sample along the wall of the oedometer cell.

Muhs and Kany (1954), Koolen (1974) and Hammel (1993) investigated the influence of sidewall friction on the compression behaviour of soil samples in oedometer tests. Muhs and Kany (1954) found for different sample sizes (0.1 m diameter, 0.01-0.1 m height) that low sample diameter-to-height ratios lead to an overestimation of sample stiffness but that the effect of sample trimming can exceed the influence of sidewall friction considerably. Comparing the influence of sample disturbance and sidewall friction, they concluded that a sample diameter-to-height ratio of approximately 1 should be ideal. Because this would led to very long consolidation times for fine-grained saturated soils,

however, they recommended a much higher ratio of about 5, i.e. flatter samples, for practical reasons. Koolen (1974) and Hammel (1993) directly measured sidewall friction. Koolen (1974) concluded that samples for oedometer tests of diameter-to-height ratios of 1.7 (at the start of the test) to about 3 (at the end of the test) are reasonable in restricting sidewall friction effects and permitting an acceptable accuracy. Hammel (1993) proposed to adapt the sample size to the specific sampling problem and to correct the influence of sidewall friction on the compression behaviour of the sample.

Beside sidewall friction and sample trimming in the laboratory, the compression behaviour of soil determined in an oedometer test can also be influenced by sampling technique in the field (Hvorslev, 1949; Clayton et al., 1995). Also 'undisturbed' samples, taken from test pits or boreholes by drilling, pushing or hammering a tube sampler into the soil, undergo a certain amount of disturbance. With large diameter, thin-walled tube samplers which are pushed continuously into the soil, sample disturbance can be minimised (Baligh et al., 1987; Vaughan et al., 1992; Clayton et al., 1998; Clayton and Siddique, 2001).

To obtain reliable results from laboratory confined uniaxial compression tests on structured soil samples, the influence of sample size on compression behaviour has to be established. For that purpose, confined uniaxial compression tests were carried out on undisturbed samples of three different diameter-to-height ratios of a silty loam and a sandy loam soil (FAO, 1990) at -6 kPa initial soil water potential.

A1.2 Material and methods

The compression tests were carried out on soil samples from two different sites, Ruckfeld and Frauenfeld, in north-eastern Switzerland. Soil properties of the two test sites are given in Table A1.1. Soil types were a Haplic Luvisol at Ruckfeld and an Eutric Cambisol at Frauenfeld (FAO, 1990). The gravel (diameter > 0.002 m) content of both soils was less than 1%. The parent material at Ruckfeld was a loess, deposited in the forefield of a glacier during the Riss glaciation. At Frauenfeld, the parent material is alluvial material from the Thur river. Both test sites were under crop rotation.

Table A1.1.   Soil parameters of the two test sites Ruckfeld and Frauenfeld

Site	Depth [m]	Sand [kg kg^{-1}]	Silt [kg kg^{-1}]	Clay [kg kg^{-1}]	Organic matter [kg kg^{-1}]
Ruckfeld	0.07-0.17	0.28	0.59	0.13	0.028
	0.27-0.37	0.31	0.56	0.13	0.023
	0.47-0.57	0.29	0.58	0.13	0.008
	0.67-0.77	0.23	0.59	0.18	0.007
Frauenfeld[†]	0.12-0.17	0.42	0.40	0.18	0.053
	0.32-0.37	0.52	0.31	0.17	0.011
	0.52-0.57	0.61	0.28	0.11	0.005

[†] Data from Gysi et al. (1999)

Table A2.2.   Size and number of samples used to determine the influence of sample size on compression behaviour

Site	Sampling depth [m]	No. of samples	Sample diameter [m]	Sample height [m]	Sample diameter-to-height ratio [-]
Ruckfeld	0.52	8	0.100	0.03	3.33
	0.52	10	0.100	0.06	1.67
	0.52	12	0.108	0.11	0.98
Frauenfeld	0.4	10	0.100	0.03	3.33
	0.4	10	0.100	0.06	1.67
	0.4	9	0.108	0.11	0.98

Samples from both test sites were taken from the subsoil. It was more difficult to prepare undisturbed samples of satisfactory quality of the Frauenfeld soil with its rather high sand and low clay content than with Ruckfeld soil. Prior to the compression test, the samples were conditioned to an initial soil water potential of -6 kPa (with respect to the sample's centre) by applying a hanging water column.

Precompression stress, compression and recompression index were determined from confined uniaxial compression tests. For the compression test, samples were kept within the coring cylinders, built into the compression cell and subsequently subjected to step-wise increased stress. A normal stress range of 8 to 800 kPa was applied through a piston, which fitted the opening of the cylinders. Each compression step lasted for 1800 s after which the pressure was increased to the next level. Precompression stress was determined from the resulting stress-strain curves (plotted as logarithm of normal stress versus vertical strain) using the graphical procedure of Casagrande (1936) (Fig. A1.1).
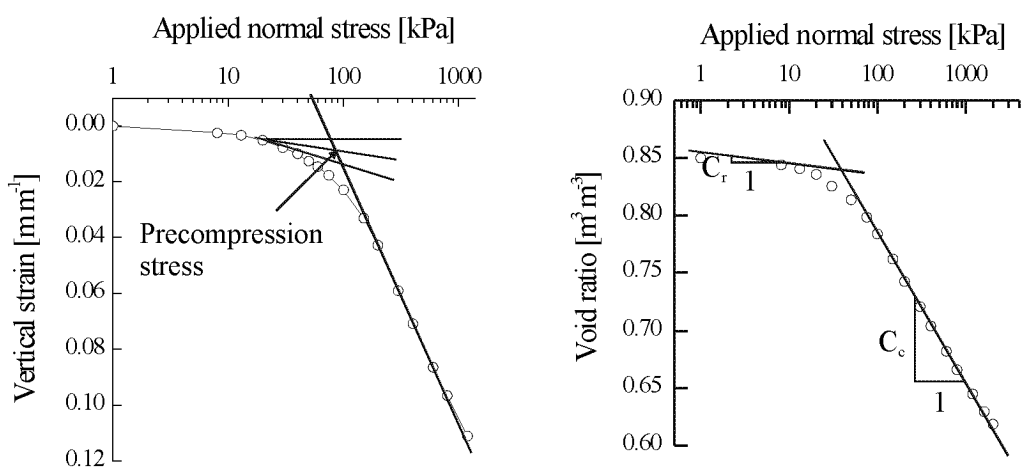
Fig. A1.1. Definition of precompression stress (left graph), compression index C_c and recompression index C_r (right graph).

The recompression index C_r was defined as the slope of the log(normal stress) versus void ratio of the post sampling recompression curve at 8 kPa normal stress and the compression index C_c as the slope of the linear virgin compression part of the applied normal stress versus void ratio curves, determined at -6 kPa initial soil water potential (see Fig. A1.1).

The samples were dried at 105 °C for at least 24 hours. The weight of the dried soil was divided by the initial sample volume to determine initial dry bulk density .

A1.3 Results

○ Ruckfeld soil, △ Frauenfeld soil
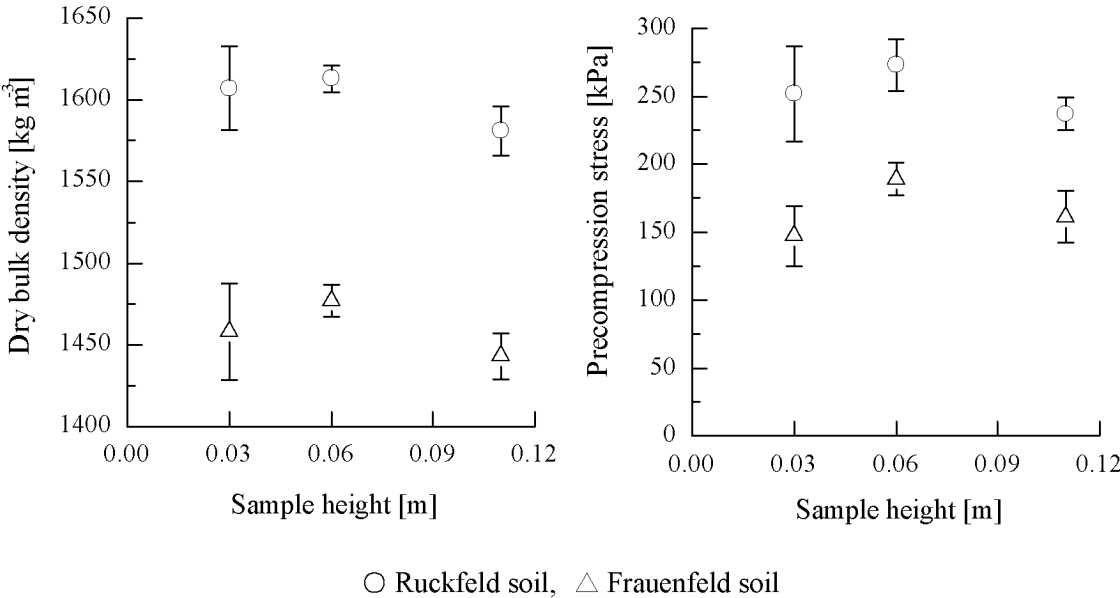
Fig. A1.2. Dry bulk density and precompression stress determined with samples of 0.03, 0.06 and 0.11 m height from the Frauenfeld (depth of the sample centre: 0.4 m, $P < 0.05$) and the Ruckfeld site (depth of the sample centre: 0.52 m, $P < 0.05$).

○ Ruckfeld soil, △ Frauenfeld soil

Fig. A1.3. Compression index C_c and recompression index C_r determined with samples of 0.03, 0.06 and 0.11 m height from the Frauenfeld (depth of the sample centre: 0.4 m, $P < 0.05$) and the Ruckfeld site (depth of the sample centre: 0.52 m, $P < 0.05$).
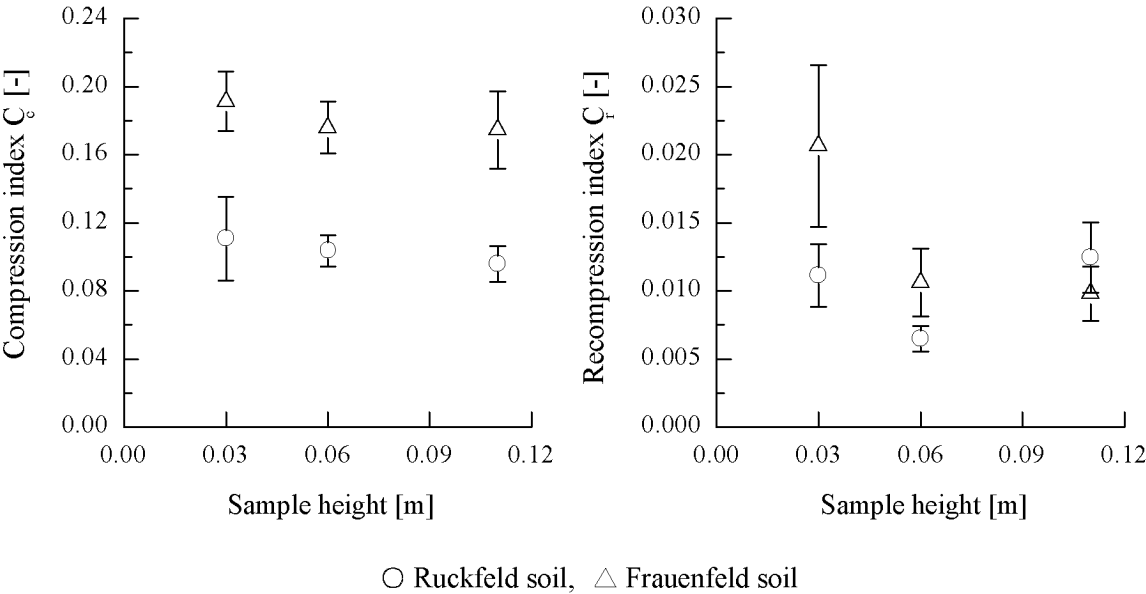
Although all samples were taken from the same depth at each site, we found significantly different bulk densities for the 0.06 and the 0.11 m high samples. Comparing the values of the two layers from the two different test sites, bulk density and precompression stress were significantly higher at Ruckfeld than at Frauenfeld. Compression and recompression indices were, with one exception, significantly higher at Frauenfeld than at Ruckfeld.

For both soils, the 0.06 m high samples showed the highest precompression stress and bulk density values with almost universally the smallest variation. The lowest precompression stress and bulk density values were measured for the 0.11 m high samples of Ruckfeld soil . For the Frauenfeld soil, bulk density of the 0.03 m high and precompression stress of the 0.11 m high samples were the lowest values. Bulk density of both soils of the 0.06 m high samples were significantly higher than those of the 0.11 m high samples. Precompression stresses of the 0.06 m high samples of both soils were significantly higher than values of the 0.11 m high samples from Ruckfeld soil and the 0.03 m high samples from Frauenfeld soil. Except for the precompression stress values from Ruckfeld soil, 95% confidence intervals of 0.03 m high samples were the largest and those of the 0.06 m high samples the smallest.

For both soils there was a slight trend to decreasing compression indices with increasing sample height. This agrees with the assumption that increasing sample height leads to increasing stiffness values due to the increasing influence of sidewall friction. However there was no significant (P<0.05) difference between the compression indices of the samples of the three different heights.

While the recompression index was significantly larger in 0.03 m than in 0.06 and 0.11 m high samples from Frauenfeld, there was no difference between the values of the 0.06 and 0.11 m high samples. The recompression index values of the Frauenfeld samples decreased with increasing sample height. The values of the Ruckfeld samples were similar for the 0.03 and 0.11 m high samples but showed significantly lower values for the 0.06 m high samples. For the Ruckfeld soil, decreasing recompression index values were related to increasing bulk density and precompression stress values.

A1.4 Discussion and conclusions

We expected to find increasing precompression stress and decreasing compression and recompression indices with decreasing diameter-to-hight ratio due to increasing influence of sidewall friction. We also expected increasing variability of the determined parameters due to the increasing influence of the top and bottom sample trimming disturbance with increasing diameter-to-hight ratio.

Fig. A1.2 and Fig. A1.3 show that the sample size influences precompression stress and recompression index as well as bulk density. The different bulk density values for different sample sizes implies that the observed differences in compression behaviour are not only due to sidewall friction. Compression behaviour at normal stresses up to precompression stress is probably more influenced by small scale spatial variability, sampling technique in the field and trimming in the laboratory than by the boundary conditions of the compression test, i.e. the sidewall friction. The gradient of the recompression curve at 8 kPa normal stress is very sensitive to loosening and roughness of the sample surface and, hence, very likely to be overestimated due to sampling disturbance. This agrees with the fact that we found no significantly different compression indices for different sample sizes, which can be explained by the decreasing influence of sample disturbance on the subsequent virgin compressing behaviour with increasing normal stress.

Baligh et al. (1987) and Clayton et al. (1998) showed that during sampling with thin-walled, long cylinders pushed in the soil, the sample undergoes compression followed by extension. This extension could explain the significantly decreased bulk density and pre-compression stress and the increased recompression index for the 0.11 m diameter compared with the 0.06 m diameter samples.

We found the smallest variability of the parameters determined from the 0.06 m high samples and not for values from the 0.11 m high samples. The largest variability was found for the 0.03 m high samples as we expected. Measurements with smaller samples are more sensitive to small scale soil layering and, hence, spatial variability, but also to disturbance by sampling and trimming.

In summary we conclude that sample size can influence bulk density, precompression stress and recompression index of undisturbed agricultural soil samples significantly. No significant effect of sample size on compression index was found. The influence of the height (at equal diameter) on the compression behaviour of a structured sample in a confined uniaxial compression test rather originates from soil spatial variability or sampling disturbance than from sidewall friction.

A1.5 References

Baligh, M.M., Azzouz, A.S. and Chin, C.T., 1987. Disturbance due to 'ideal' tube sampling. Journal of Geotechnical Engineering, 113(7): 739-757.

Casagrande, A., 1936. The determination of pre-consolidation load and its practical significance. 1st International Conference on Soil Mechanics and Foundation Engineering, Harvard University, Cambridge, Massachusetts. pp. 60-64.

Clayton, C.R.I., Matthews, M.C. and Simons, N.E., 1995. Site investigation. Blackwell Scientific, Oxford, 573 pp.

Clayton, C.R.I. and Siddique, A., 2001. Tube sampling disturbance - forgotten truths and new perspectives. Proceedings of the Institution of Civil Engineers, Geotechnical Engineering, 149(3): 195-200.

Clayton, C.R.I., Siddique, A. and Hopper, J., 1998. Effects of sampler design on tube sampling disturbance - numerical and analytical investigations. Géotechnique, 48(6): 847-867.

FAO, 1990. FAO-Unesco Soil Map of the World, Food and Agriculture Organisation of the United Nations (FAO), Revised Legend, Rome.

Gysi, M., Ott, A. and Flühler, H., 1999. Influence of single passes with high wheel load on a structured , unploughed sandy loam soil. Soil & Tillage Research, 52: 141-151.

Hammel, K., 1993. Spannungsverteilung und Bodenverdichtung unter profilierten Reifen am Beispiel zweier Böden unter Grünland. PhD Thesis, Institut für Bodenkunde und Standortlehre, Universität Hohenheim, Stuttgart, 141 pp.

Hvorslev, M.J., 1949. Subsurface Exploration and Sampling of Soils for Civil Engineering Purposes. Waterways Experimental Station, Vicksburg, Mississippi, 512 pp.

Koolen, A.J., 1974. A method for soil compactibility determination. Journal of Agricultural Engineering Research, 19: 271-278.

Muhs, H. and Kany, M., 1954. Einfluss von Fehlerquellen bei Kompressionsversuchen. Fortschritte und Forschungen im Bauwesen, 17(1). Franckh'sche Verlagshandlung, Stuttgart, 125-152 pp.

Vaughan, P.R., Chandler, R.J., Apted, J.P., Maguire, W.M. and Sandroni, S.S., 1992. Sampling disturbance - with particular reference to its effect on stiff clays. In: G.T. Houlsby and A.N. Schofield (Editors). Wroth Memorial Symposium, Oxford. Thomas Telford, London, . pp. 685-708.

Appendix A2

Additional details and results to chapter 5

'Modelling compaction of agricultural subsoils by tracked heavy construction machinery under various moisture conditions'

The aim of appendix 2 is

1. to give details about the determination of the slope of the virgin compression line λ, the slope of the recompression line κ, the void ratio on the critical state line at $\ln(p'=1$ kPa) e_{cs} and the slope of the critical state line M from confined uniaxial compression and direct shear tests and

2. to present additional results from the critical state modelling described in chapter 5.

A2.1 Determination of critical state parameters

Numerical analysis was carried out using a constitutive model based on critical state soil mechanics reported in chapter 5. The slope of the virgin compression line λ, the slope of the recompression line κ, the void ratio on the critical state line at $\ln(p'=1 \text{ kPa})$ e_{cs} and the slope of the critical state line M (definition see chapter 2.2) were determined for the topsoil (0-0.25 m), the ploughpan (0.25-0.35 m) and the intermediate subsoil (0.35-0.8 m). To this end, confined uniaxial compression tests and direct shear tests were carried out on samples of -6 kPa initial soil water potential (for description of the soil properties see chapter 3.2). For the lower subsoil (0.8-2.8 m), λ and κ were taken from confined uniaxial compression tests carried out by Rosal (1997) on undisturbed samples at initial moisture conditions equal to the field moisture content. The initial void ratio e_o and the angle of internal friction ϕ' of the lower subsoil were also taken from Rosal (1997).
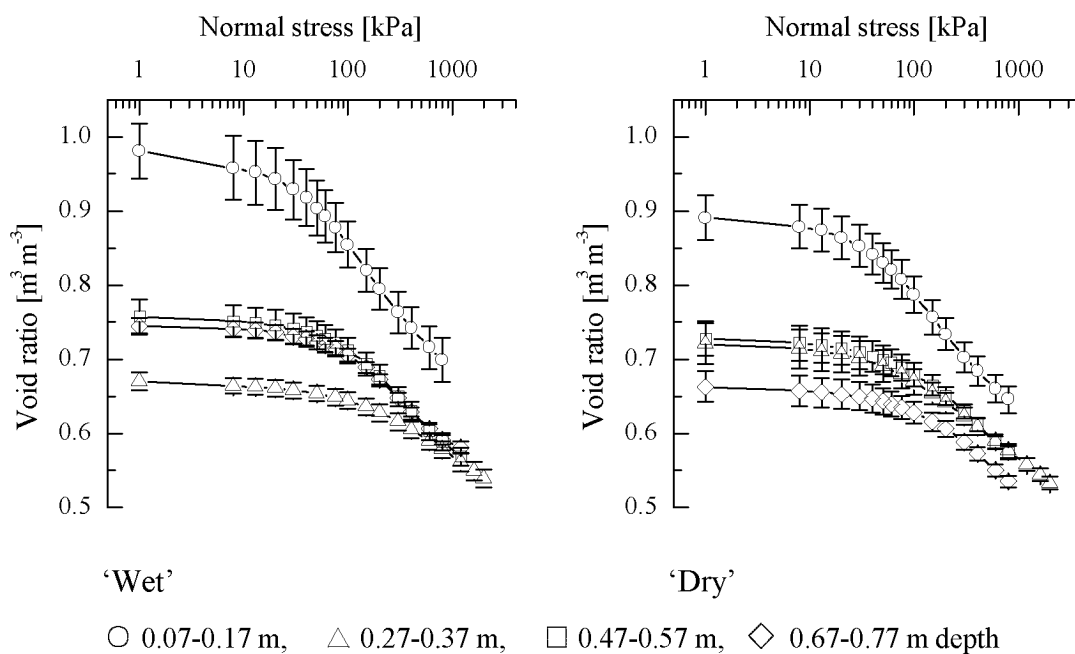

Fig. A2.1. Applied normal stress versus void ratio of the 'wet' and 'dry' non-trafficked Ruckfeld soil at -6 kPa initial soil water potential. Points represent mean values of 4 to 6 replicate measurements, error bars are standard errors.

Fig. A2.1 shows the ln(normal stress) versus void ratio curves from the 'wet' and 'dry' Ruckfeld plot of samples from 0.07-0.17, 0.27-0.37, 0.47-0.57 and 0.67-0.77 m depth. κ was calculated as the slope of the ln(normal stress) versus void ratio curve at 8 kPa normal stress, λ as the slope of the linear virgin compression part of the ln(normal stress) versus void ratio curve.
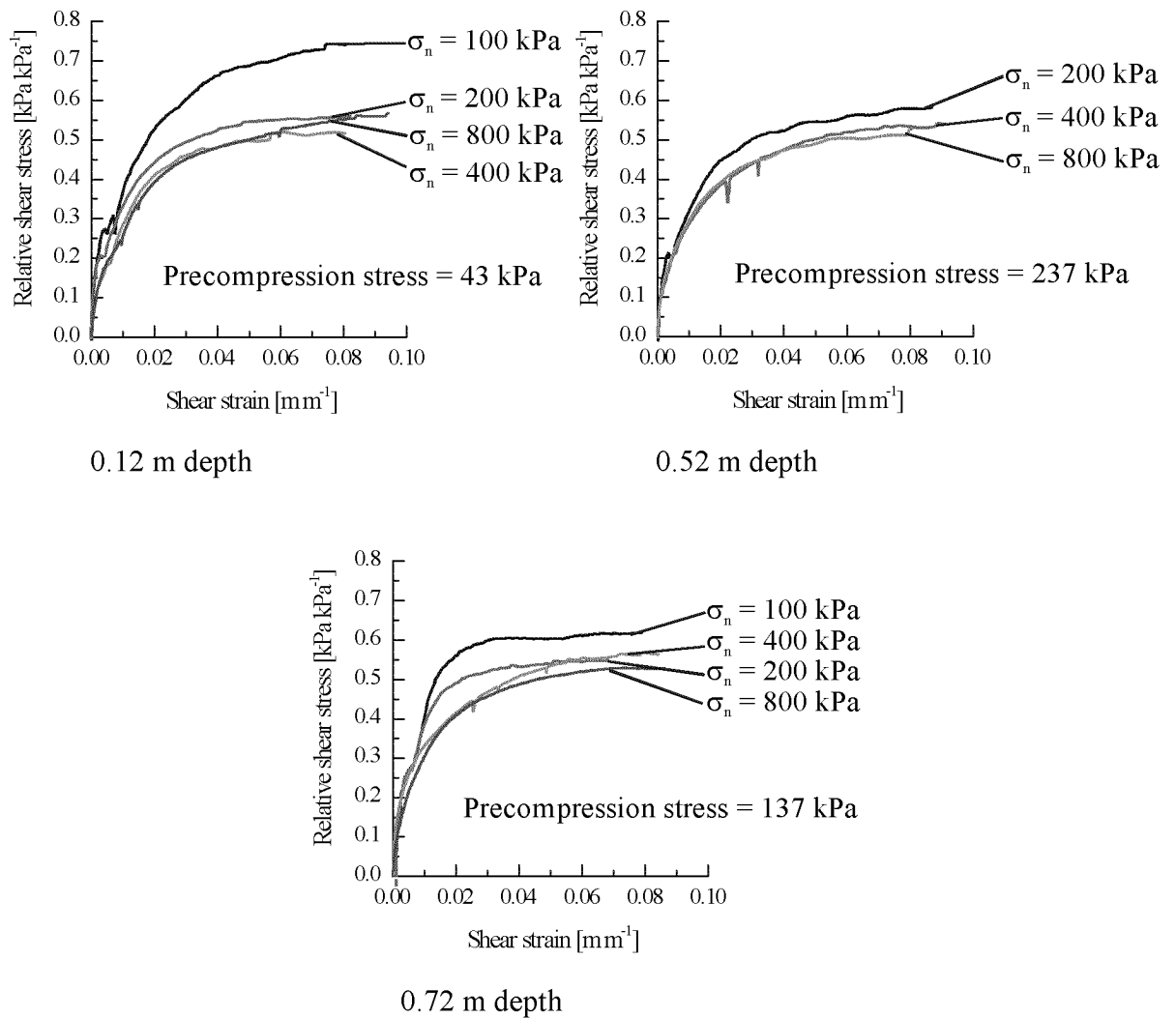
Fig. A2.2. Relative shear stress (the shear stress τ to applied normal stress σ$_n$ ratio) versus shear strain of the non-trafficked Ruckfeld soil at 0.07-0.17, 0.47-0.57 and 0.67-0.77 m depth at -6 kPa initial soil water potential.

The stress-strain curves from the direct shear tests are given in Fig. A2.2. With the normal and shear stress values obtained at failure, the Mohr-Coulomb failure line was plotted in order to determine the angle of internal friction in direct shear. Failure was defined as the range where the relative shear stress versus shear strain curve became approximately horizontal. We tried to carry out the direct shear test under effective stress conditions ($\sigma_n = \sigma_n$') using a low shear velocity of 5×10^{-7} m s^{-1} in order to obtain the effective angle of internal friction ϕ'. However, since the pore water pressure of the sample cannot be controlled in the direct shear test, we probably did not reach pure effective stress conditions. An angle of internal friction ϕ' of 26° was determined for the topsoil and a ϕ' of 27° for the intermediate subsoil was found. For the ploughpan, the angle of internal

friction was estimated as 27° based on the measurements from the top- and the interme-diate subsoil (see also Table A2.1). The samples from the ploughpan were not homogeneous enough to cut undisturbed 0.02 m thin samples of satisfactory quality for the direct shear test. Rosal (1997) determined ϕ'-values between 28° and 33° for the lower subsoil, using a triaxial apparatus.

With the angle of internal friction ϕ' the slope of the critical state line M in compression (definition see chapter 2.4.1) was calculated with

$$M = \frac{6 \sin \phi'}{3 - \sin \phi'} \tag{A2.1}$$

The void ratio on the critical state line at $\ln(p'=1 \text{ kPa})$, e_{cs}, can be calculated from the initial void ratio e_0 with equation (A2.2)

$$e_{cs} = e_0 + \left(\lambda - \kappa\right) \ln\left(\frac{p_0'}{2}\right) \tag{A2.2}$$

Equation (A2.2) is derived from equations (2.11) and (2.12) from chapter 2.4.1

$$v_{cs} = \Gamma - \lambda \ln p'_{cs} \tag{2.11}$$

$$v = v_\kappa - \kappa \ln p', \tag{2.12}$$

using the definitions $v_\kappa = e_o + 1$; $\Gamma = e_{cs} + 1$.

For the constitutive model 'Modified Cam Clay',

$$p'_{cs} = \frac{p_0'}{2} \tag{A2.3}$$

for $v_{cs} = v$ with p_0' the precompression stress under isotropic triaxial compression stress conditions.

p_0' is transformed from precompression stress determined with oedometer tests, $\sigma'_{v,max}$, using the equations (A2.4) and (A2.5).

$$p'_{max} = \frac{(1 + 2\,K_{nc})\,\sigma'_{v,max}}{3} \tag{A2.4}$$

$$q_{max} = (1 - K_{nc})\,\sigma'_{v,max} \tag{A2.5}$$

$$p'_0 = \frac{q_{max}^2}{M^2 p'_{max}} + p'_{max} \tag{A2.6}$$

M is the slope of the critical state line and K_{nc} the in-situ earth pressure at rest under normally consolidated conditions.

Equation (2.6) is based on the elliptical yield surface of 'Modified Cam Clay' in the p'-q space (Fig. A2.3).
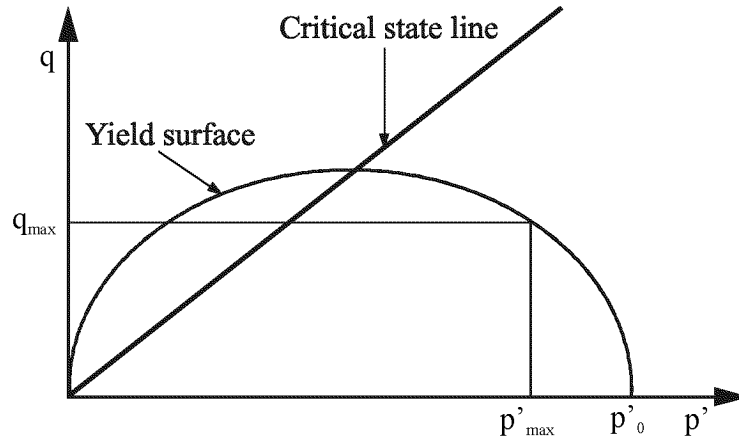

Fig. A2.3. p'_{max} and q_{max} in the p'-q space for an elliptical 'Modified Cam Clay' yield locus.

Using equations (A2.4) to (A2.6) together with (A2.2), equation (A2.7) yields for the void ratio on the critical state line at $\ln(p'=1 \text{ kPa})$, e_{cs},

$$e_{cs} = e_o + (\lambda - \kappa)\ln\left[\frac{\sigma'_{v,max}}{2}\left(\frac{3(1 - K_{nc})^2}{M^2(1 + 2\,K_{nc})} + \frac{1 + 2\,K_{nc}}{3}\right)\right] \tag{A2.7}$$

Table A2.1. Measured values for the angle of internal friction ϕ' and calculated values for the in-situ earth pressure at rest K_{nc} and the slope of the critical state line M used for the modelling in chapter 5

Parameter	Topsoil	Ploughpan	Intermediate subsoil
Angle of internal friction ϕ' [°]	26	27	27
In-situ earth pressure at rest K_{nc} [-]	0.56	0.55	0.55
Slope of the critical state line M [-]	1.02	1.07	1.07

The in-situ earth pressure at rest was calculated according to Jaky's formula $K_{nc} = 1 - \sin(\phi')$.

Table A2.2. Critical state properties λ, κ, and e_{cs} of the 'wet' and the 'dry' plots, determined at -6 kPa initial water potential. Mean values of 4 to 6 replicate measurements, error bars given in parentheses as standard errors

Critical state soil properties	Topsoil 0.07–0.17 m depth	Ploughpan 0.27–0.37 m depth	Intermediate subsoil 0.47–0.57 m depth	Intermediate subsoil 0.67–0.77 m depth
'Wet' plot				
Slope of the virgin compression line, λ [-]	8.58×10^{-2} (6.32×10^{-3})	3.99×10^{-2} (1.94×10^{-3})	7.12×10^{-2} (3.16×10^{-3})	6.29×10^{-2} (3.43×10^{-3})
Slope of the recompression line, κ [-]	1.18×10^{-2} (2.31×10^{-3})	2.93×10^{-3} (3.74×10^{-4})	4.06×10^{-3} (5.58×10^{-4})	2.75×10^{-3} (4.18×10^{-4})
Initial void ratio on the critical state line at $\ln(p'=1$ kPa), e_{cs} [-]	1.21 (4.92×10^{-2})	0.82 (1.58×10^{-2})	1.01 (3.13×10^{-2})	0.97 (2.32×10^{-2})
'Dry' plot				
Slope of the virgin compression line, λ [-]	7.76×10^{-2} (6.44×10^{-3})	4.57×10^{-2} (1.66×10^{-3})	6.04×10^{-2} (3.36×10^{-3})	5.69×10^{-2} (4.03×10^{-3})
Slope of the recompression line, κ [-]	8.42×10^{-3} (1.16×10^{-3})	3.64×10^{-3} (7.20×10^{-4})	4.21×10^{-3} (6.83×10^{-4})	2.98×10^{-3} (7.59×10^{-4})
Initial void ratio on the critical state line at $\ln(p'=1$ kPa), e_{cs} [-]	1.11 (4.71×10^{-2})	0.86 (2.08×10^{-2})	0.94 (2.74×10^{-2})	0.88 (3.73×10^{-2})

A2.2 Critical state stress-strain-displacement modelling for the 'wet' trafficked Ruckfeld soil under a tracked heavy construction machinery

Soil-vehicle interaction calculations were performed on the continuum with the finite element program 'Sage Crisp' Version 4.02. The constitutive model 'Modified Cam Clay' was used to describe the mechanical behaviour of the soil in terms of critical state soil mechanics (Britto and Gunn, 1987).

The experiment was modelled as a plane strain problem with the rigid track acting as an infinite strip load. Symmetry required only half the problem domain to be modelled, which was chosen to be 2 m wide and 2.8 m deep (Fig. A2.3). The finite element mesh comprised 420 linear strain triangular elements ranging in size from 0.05 by 0.05 m near the track to 0.2 by 0.6 m in the corner farthest away from the track. The mesh was divided into four layers (topsoil, ploughpan, intermediate and lower subsoil) with different critical state parameters (see Table A2.2).
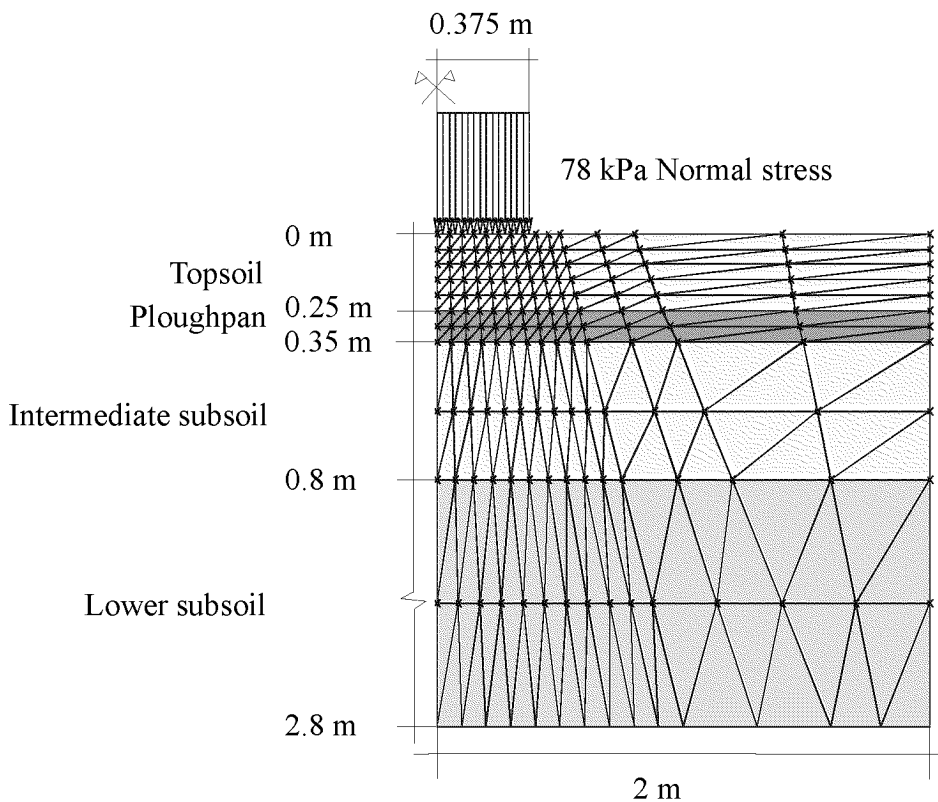

Fig. A2.3. The finite element mesh chosen for the calculation in chapter 5.

The load exerted by the rigid steel track onto the soil surface was considered to be uniformly distributed over the entire contact area. The load was assumed to be a normal stress of 78 kPa applied on a 0.75 m wide strip, which is equivalent to the mean normal stress and the width of the contact area under the heaviest machine used for the experiment. Shear tractions at the surface were ignored, because the vehicles were either standing still or moving slowly without draft.

The following plots give results of displacement, stress and strain calculations for the 'wet' trafficked Ruckfeld soil under drained conditions in order to complement the results presented in chapter 5.
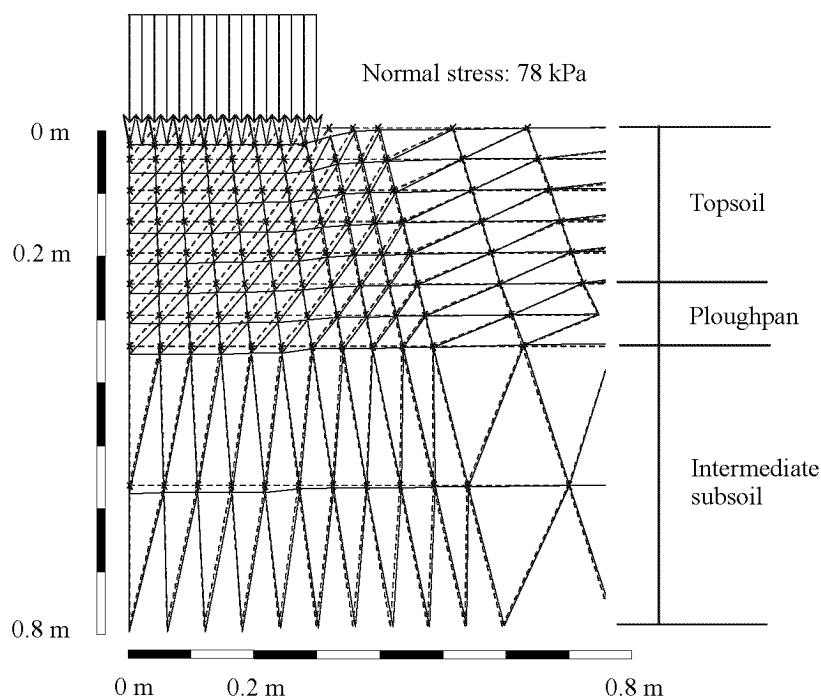

Fig. A2.4. The deformed finite element mesh (in scale) calculated for the 'wet' trafficked Ruckfeld soil under drained conditions.

The model calculations predicted a rut depth of 0.025 m at the soil surface under a constant normal stress of 78 kPa (Fig. A2.4). In the field experiment (see chapter 3), rut depths between 0.02 and 0.04 m were measured after the passage of the tracked machines. A key assumption in the use of the 'Cam Clay' models is that straining within the yield surface is directed by isotropic elasticity. In consequence, 'Modified Cam Clay' cannot exactly predict the surface profile and in particular the heave at the side of the tracks as seen in the field. This was also observed by Stallebrass and Taylor (1997) and is

due to the variation of stiffness with strain (even within the yield surface) as well as effects of anisotropy.
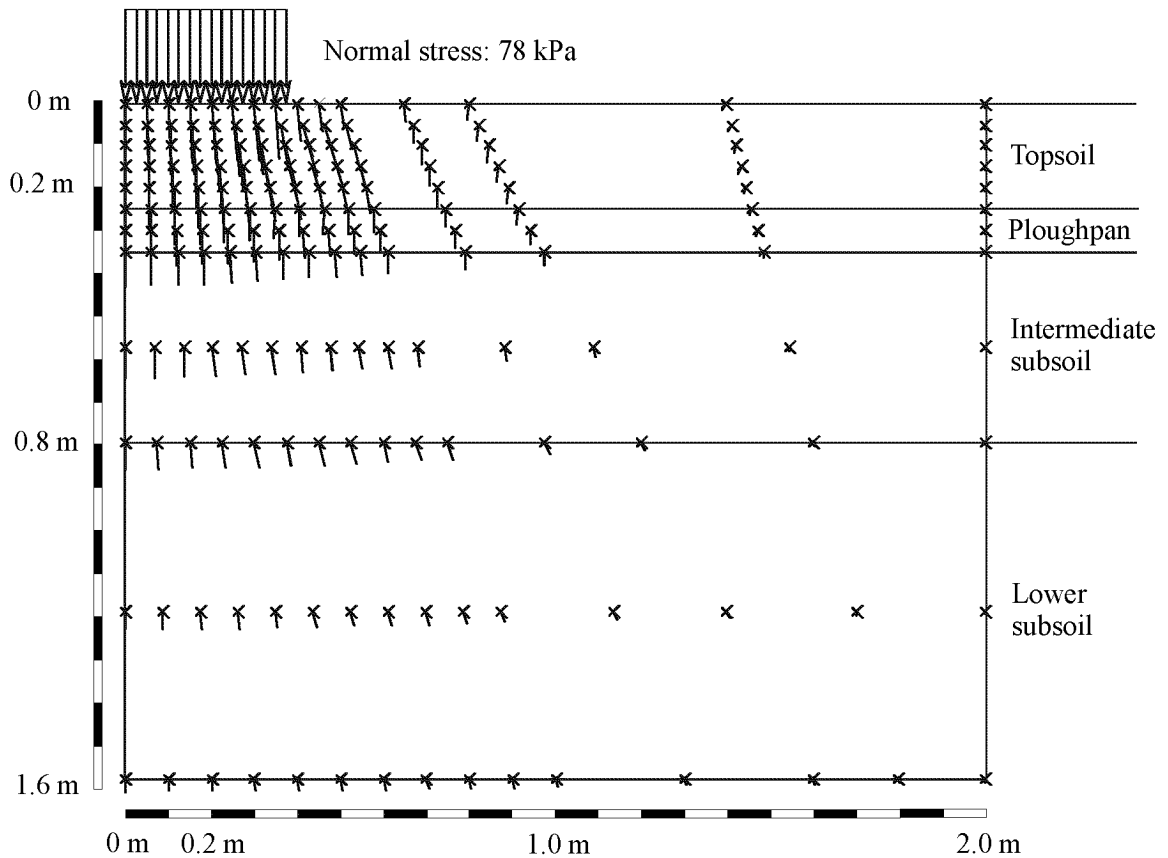

Fig. A2.5. The deformation vectors (scale 5:1) calculated at the nodes of the finite element mesh for the 'wet' trafficked Ruckfeld soil under drained conditions.

Mainly vertical displacements occurred under the strip load (Fig. A2.5). This supports the assumption that the stress-strain behaviour of a soil sample in a confined uniaxial compression tests is similar to the stress-strain behaviour of the soil under an infinite strip load.
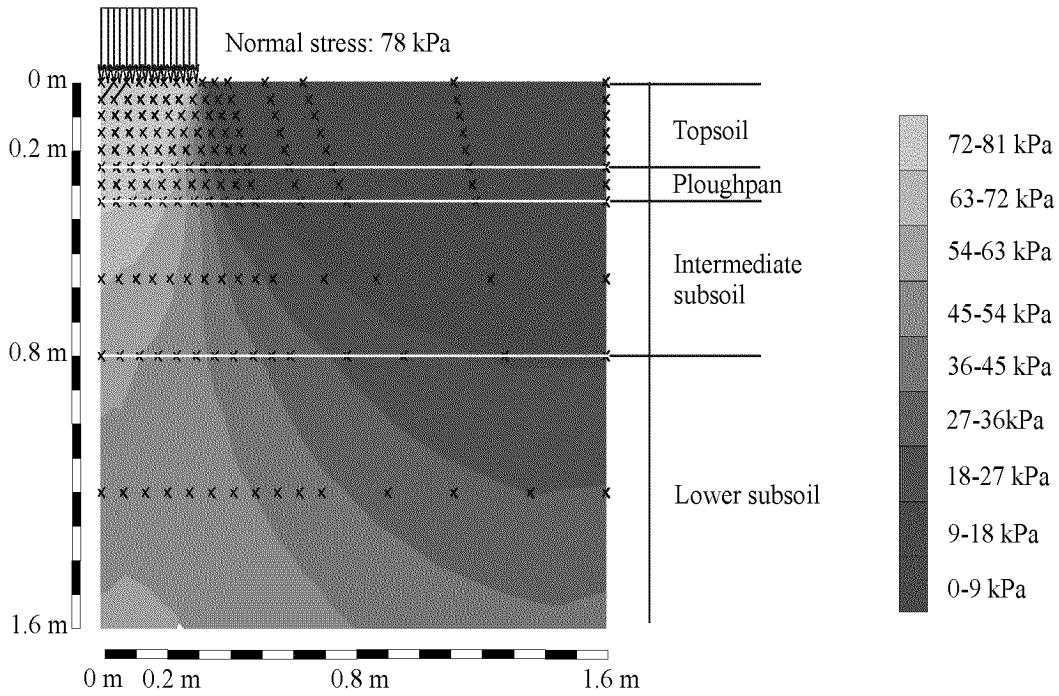
Fig. A2.6. Total vertical stress calculated for the 'wet' trafficked Ruckfeld soil under drained conditions.
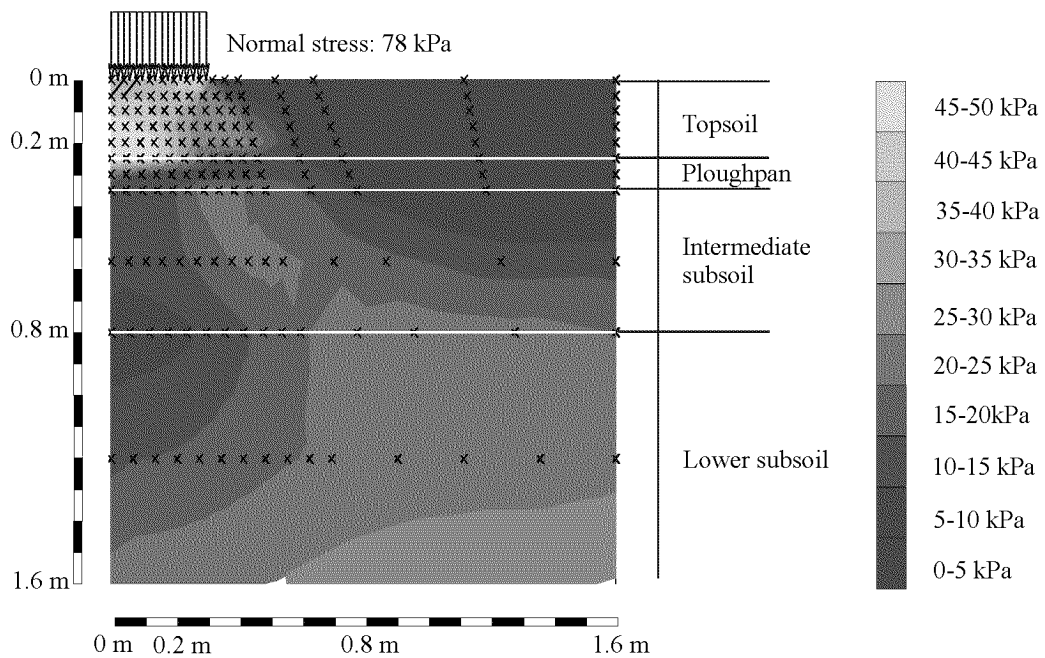

Fig. A2.7. Total horizontal stress calculated for the 'wet' trafficked Ruckfeld soil under drained conditions.
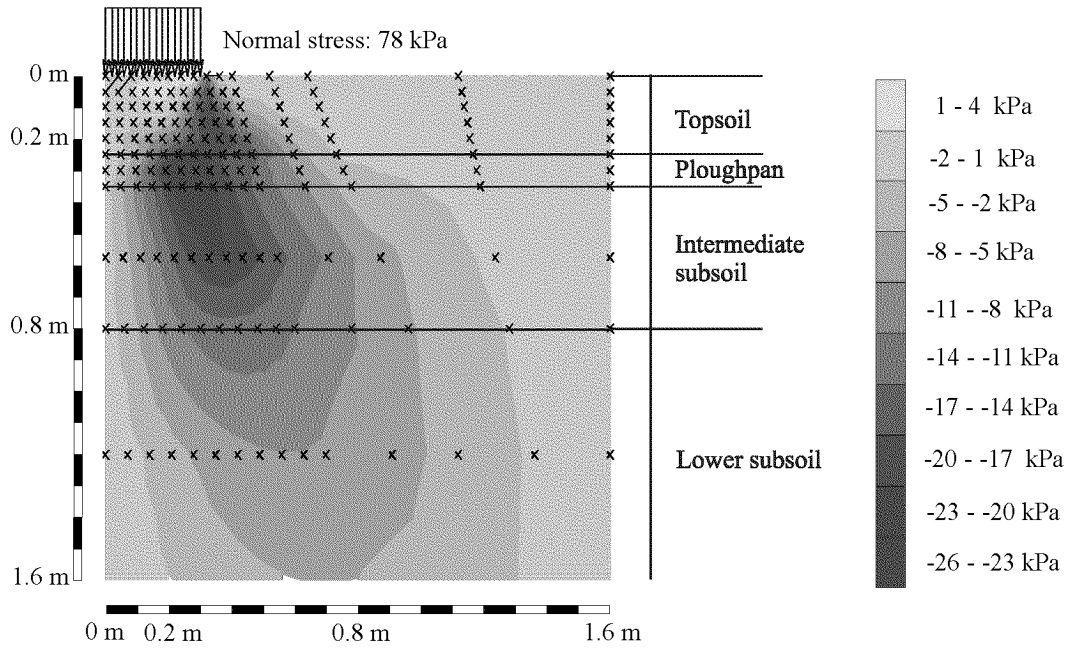
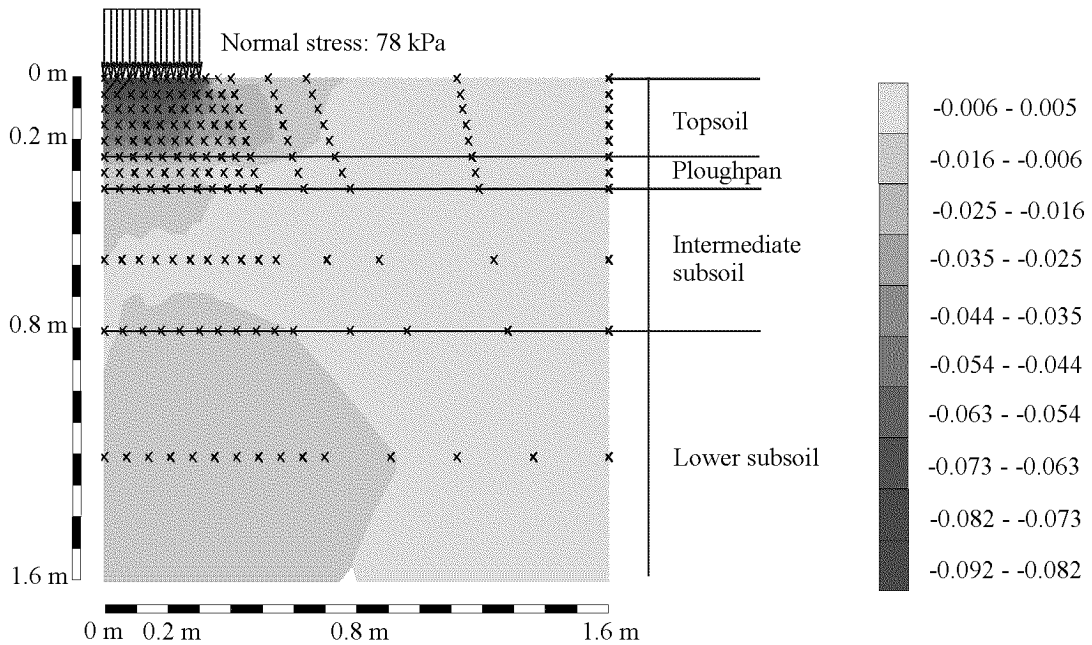Fig. A2.8. Plane shear stress calculated for the 'wet' trafficked Ruckfeld soil under drained conditions.

Fig. A2.9. Void ratio changes calculated for the 'wet' trafficked Ruckfeld soil under drained conditions.

The soil layering influenced the calculated horizontal and shear stress propagation (Fig. A2.7 and A2.8) as well as the change in void ratio (Fig. A2.9). The layering has, in con-

trary to expectation, only a slight influence on vertical stress propagation (Fig. A2.6). The ploughpan, although stiffer than top- and subsoil, did not appear to affect the distribution of the vertical stress considerably and, hence, protect the subsoil below from compaction. Perhaps this was because the ploughpan was only 0.1 m thick, which is less than 1/3 of the half track width at a depth of 3/4 of the half track with. The ploughpan caused a slight build up in horizontal stresses and a small complementary reduction in void ratio, which was concentrated in the topsoil. This agreed with the fact that the calculated vertical stress was higher than the precompression stresses only in the topsoil (see chapter 5, Fig. 5.6) which led to plastic compression. Shear stresses occurred around the 'compression zone' in the topsoil and propagated down to the lower subsoil. Shear stresses appeared to be horizontally distributed by the ploughpan.
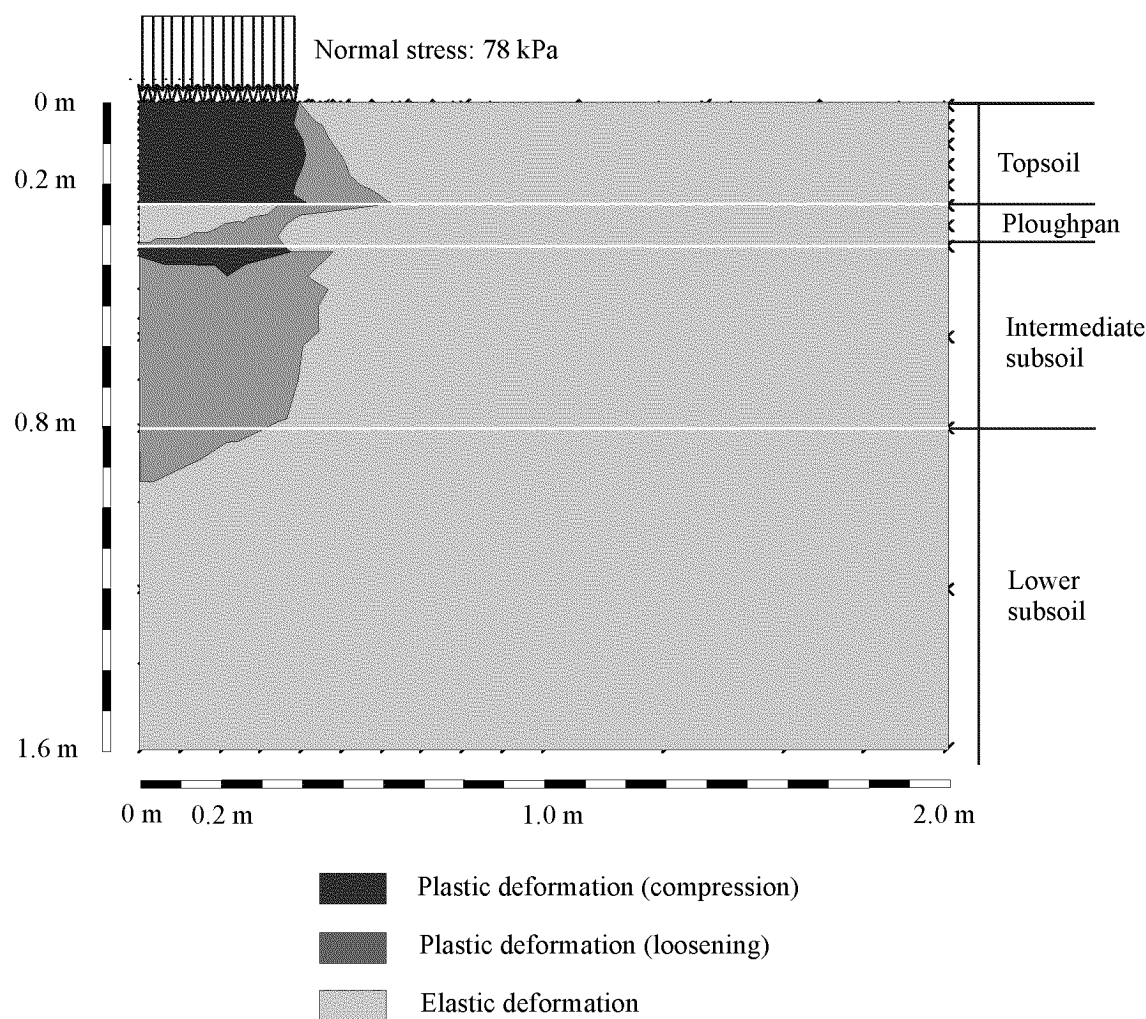

Fig. A2.10. Zones of elastic and plastic deformation calculated for the 'wet' trafficked Ruckfeld soil under drained conditions.

Fig. A2.10 shows the extent of elastic and plastic deformation in the 'wet' trafficked soil according to the calculations with 'Modified Cam Clay'. 'Modified Cam Clay' predicted plastic compression for the topsoil but also for a thin zone in the subsoil, directly underneath the ploughpan. In a rather large zone in the intermediate subsoil, plastic loosening due to shear processes was predicted. With focus on avoiding plastic deformation in the subsoil, not only the plastic compression but also possible plastic loosening zones should be of further interest for soil protection research.

References

Britto, A.M. and Gunn, M.J., 1987. Critical State Soil Mechanics via Finite Elements. Ellis Horwood, Chichester, 488 pp.

Rosal, C., 1997. Drucksondierungen in Loess, Ruckfeld. Diploma Thesis, Institut für Geotechnik (IGT), Eidgenössische Technische Hochschule (ETHZ), Zürich, 36 pp.

Stallebrass, S.E. and Taylor, R.N., 1997. The development and evaluation of a constitutive model for the prediction of ground movements in overconsolidated clay. Géotechnique, 47(2): 235-253.

Curriculum Vitae

Surname	:	Berli
First name	:	Markus
Date of birth	:	1 January 1968
Citizen of	:	Birmensdorf and Ottenbach, Switzerland

School education	:	1975 - 1981	Primary school in Birmensdorf
		1981 - 1984	Secondary school in Birmensdorf
		1984 - 1988	Mathematisch-Naturwissenschaftliches Gymnasium Rämibühl, Zurich, Matura Typus C
Military service	:	1989	
Higher education	:	1989 - 1991	Studies in physics, Swiss Federal Insitute of Technology (ETH), Zurich, Switzerland
		1991 - 1996	Studies in environmental engineering, ETH Zurich Diploma in environmental engineering (Dipl. Umwelting. ETH)
		1996 - 2001	PhD-Studies in technical engineering, ETH Zurich
Occupation	:	1996 - 2001	Research and teaching assisstant, ETH Zurich

Birmensdorf, October 2001